

A microscopic image of a protein particle, likely a virus or a large protein complex, showing a hexagonal lattice structure. The particle is yellowish and has a porous, honeycomb-like appearance. It is centered in the frame, with other similar particles visible in the background and foreground, slightly out of focus. The background is dark, and the lighting highlights the texture of the particle.

# WATER-BINDING OF PROTEIN PARTICLES

*Jorien P.C.M. Peters*

# **WATER-BINDING OF PROTEIN PARTICLES**

*Jorien P.C.M. Peters*



**Thesis committee****Promotors**

Prof. Dr A.J. van der Goot

Personal chair at the Laboratory of Food Process Engineering  
Wageningen University

Prof. Dr R.M. Boom

Professor of Food Process Engineering  
Wageningen University

**Other members**

Prof. R. Ipsen, University of Copenhagen, Denmark

Prof. Dr J.P.M. van Duynhoven, Wageningen University

Prof. Dr E. van der Linden, Wageningen University

Dr L.E. van Riemsdijk, Bel Leerdammer B.V., Schoonrewoerd

This research was conducted under the auspices of the Graduate School VLAG (Advanced studies in Food Technology, Agrobiotechnology, Nutrition and Health Sciences)

# **WATER-BINDING OF PROTEIN PARTICLES**

*Jorien P.C.M. Peters*

## **Thesis**

submitted in fulfilment of the requirements for the degree of doctor  
at Wageningen University  
by the authority of the Rector Magnificus,  
Prof. Dr A.P.J. Mol,  
in the presence of the  
Thesis Committee appointed by the Academic Board  
to be defended in public  
on Friday 16 September 2016  
at 4 p.m. in the Aula

Jorien P.C.M. Peters  
Water-binding of protein particles,  
200 pages.

PhD thesis, Wageningen University, Wageningen, NL (2016)

With references, with summary in English

ISBN: 978-94-6257-862-3

DOI: <http://dx.doi.org/10.18174/385963>



Voor pap en mam



## TABLE OF CONTENTS

<b>Chapter 1</b>	Introduction	13
<b>Chapter 2</b>	Effect of crosslink density on the water-binding capacity of whey protein microparticles	25
<b>Chapter 3</b>	Time domain nuclear magnetic resonance as a method to determine and characterise the water-binding capacity of whey protein microparticles	49
<b>Chapter 4</b>	Unravelling of the water-binding capacity of cold-gelated whey protein microparticles	75
<b>Chapter 5</b>	Water-binding capacity of protein-rich particles	107
<b>Chapter 6</b>	General discussion	135
<b>Summary</b>		159
<b>Appendix</b>		163
<b>References</b>		173
<b>Acknowledgements</b>		191
<b>About the author</b>		193
<b>List of publications</b>		195
<b>Overview of completed training activities</b>		197





## LIST OF ABBREVIATIONS

CG MPs	cold-gelated whey protein microparticles
CLSM	confocal laser scanning microscope/microscopy
CPMG	Carr–Purcell–Meiboom–Gill
DH	degree of hydrolysis
DRCOSY	diffusion relaxation correlation spectroscopy
DTNB	5,5'-dithio-bis-(2-nitrobenzoic acid)
DTT	dithiothreitol
DTT MPs	unwashed microparticles treated with 40 mM dithiothreitol
DVS	dynamic vapour sorption
GDL	glucono- $\delta$ -lactone
GRAS	generally recognized as safe
HG MPs	heat-gelated whey protein microparticles
IEP	isoelectric point
LBG	locust bean gum
LPC	lupin protein concentrate
MPs	whey protein microparticles
NEM	<i>N</i> -ethylmaleimide
NMs	nanomaterials
NMR	nuclear magnetic resonance
NPs	nanoparticles
OPA	<i>o</i> -phthaldialdehyde
PFG-STE	pulsed field gradient stimulated echo
pH MPs	whey protein microparticles made at pH 5.8
PPI	pea protein isolate
RH	relative humidity
SAP	super-absorbing polymer
SDS	sodium dodecyl sulphate
SPI	soy protein isolate
ST MPs	standard whey protein microparticles
TD NMR	time domain nuclear magnetic resonance
Tgase	transglutaminase
VWG	vital wheat gluten
WBC	water-binding capacity
WBC-MPs	water-binding capacity of microparticles
WBC-P	water-binding capacity of the pellet
WHC	water-holding capacity
WPC	whey protein concentrate
WPI	whey protein isolate

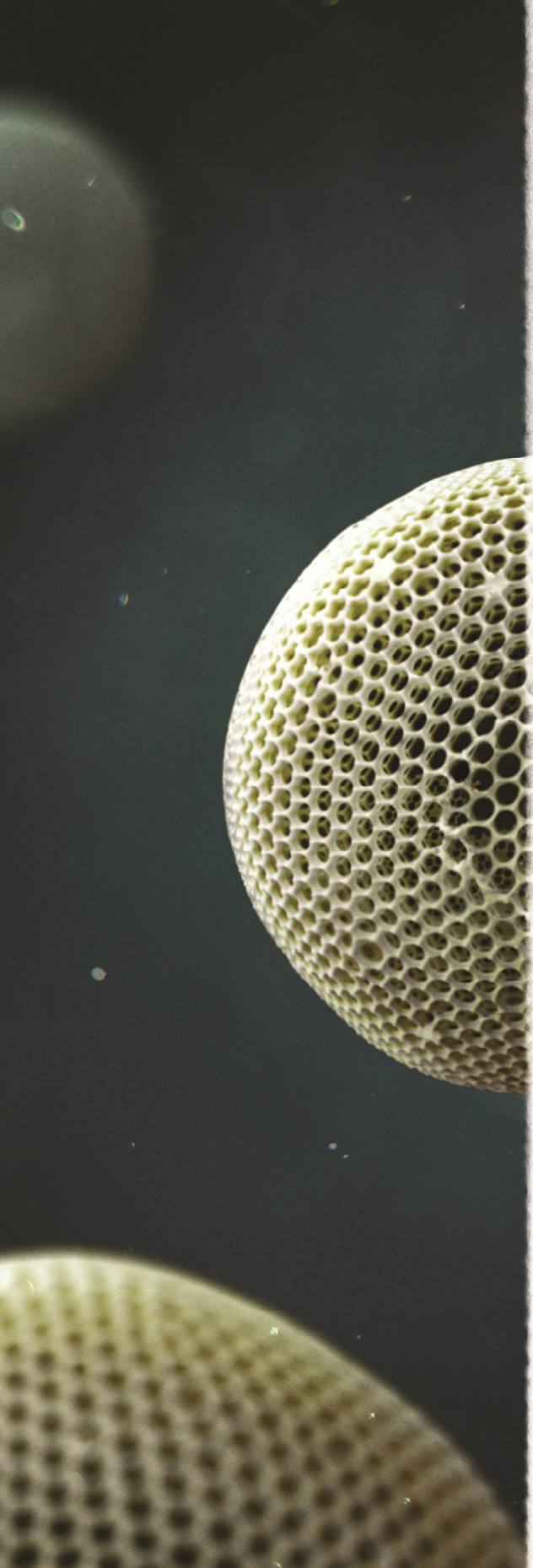
## LIST OF SYMBOLS

$a_w$	water-activity (-)
$D$	diffusion coefficient ( $\text{m}^2 \text{s}^{-1}$ )
$d_{4,3}$	volume mean diameter (m)
$E$	elastic modulus ( $\text{m kg s}^{-2}$ )
$M_c$	molecular weight between crosslinks ( $\text{kg mol}^{-1}$ )
$M_{\text{dm\_between}}$	weight of dry matter between the particles (kg)
$M_{\text{dm\_s}}$	weight remaining dry matter after drying the supernatant (kg)
$M_{\text{dpp}}$	weight of all dry particles in the pellet (kg)
$M_{\text{dry\_pellet}}$	weight of the remaining pellet after oven drying (kg)
$M_{\text{wet\_pellet}}$	weight of the pellet immediately after centrifugation (kg)
$p_2$	weight fraction (-)
$R$	ideal gas constant ( $8.314 \text{ J mol}^{-1} \text{ K}^{-1}$ )
$R_2$	transverse relaxation rate ( $\text{s}^{-1}$ )
$T$	absolute temperature (K)
$T_2$	transverse relaxation time (s)
$V_{\text{hpp}}$	total volume of all hydrated particles in the pellet ( $\text{m}^3$ )
$V_{\text{wet\_pellet}}$	volume of the pellet immediately after centrifugation ( $\text{m}^3$ )
$w_{\text{dm\_between}}$	weight-fraction of dry matter in between the particles (-)
$w_{\text{w\_between}}$	weight-fraction of water in between the particles (-)
$\Delta$	diffusion encoding time (s)
$\rho_p$	density protein ( $\text{kg m}^{-3}$ )
$\rho_w$	density water ( $\text{kg m}^{-3}$ )
$\varphi_1$	volume fraction of polymer (-)
$\varphi_2$	volume fraction of water (-)
$\chi$	polymer-solvent interaction parameter (-)
$\chi_1$	polymer-solvent interaction parameter of the dry system (-)









*Chapter 1*

# INTRODUCTION



## 1 THE DEMAND FOR LOW-CALORIC PRODUCTS

One of the world's largest health issues nowadays is the increase in people who are overweight or obese. In the Netherlands, the number of children (4 to 20 years) and adults (20 years or older) that are obese, and adults that are overweight, have been increasing at least since 1981, even though a small decrease in overweight children has been observed since 2012.<sup>[28]</sup> Body overweight increases the risk of developing other health problems such as cardiovascular diseases and diabetes type II.<sup>[97][138]</sup> Furthermore, there is an increase in the number of people who wish to live and eat healthier.<sup>[102][163]</sup> These consumers would benefit from low-caloric foods to better manage their weight.

Dairy is one of the main product categories in the Western diet, and is therefore a category for which low-caloric products are important. Gouda cheese is an example of such a product. To reduce the caloric content of cheese, its fat content may be decreased; another starter culture may be used; the process conditions may be altered; stabilizers may be added; or fat substitutes may be incorporated.<sup>[95][10]</sup> However, raising the sensory quality of low-caloric cheese to near its full-fat equivalent remains a challenge. Often, low-fat cheeses are firmer, and lack the ability to 'melt in the mouth,' which is a sensory attribute of full-fat cheeses.<sup>[22][64]</sup>

The research reported in this thesis is based on the ambition to decrease the caloric content of Gouda cheese by increasing its water content, thereby decreasing its fat and protein content. Merely adding water will likely soften the cheese or may result in the expulsion of water, which is undesired. Therefore, the chosen approach is to incorporate particles that can bind at least 90% w/w water, increasing the overall moisture content of the cheese. In addition, incorporation of these particles should not negatively affect the sensory attributes of the cheese. To prepare these strongly water-binding particles, we investigated the use of whey proteins in this thesis.

## 2 WHEY PROTEIN MICROPARTICLES

Microparticulated proteins (gelated protein particles that have a maximum size in the microscale (1 to 1000  $\mu\text{m}$ )) seem to have promising characteristics as fat replacers and water-binding particles. In addition, both the nano- and microstructure of the gels can be easily adapted during the microstructuring process.<sup>[124]</sup> Within this thesis, two structuring methods were used to make protein microparticles (MPs): heat- and cold gelation. For both methods, whey protein was taken as starting material.

### 2.1 PROPERTIES OF WHEY PROTEINS

Whey proteins are obtained when caseins in milk are precipitated with rennet enzymes and bacteria, during cheese formation or casein production (sweet whey); or with an acid, during acidic casein production (acid whey).<sup>[81][171]</sup> The fluid that is left after precipitation of the proteins is whey, and contains about 6% of solids.<sup>[81]</sup> This solid fraction contains lactose, proteins and minerals. After the formation of whey, it is concentrated (e.g., by evaporation); minerals and lactose may be removed from it (e.g., by ultrafiltration or ion-exchange); and it is dried (e.g., by spray drying), to obtain whey protein concentrate (WPC; 35–80% proteins) or the even purer whey protein isolate (WPI;  $\geq 90\%$  proteins).<sup>[81][171]</sup> The WPI used in this research is made through spray drying sweet, purified whey and contains more than 95% globular proteins, which can be present in their undenatured state.<sup>[37][115][169]</sup> WPI consists of several proteins, each with their own characteristics (Table 1) that determine the overall characteristics of WPI.

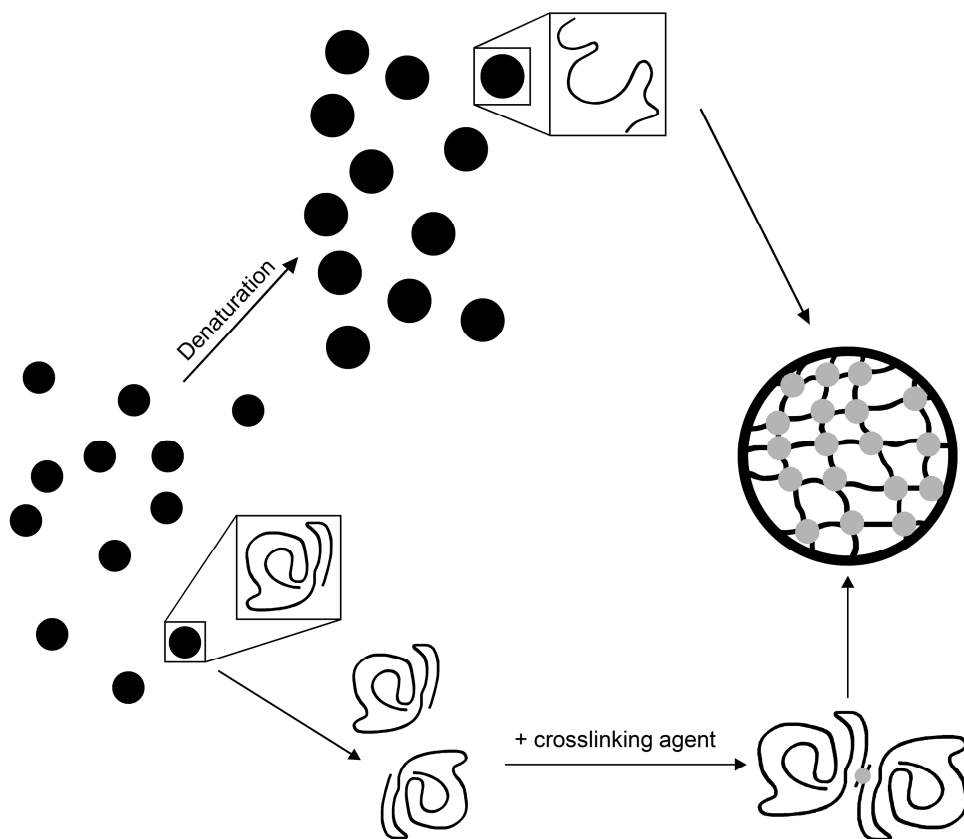
**Table 1.** Composition and characteristics of the various proteins in whey protein isolate (WPI).<sup>[161][169]</sup>

Protein fraction	Concentration in WPI (% w/w)	Molecular weight (kDa)	pH isoelectric point (-)	Cysteine (mole residues/mole protein)
$\beta$ -lactoglobulin	70	18.3–36.9	5.2	5
$\alpha$ -lactalbumin	18	14.2	4.3–5.1	8
Bovine serum albumin	6	66–69	4.8	35
Immunoglobulins	6	160	5.5–6.8	

## 2.2 WHEY PROTEIN GELATION

Whey proteins can bind extra water through entrapment in a protein network; i.e., a gel.<sup>[68][186]</sup> There exist various procedures that may be used to make a gel from whey proteins, such as applying heat, changing the solvent conditions (pH and ionic strength), or applying an enzymatic treatment.<sup>[167]</sup> These procedures, with the exception of the enzymatic treatment, are based on the ability of whey proteins to denature (unfold).<sup>[44][61][103]</sup> Due to denaturation, the hydrophobic part inside the proteins is exposed, increasing the hydrophobic interactions between the proteins.<sup>[23]</sup> These intermolecular interactions induce protein aggregation and the formation of a space-spanning network—if and when the attractive interactions dominate.<sup>[23][61]</sup> When the repulsive interactions dominate, or if the concentration is too low to form a gel, individual fibrils or aggregates are formed from the proteins.<sup>[23]</sup> Inside the protein gel, interactions between the proteins can be of a non-covalent or covalent nature.<sup>[145]</sup> Both types of interactions act as crosslinks in the network (Fig. 1).

Crosslinks between whey proteins can also be created with the use of an enzyme or a chemical crosslinking agent, which may additionally result in the formation of a gel (Fig. 1). These crosslinking agents catalyse or initiate a specific chemical reaction between certain amino acids. A well-known enzyme that is used for this purpose is transglutaminase (Tgase),<sup>[8][100][146][176]</sup> which catalyses the formation of a covalent bond between two amino acids: lysine and glutamine.<sup>[73][182]</sup> Other examples of crosslinking agents for whey proteins are enzymes that catalyse oxidation, such as tyrosinase,<sup>[144]</sup> peroxidase, and laccase.<sup>[47]</sup> A chemical that induces crosslinking of whey proteins is genipin.<sup>[121]</sup> In contrast to transglutaminase, genipin is not a catalyst, but a reactant that can crosslink free amino groups of proteins in a two-step reaction mechanism. As a side effect, the protein acquires a bluish colour.<sup>[26]</sup> Overviews of crosslinking agents that can be used for proteins are available from Gerrard (2002)<sup>[59]</sup> and Buchert et al. (2010),<sup>[24]</sup> among others.



**Fig. 1.** The formation of a protein gel, due to denaturation (upper row), or due to the presence of a crosslinking agent (lower row).

## 2.3 MICROSTRUCTURING OF WHEY PROTEINS

In this thesis we made use of two gelation methods to produce MPs: heat- and cold gelation. Heat-induced gelation is a frequently used method to create protein gels from a protein dispersion, with a concentration above the gelation concentration, which is 11–12% w/w for whey proteins.<sup>[7][90]</sup> Heating such a dispersion results in the formation of a volume-spanning network, if the repulsive forces are sufficiently shielded to allow proteins to attract each other.<sup>[23][61]</sup> With intermediate screening, the proteins attach at their far end, resulting in a filamentous structure. Stronger screening of the repulsive forces allows the proteins to interact over the whole length of the protein chain, and results in the formation of a network of large, spherical aggregates.<sup>[23]</sup> Heat-gelated microparticles (HG MPs) are obtained by first heating and simultaneously mixing a 40% w/w WPI dispersion, resulting

in broken gel pieces. These pieces are then dried and milled to micro-sized particles.<sup>[115][116][118][119]</sup>

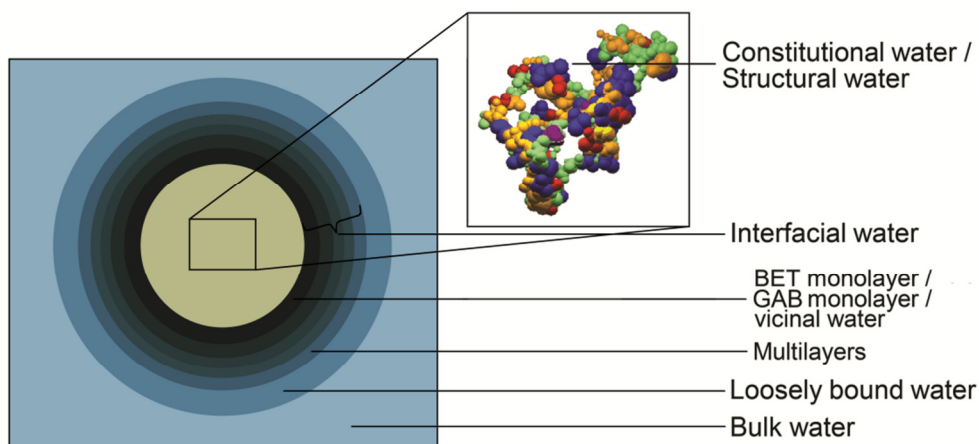
Cold gelation is a two-step process in which denaturation and gelation occur sequentially, instead of simultaneously as during heat gelation.<sup>[3][23]</sup> The use of cold gelation is preferred when the product may not be (strongly) heated due to the presence of heat-sensitive ingredients.<sup>[23]</sup> The process of forming cold-gelated microparticles (CG MPs) starts with heating a protein dispersion with a concentration that is lower than the gelation concentration. This leads to the formation of small protein aggregates, provided that the repulsive forces are stronger than the attractive forces.<sup>[3]</sup> Therefore, the solvent should have a low ionic strength and a pH that is not too near the isoelectric point (IEP) of the proteins (pH 5.2–5.4).<sup>[23][58][147]</sup> After the formation of reactive aggregates (i.e., aggregates still having groups or patches that would allow further binding to other proteins or aggregates), the electrostatic repulsion between the aggregates is shielded, allowing the aggregates to come together, form strands, and eventually form a gel.<sup>[23]</sup> This can be induced by reducing the pH to the IEP of the proteins,<sup>[3][5][150][160]</sup> or by the addition of salts.<sup>[3][12][72]</sup> When a polysaccharide is added prior to gelation, phase separation takes place during gel formation, which can produce CG MPs.<sup>[39][40][159][160]</sup>

### 3 PROTEIN(STRUCTURE)-WATER INTERACTIONS

#### 3.1 TYPES OF WATER AND THEIR IMPORTANCE

Protein(structure)–water interactions largely determine the ultimate properties of a protein gel, including its ability to bind water.<sup>[186]</sup> This and other protein gel properties are additionally influenced by protein–protein interactions.

Protein and water interact in a protein gel over length-scales that range from nano-scale (1 to 100 nm) to macro-scale (the scale that is visible without use of microscopy).<sup>[68]</sup> Depending on the scale that is observed, there are differences in the strength of water-binding. Water near protein molecules, for example, is bound more strongly than water that is present in the middle of a big pore. This strongly affects the properties of water near the protein molecule, resulting in significant deviation from the properties of bulk water. These differences are often used to divide water into different “types” or “layers” (Fig. 2 and 3).<sup>[30][82][185]</sup> However, in reality, the water molecules exchange quickly from one water layer to the other (it might take only  $10^{-9}$  s for a water molecule to exchange between free and bound water),<sup>[71]</sup> implying that water molecules are not truly irreversibly bound in a water layer, and that the layers are not stagnant. In literature, a distinction is frequently made between constitutional water or structured water, interfacial water (consisting of the BET or GAB monolayer, and multilayers), loosely bound water and bulk water (Fig. 2).<sup>[30][82][185]</sup>



**Fig. 2.** The various types and layers of water that may be present around proteins.

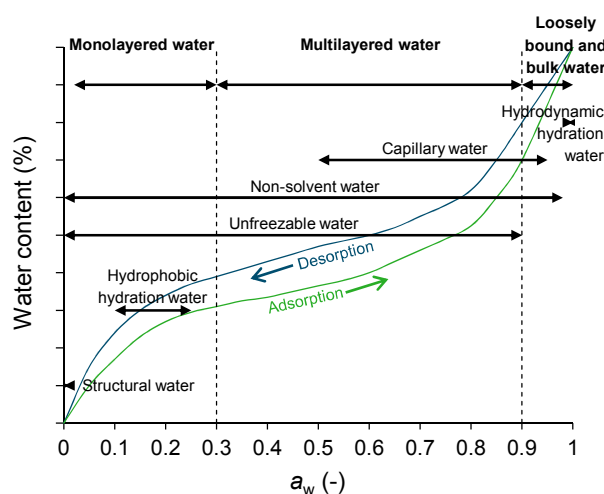
Water in any molecular network is retained in the network, due to the attractive interactions between the solvent (water) and the matrix. In a network of protein molecules, the crosslinks between them prevent the protein molecules from simply dissolving in excess water, and also counteract swelling. This balance between a good solvent–network interaction and the counteracting of swelling by strained crosslinks is described for synthetic polymers by the Flory–Rehner equation.<sup>[53][54]</sup> It was shown recently that it is possible to expand the Flory–Rehner theory to describe the swelling behaviour of food materials, despite the fact that this theory is based on a concept in polymer science for solvents and crosslinked polymers that have no hydrogen bonding.<sup>[111][152][153][154][155][156]</sup> This theory shows that swelling at low water-activities ( $a_w$ ) is predominately governed by the interaction between the networked polymer (protein) and the solvent (water) (i.e., the hydrophilicity of the proteins), whereas the swelling of a particular gel at high  $a_w$ -values is mostly governed by the crosslink density. However, no remarkable effect on the water-binding was found in the  $a_w$ -range 0 to 0.92 for a series of proteins with different structures, especially in comparison with the maximum amount of water that can be bound by a protein gel.<sup>[30][83]</sup> This suggests that the characteristics that have the largest effect on the water-binding are those that play a role at  $a_w$ -values from 0.92 to 1, and which thus determine the amount of loosely bound water in the network: the pores in the network, and its crosslink density.<sup>[30][82]</sup>

### 3.2 METHODS TO QUANTIFY PROTEIN(STRUCTURE)-WATER INTERACTIONS

Various experiments exist that can be used to gain insight into the protein(structure)–water interactions, depending on the material used and which protein(structure)–water interactions are of interest. A good overview of those methods is given by Chou (1979)<sup>[30]</sup> and Kneifel et al. (1991),<sup>[84]</sup> among others.

A frequently used method to determine the water-binding capacity (WBC; *the amount of water that is bound to the MPs after applying an external force to a protein dispersion*) of protein particles, is to first make a dispersion of the particles in water, and subsequently centrifuging it.<sup>[1][15][76][115]</sup> The weight of the pellet that is obtained after centrifugation is used to calculate the WBC, making the assumption that no significant amount of water is present between the particles.

An isotherm (Fig. 3) provides information about the approximate amount of water in the structural water layer, monolayer, multilayers, and the loosely bound water layer separately. To make an isotherm, samples are subjected to a certain relative humidity, and the weight of the water uptake is measured. A rough distinction between the types of water can be made via the isotherm, taking into account the  $a_w$ -ranges in which these types of water are present (Fig. 3).<sup>[82][83]</sup>



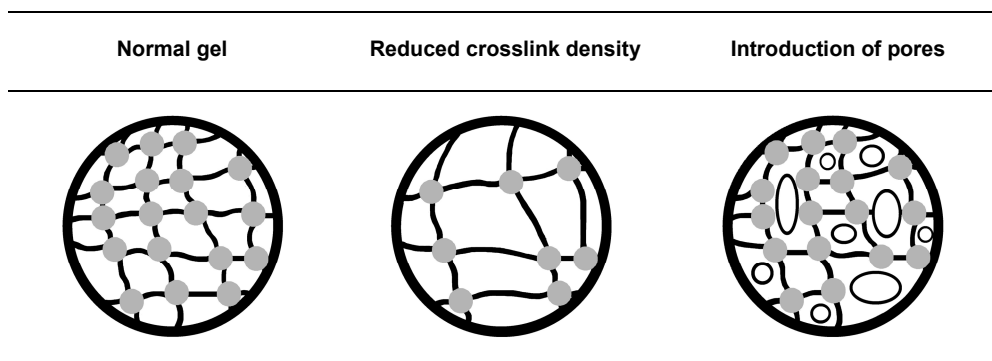
**Fig. 3.** The different types and layers of water that may be present in a protein gel at varying water-activities ( $a_w$ ).

Another method that gets increased attention is time domain nuclear magnetic resonance (TD NMR).<sup>[17][18][21][141]</sup> A frequently performed measurement with TD NMR is a  $T_2$ -relaxation time measurement: first a sample is placed into a magnetic field, which induces the  $^1\text{H}$  protons to align. Then, a radio frequency pulse is applied to the  $^1\text{H}$  protons, resulting in a shift of the proton alignment. As soon as the pulse is removed, the protons will return to their equilibrium state (relaxation), and the echo of the proton relaxation is recorded. The obtained relaxation decay curve is then subjected to an inverse Laplace transformation to acquire transverse relaxation time ( $T_2$ )-spectra.<sup>[139]</sup>  $T_2$ -spectra show the number of water domains that are detected and give an indication of the amount of water in those domains. However, the number of domains is influenced by the rate of water exchange between the various domains. Fast exchange of water between the different domains results in averaging of the  $T_2$ -peaks.<sup>[91]</sup> In addition,  $T_2$ -spectra give an indication about the strength of water-binding. Pure water has a large  $T_2$ -value, because water molecules diffuse relatively quickly and therefore need more time before relaxation occurs. The presence of proteins lowers the  $T_2$ -value, because the mobility of water is decreased by its being “bound” to the proteins, resulting in faster relaxation.<sup>[104]</sup> In case of meat, fresh cheese, carrageenan gels and solutions, whey gels, and yogurt, TD NMR provided insight into the total water-binding, and the water fractions that affect the water-binding.<sup>[17][18][21][69][70][141]</sup>



## 4 THE USE OF STRUCTURING TO AFFECT THE SWELLING PROPERTIES

HG MPs are able to swell in water and can bind more water when a dispersion of HG MPs is reheated.<sup>[116][119]</sup> The challenge is to produce MPs that are able to absorb even more water, because a water content of  $\geq 90\%$  makes the concept presented in Section 1 most feasible. In addition, water should be bound sufficiently strongly, thereby preventing net exchange with the continuous phase of the product, thus keeping the water in the MPs. Structuring the protein at different length-scales can be a tool to alter the swelling capacity of protein gels. The potential of micro- and nanostructuring becomes evident when looking at synthetic super-absorbing polymer gels (SAPs;  $> 95\%$  water). The properties of SAPs suggest that the following characteristics of the polymer and polymer network determine the swelling capacity: the crosslink density<sup>[106]</sup> and types of crosslinks, the hydrophilicity of the polymers,<sup>[71][106][107][188]</sup> and the pores present in the gel<sup>[107]</sup> (Fig. 4). These findings are consistent with the Flory–Rehner theory, which confirms the importance of the crosslink density and the hydrophilicity of polymers, in relation to the swelling ability of polymer gels.<sup>[152][153]</sup> As stated in Section 3, the hydrophilicity only affects swelling at low water contents. Hence there seem to be two ways in which the structure of MPs can be changed to enhance its ability to bind water (Fig. 4): by decreasing the number of crosslinks in the gel (nanostructuring), or by introducing pores (nano- or microstructuring) that can bind water via capillary forces. A combination of these parameters will further increase the water-binding.



**Fig. 4.** Possible structural changes to protein gels that might result in a larger water-binding capacity.

## 5 OBJECTIVE AND OUTLINE OF THE THESIS

The aim of this thesis was to gain a better understanding of the water-binding properties of protein particles, both on nanometer (e.g., crosslink density) and micrometer length-scales (e.g., particle size and shape). This understanding is the basis for developing guidelines on the requisite characteristics of protein particles that allow them to absorb a lot of water ( $\geq 90\%$ ). A schematic overview of this thesis is shown in Fig. 5.

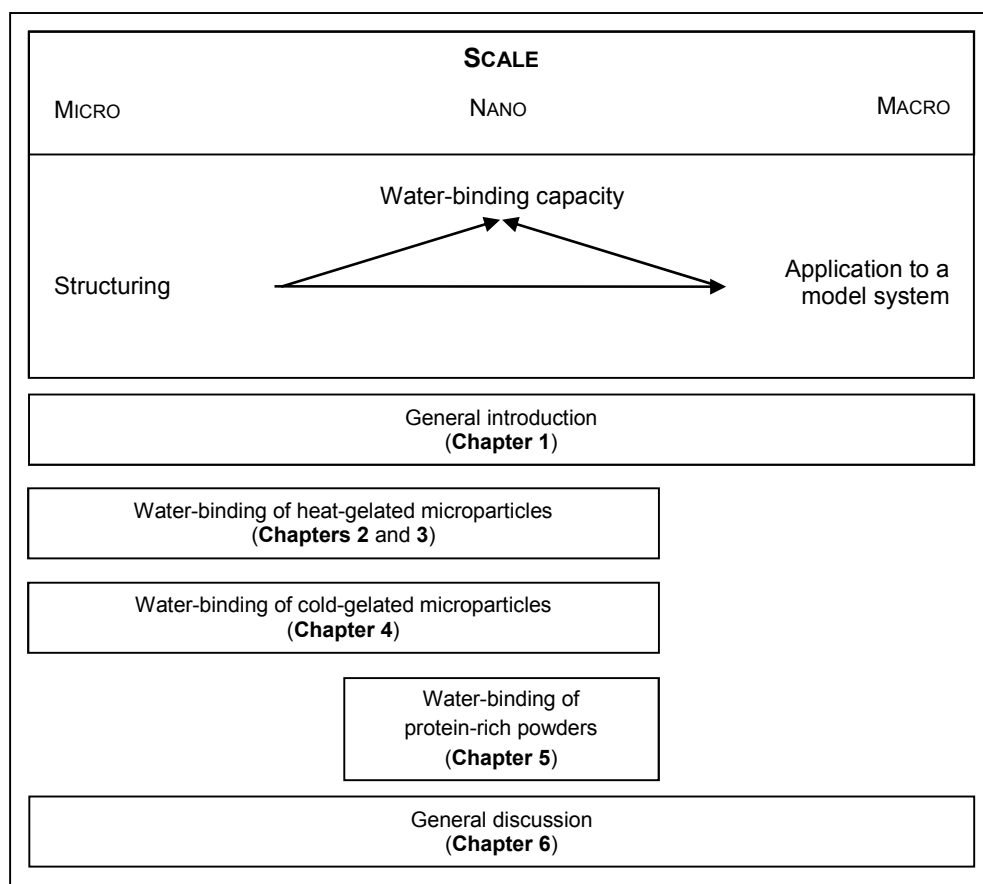
**Chapter 2** shows the effect of changing the parameter that has the greatest influence on the swelling capacity of MPs according to the Flory–Rehner theory: the crosslink density. HG MPs were made with various crosslink densities, and their effect on the WBC of pellets (WBC-P) of these MPs was tested, as well as their effect on swelling of the HG MPs.

In **Chapter 3** the WBC-P of these HG MPs with various crosslink densities was further investigated with TD NMR. This provided deeper insight into the factors that affect the WBC-P, and demonstrated that TD NMR could provide a more accurate determination of the WBC-P.

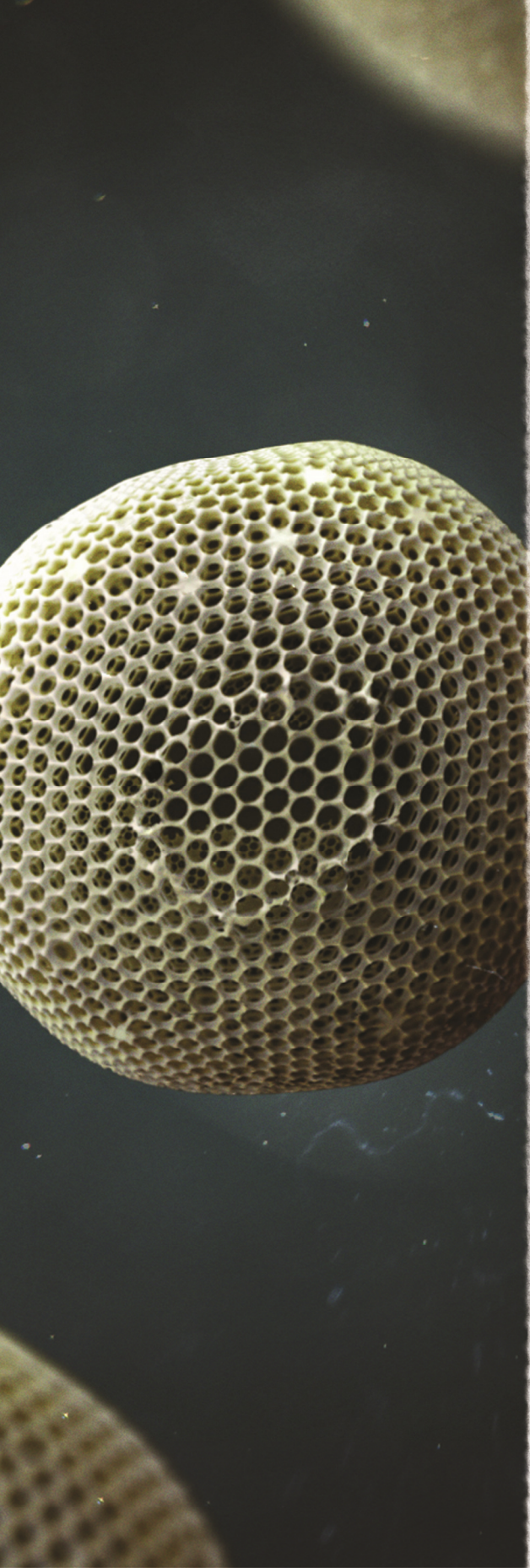
The second type of MPs was made via cold gelation. In **Chapter 4** their WBC-P characteristics were explored. Remarkable differences in the behaviour of CG MPs were found, as compared to the HG MPS that were studied in **Chapters 2** and **3**.

In **Chapter 5**, the WBC-P of other proteins was studied as well. This resulted in some general principles that play a role in the determination of the WBC via the pellet.

Finally, **Chapter 6** reviews the results that were presented in the previous chapters. It evaluates the applicability of MPs as highly water-binding particles. Furthermore, it describes the scientific challenges to gaining further insight into the water-binding of protein systems. The chapter ends with a risk assessment of the particles that were made in this thesis.



**Fig. 5.** A schematic overview of the various chapters in this thesis.



## *Chapter 2*

# **EFFECT OF CROSSLINK DENSITY ON THE WATER-BINDING CAPACITY OF WHEY PROTEIN MICROPARTICLES**

## ABSTRACT

The ability of whey protein microparticles (MPs) to bind water and consequently to swell is determined by the crosslink density of the MPs, among other properties. The Flory–Rehner model states that a decrease in crosslink density should lead to an increase in swelling of the MPs. Decreasing the crosslink density of MPs with dithiothreitol (DTT) decreased the amount of disulphide bridges and increased the water-binding capacity (WBC) from 6 to 9 g water/g protein. Increasing the crosslink density with transglutaminase or genipin resulted in a decreased number of primary amino groups, although the WBC did not change significantly. The WBC of the MPs was determined using a centrifugation method that resulted in the formation of a pellet, so water inside and between the MPs was measured simultaneously. Therefore, additional microscopy and swelling tests were performed, which suggested that an increased WBC of the pellet of MPs was not only related to an increased swelling of the MPs, but also to an increased amount of water between the MPs.

### THIS CHAPTER IS PUBLISHED AS:

Peters, J. P. C. M., Luyten, H., Alting, A. C., Boom, R. M., van der Goot, A. J. (2015). Effect of crosslink density on the water-binding capacity of whey protein microparticles. *Food hydrocolloids*, 44, 277–284.

# 1 INTRODUCTION

Controlling the water-binding properties of protein materials is relevant for various applications, including foods. A route to control the water-binding properties of proteinaceous materials is through the inclusion of whey protein microparticles (MPs). In case the water-binding properties of MPs can be controlled, they can be used to alter the water-binding properties of a full product by adding the particles as an additional dispersed phase.<sup>[115][116]</sup> However, the possibilities to control the water-binding properties of MPs are not yet well understood.

The Flory–Rehner model can be used to obtain guidelines on increasing the swelling capacity of MPs. Originally, this model was developed to describe the swelling behaviour of crosslinked synthetic polymers in apolar solvents.<sup>[53][54]</sup> Recent research showed that the Flory–Rehner model can be adapted to describe the swelling behaviour of much more complex biological materials such as meat,<sup>[152][153][154]</sup> and could be a good model for vegetables and fruits.<sup>[155]</sup> According to the Flory–Rehner model,<sup>[62][154]</sup> the total water-activity ( $a_w$ ) of MPs originates from the interaction between the proteins and the solvent (first part of the equation) and the elastic contribution of the MPs (second part of the equation):

$$\ln a_w = \ln (1 - \varphi_1) + \varphi_1 + \chi \varphi_1^2 + \frac{E v_w}{R T} \left[ \varphi_1^{1/3} \varphi_0^{2/3} - \frac{\varphi_1}{2} \right] \quad (1)$$

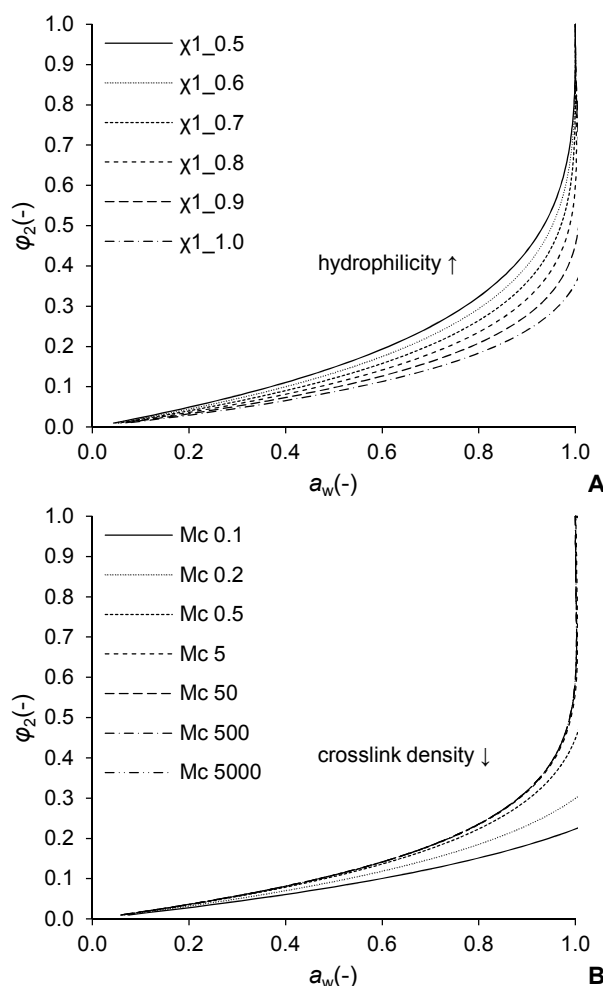
In this equation,  $\varphi_1$  is the polymer volume fraction,  $\chi$  is the polymer-solvent interaction parameter,  $E$  is the elastic modulus,  $v_w$  is the molar volume of water, and  $\varphi_0$  is the volume fraction of the gel in the relaxed state. In later contributions,<sup>[155]</sup>  $\chi$  was made concentration dependent and adapted to:

$$\chi = \chi_1 + (\chi_0 - \chi_1)(1 - \varphi_1)^2 \quad (2)$$

where  $\chi_1$  is the interaction parameter of the dry system and  $\chi_0$  is the interaction parameter of a dilute system with proteins. The elastic contribution of the Flory–Rehner model depends on the crosslink density (the number of linkages (covalent and non-covalent) between two polymer chains) of the polymer network according to the following formula:

$$\frac{E}{R T} = \frac{\rho_s}{M_c} \quad (3)$$

where  $\rho_s$  is the density of the polymers and  $M_c$  is the molar weight of the polymeric units between the crosslinks,<sup>[62][154]</sup> which is considered as the inverse of the crosslink density. These equations show that the swelling capacity can be influenced by changes to two parameters:  $\chi_1$  and/or  $M_c$ . Modelling these two parameters illustrates that  $\chi_1$  and  $M_c$  change the water absorption mostly above  $a_w = 0.2$  (Fig. 6A and B). In addition, Fig. 6B shows that the effect of a change in  $M_c$  on water absorption decreases for lower crosslink densities.



**Fig. 6.** The isotherm of a polymer, where  $\phi_2$  is the volume fraction of water and  $a_w$  is the water-activity, as affected by (A) hydrophilicity ( $\chi_1$ ) of the polymers and (B) the molecular weight between the crosslinks ( $M_c$ ). The arrows show, in the direction the arrow points, an increase in the hydrophilicity (A) and crosslink density (B).

In this research, the swelling capacity of MPs was studied by adding ingredients that have been reported to change the crosslink density of proteins.<sup>[35][133]</sup> The crosslink density was decreased with dithiothreitol, and increased with genipin and transglutaminase. After the formation of various MPs, their water-binding capacity (WBC) was determined using a centrifugation method. In addition, microscopy, light scattering and sorption isotherms were used to investigate whether the WBC changed as a result of a change in swelling of the MPs or a change in the amount of water between the MPs.



## 2 MATERIALS AND METHODS

### 2.1 MATERIALS

Whey protein isolate (WPI; BiPRO, lot no. JE 034-7-440; Davisco Food International Inc., Le Sueur, MN) was used to produce whey protein microparticles (MPs). WPI has a reported protein content of 97.7% on a dry weight basis. The MPs were treated with dithiothreitol (DTT), genipin (both from Sigma–Aldrich, Germany) or microbial  $\text{Ca}^{2+}$ -independent transglutaminase (Tgase; Activa WM; activity of 81–135 units  $\text{g}^{-1}$  according to the manufacturer) derived from *Streptoverticillium mobaraense* (Barentz Raw Materials, The Netherlands), to obtain MPs with various crosslink densities. Other chemicals used for the analysis of the MPs were 5,5'-dithio-bis-(2-nitrobenzoic acid) (DTNB), Bis-Tris, *o*-phthalaldehyde (OPA), ethanol, sodium tetraborate decahydrate (borax), sodium dodecyl sulphate (SDS), Rhodamine B (all from Sigma–Aldrich, Germany) and isopropanol Emplura (Merck, Germany). D-Methionine (Acros Organics, Belgium) was used as a standard for the protein content analysis, cysteine hydrochloride monohydrate (Sigma–Aldrich, Germany) as a standard for the method to determine the sulphhydryl content and L-lysine (Sigma–Aldrich, Germany) as the standard for the OPA method. Milli-Q water (resistivity of 18.2  $\text{M}\Omega$  cm at 25 °C, total oxidisable carbon <10 ppb, Merck Millipore, France) was used in all experiments unless stated otherwise.

### 2.2 METHODS

#### 2.2.1 PRODUCTION OF STANDARD WHEY PROTEIN MICROPARTICLES

MPs were made according to Purwanti, van der Veen, van der Goot, and Boom (2013)<sup>[119]</sup> by first dispersing WPI in water to form a 40% w/w dispersion. The dispersion was stirred with an overhead mixer at room temperature for at least 2 h, and then mixed at 4 °C with a magnetic stirrer overnight. The WPI dispersion was then centrifuged at 1000 rpm and 20 °C for 10 min. Centrifugation resulted in the formation of a foam layer on top of the dispersion, which was removed manually. Subsequently, the dispersion was placed in a bowl mixer (type W50) that was connected to a Brabender Do-corder E330 (Brabender OHG, Duisburg, Germany) and heated with water at 95 °C from a water bath. Within the mixer, the dispersion was mixed at 0 rpm for 5 min, 5 rpm for 5 min and 200 rpm for 40 min. After mixing, the mixer was cooled with water at 4 °C for approximately 5 min, and then the wet gel particles were removed. The wet gel particles were placed in an oven at 50 °C for 2 days and subsequently ground with an ultracentrifuge mill (Retsch ZM 1000). The mill had a 24-tooth stainless steel rotor to which an 80- $\mu\text{m}$  sieve was attached. The rotor was operated at 15,000 rpm for 120 s. After grinding, standard MPs were obtained.

## **2.2.2 PRODUCTION OF WHEY PROTEIN MICROPARTICLES WITH AN ALTERED CROSSLINK DENSITY**

Variations in crosslink density were induced through the addition of DTT, genipin or Tgase in one of the processing steps used to make the MPs. The MPs that were treated with DTT or genipin were prepared by adding 25 g of wet gel particles to a 50 mL solution containing either 10, 20 or 40 mM DTT; or 0.5, 1, 2, or 4 mM genipin. The dispersion was mixed at 20 °C for 24 h. Then, the procedure was continued as described for the standard MPs (i.e., oven drying at 50 °C and milling). Those particles will be referred to as MPs treated with DTT and MPs treated with genipin.

The preparation of MPs treated with Tgase was performed as follows. A 20% w/w Tgase solution was prepared and kept in a fridge (about 4 °C) for 1 week. Before use, the Tgase solution was mixed for 10 min and filtered over a 0.45- $\mu$ m filter. The effect of the addition of Tgase on the MPs was investigated, either by incubating the WPI dispersion before mixing with Tgase, or by incubating wet gel particles in a Tgase solution. In both cases, an enzyme:protein ratio of 1:5 was used. When the WPI dispersion was incubated with Tgase before mixing, the required amount of Tgase solution was kept at 50 °C for 10 min. The WPI dispersion was then mixed with the Tgase solution and further incubated at 50 °C for 1, 2, 6 or 24 h. Subsequently, the dispersion was placed in a bowl mixer (type W50) and heated at 95 °C, while it was mixed at 0 rpm for 5 min, 5 rpm for 5 min and 200 rpm for 40 min. After mixing, the mixer was cooled with water of 4 °C and the wet gel particles were oven-dried and ground as described for the standard MPs in Section 2.2.1. To test the effect of Tgase on the MPs after mixing, 25 g of wet gel particles were incubated in a Tgase solution (50 mL preheated for 10 min) at 50 °C for 1, 2, 6 or 24 h. This procedure was completed with oven drying and milling as described above for the standard MPs. Those MPs will be referred to as MPs treated with Tgase before mixing (incubation of the WPI dispersion with Tgase), and MPs treated with Tgase after mixing (incubation of wet gel particles in a Tgase solution). All MPs were made in duplicate (called batch 1 and batch 2).

## **2.2.3 AMOUNT OF SULPHYDRYL GROUPS**

The amount of sulphhydryl groups present on the surface of the standard MPs and of the MPs treated with DTT of batch 1, was determined using Ellman's reagent (DTNB).<sup>[46]</sup> It was assumed that all of the DTT had reacted with the MPs, and therefore could no longer react with Ellman's reagent. The method described by Alting, Hamer, de Kruif, Paques, and Visschers (2003)<sup>[4]</sup> and Purwanti et al. (2011)<sup>[117]</sup> was used, with some adaptations. First, a dispersion of MPs was made with water (5 g protein L<sup>-1</sup>). In 10-mL tubes, 5 mL of 50 mM Bis-Tris buffer (pH 7) was added, together with 0.5 mL of DTNB solution (1 mg mL<sup>-1</sup> Bis-Tris buffer) and 0.4 mL of MP dispersion. The tubes were wrapped in aluminium foil and rotated for 10 min. Subsequently, the dispersion was centrifuged at 4700 g for 1 min

and 3 mL of the supernatant was transferred to a cuvette. After 15 min of incubation, the absorbance was measured at 412 nm with a spectrophotometer (Genesys 20, Thermo Scientific). For the standard series, cysteine hydrochloride monohydrate was used instead of the MP dispersions. The MPs were measured in quadruplicate; the standards in triplicate.

#### 2.2.4 AMOUNT OF PRIMARY AMINO GROUPS

The amount of primary amino groups present in batch 1 of the standard MPs; the MPs treated with Tgase; and the MPs treated with genipin, was determined using the OPA method, as described by Nielsen, Petersen, and Dambmann (2001),<sup>[101]</sup> with some adaptations. First, 10 mg of MPs were mixed with 1 mL of a 10% w/w SDS solution and 4 mL of a 15.625 mM borax solution for 1 h. After incubation, the tubes were centrifuged at 4500 rpm for 15 min. In the meantime, the OPA reagent was prepared by dissolving 9.53 g of borax and 2.5 g of SDS in 200 mL of water. Then, 200 mg of OPA, dissolved in 5 mL of ethanol, was added. Subsequently, 220 mg of DTT was mixed into the solution and the solution was made up to 250 mL with water. The solution was filtered over a 0.45- $\mu$ m filter and stored in a bottle wrapped in aluminium foil. After preparation of the samples and the OPA reagent, the samples were subjected to the reagent. First, 1.5 mL of OPA reagent was transferred to a cuvette and measured at 340 nm with a spectrophotometer (Genesys 20, Thermo Scientific). The OPA reagent was transferred to an Eppendorf tube, 200  $\mu$ L of the supernatant of the sample was added, and the tube was mixed with a vortex. After 5 min of incubation, the absorbance was measured again. In addition to the samples, different concentrations of an L-lysine solution were measured to obtain a standard curve. The MPs were measured at least in quadruplicate; the standards in triplicate.

#### 2.2.5 WATER-BINDING CAPACITY OF THE WHEY PROTEIN MICROPARTICLES

The water-binding capacity (WBC) of both batches of all MPs was measured by first preparing a 10% w/w dispersion. The dispersion was mixed at 25 °C with a rotor at a speed of 16 rpm for 3 h. Every 15 min, the dispersion was mixed with a vortex. Then the dispersion was centrifuged at 3000 rpm and 25 °C for 20 min to form a supernatant and pellet. The supernatant was decanted and the pellet was dried in an oven at 105 °C for 24 h. From the weight difference between the wet pellet and the dry pellet and the protein content of the dry pellet, the WBC (g water/g protein) was calculated using the following formula:

$$\text{WBC (g water/g protein)} = \frac{(M_{\text{wet\_pellet}} - M_{\text{dry\_pellet}})}{M_{\text{dry\_pellet}} \text{Protein\_content}_{\text{dry\_pellet}}} \quad (4)$$

In this formula,  $M_{\text{wet\_pellet}}$  is the weight of the wet pellet,  $M_{\text{dry\_pellet}}$  is the weight of the dry pellet and  $\text{protein\_content}_{\text{dry\_pellet}}$  is the protein content of the dry pellet.

The effect of reheating on the WBC of MPs was also tested. Therefore, the same procedure was used as described above; however, before the dispersion was centrifuged, it was heated in a water bath at 90 °C for 30 min. The tube was then put into ice water for 10 min and placed at room temperature for another 10 min. The WBC of each batch of MPs was measured in triplicate, and the average for each treatment was calculated.

## 2.2.6 MICROSCOPIC OBSERVATION OF THE PELLETS

The pellets from batch 1 of the unheated standard MPs and of MPs treated with 40 mM DTT were observed with a confocal laser scanning microscope (CLSM). The same procedure was applied to the MPs, as described in Section 2.2.5. Only one drop of a  $2 \times 10^{-3}\%$  w/w Rhodamine B solution was added to the 10% w/w MP dispersion before hydration, and the tubes were covered with aluminium foil. After centrifugation, the pellet was transferred to a chambered cover glass. The pellets were then visualized with a LSM 510 microscope (Zeiss, Germany). To induce fluorescent emission of Rhodamine B, a 543-nm laser was used for excitation to detect emissions between 600 and 650 nm.

## 2.2.7 SWELLING OF THE WHEY PROTEIN MICROPARTICLES

To calculate the swelling of the MPs during the WBC experiment, the size distribution of the unhydrated (i.e., the MPs as obtained after oven drying and milling and further referred to as dry MPs); hydrated; and hydrated and heated standard MPs, and MPs treated with 40 mM DTT from batch 1; were determined with static light scattering (Mastersizer 2000, Malvern Instruments). In the determination of the particle size of the dry MPs, isopropanol was used as a carrier fluid, because MPs do not absorb this solvent. The effect of hydration, and hydration and heating, was measured using water as a carrier fluid. The stirring speed in the vessel containing the carrier fluid was set at 1200 rpm. Refractive indices of 1.545 (MPs), 1.33 (water) and 1.39 (isopropanol) were used, and the absorption of the MPs was set at 0.001.<sup>[164]</sup> To determine the size of the dry MPs, a 10% w/w dispersion of MPs in isopropanol was prepared. The size of the hydrated, and hydrated and heated MPs was determined after hydrating a 10% w/w MP dispersion for 3 h (hydrated MPs) and subsequently heating, cooling and equilibrating (hydrated and heated MPs) as described in Section 2.2.5. The measurements were taken for three dispersions per treatment; the size distribution was measured in quintuplicate. From the results, the average particle diameter ( $d_{4,3}$ ) was calculated.

### 2.2.8 SORPTION ISOTHERMS OF THE WHEY PROTEIN MICROPARTICLES

The water vapour sorption isotherms of the MPs were used to analyse the effect of the treatment on their swelling capacity. Sorption isotherms for batch 1 of the standard MPs and of MPs treated with 40 mM DTT were obtained by putting 10–15 mg of MPs in a stainless steel mesh basket and placing this basket in a Dynamic Vapour Sorption (DVS) Advantage apparatus (Surface Measurement Systems NA, Allentown, PA). The temperature of the DVS was set at 25 °C. The material was subjected to a full loop relative humidity (RH) circle, starting from 30.4% RH, which was the approximate initial RH of the MPs. The RH was increased stepwise to approximately 97%, decreased in several steps to 0% RH, and increased again to the starting RH. When the mass of the MPs did not change by more than 0.002 mg min<sup>-1</sup> for 300 min, or the material was subjected to a certain RH for a maximum of 1500 min, the program went to the next step. The weight of the dry particles obtained from the isotherm at 0% RH was used to calculate the amount of water present at each RH point. The measurement of the isotherm for each type of MP was performed in duplicate.

### 2.2.9 PROTEIN CONTENT

The protein content of the pellets formed during the WBC experiment and the supernatant obtained from the solubility experiment was determined using Dumas analysis (Nitrogen Analyzer, FlashEA 1112 series, Thermo Scientific, Interscience). A conversion factor of 6.38 was used to convert the nitrogen content to the protein content. To calculate the protein content of the pellets, the average protein content of three independent samples was taken from one batch. For the protein content in the supernatant, the average of all supernatants was used.

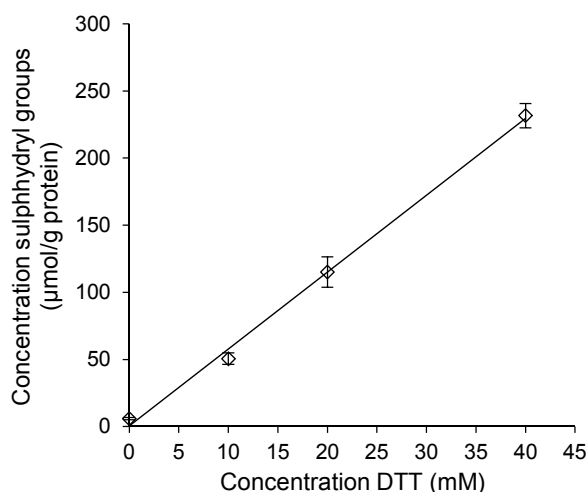
### 2.2.10 SOLUBILITY OF THE PROTEINS

To determine the amount of proteins that solubilized during the incubation of wet gel particles in a DTT solution, wet incubated gel particles with supernatant were filtered over a sieve (0.090 mm). This resulted in separation of the MPs from the supernatant, though some small protein aggregates remained in the supernatant. The supernatant was dried at 105 °C for 24 h. The protein content of the dried supernatant was determined and the solubility of the proteins was calculated.

### 3 RESULTS

#### 3.1 THE EFFECT OF DITHIOTHREITOL, GENIPIN AND TRANSGLUTAMINASE ON THE CONTENT OF SULPHHYDRYL AND PRIMARY AMINO GROUPS

To decrease the crosslink density of MPs, dithiothreitol (DTT)—a reducing agent that is able to break disulphide bridges into sulphhydryl groups—was added. However, the sulphhydryl groups are able to form new disulphide bridges, which makes the overall effect of DTT uncertain.<sup>[187]</sup> Here, it was found that the number of sulphhydryl groups measured scaled linearly with the amount of DTT added (Fig. 7). The high sulphhydryl content on the surface of the MPs made with 40 mM DTT might be partly caused by the presence of some DTT, still in its reduced form, that had reacted with Ellman's reagent. The increase in sulphhydryl groups confirms the breakdown of disulphide bridges and suggests a decrease in the crosslink density.

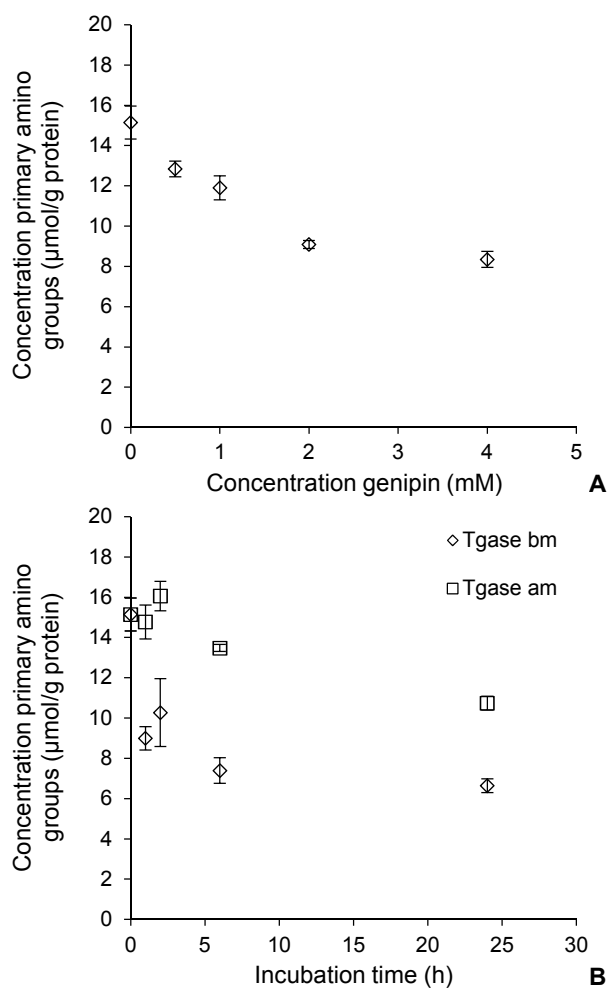


**Fig. 7.** The concentration of sulphhydryl groups ( $\mu\text{mol/g protein}$ ) present in the standard whey protein microparticles (MPs) (0 mM) and MPs incubated in solutions with various amounts of dithiothreitol (DTT). The bars show the standard deviation. The line guides the eye.

Genipin and transglutaminase (Tgase) were used to increase the crosslink density. Genipin is a crosslinker that has been used previously in combination with, for example, chitosan<sup>[26][184]</sup> and the proteins gelatin,<sup>[26][174]</sup> bovine serum albumin,<sup>[26]</sup>  $\beta$ -lactoglobulin,<sup>[121]</sup> and casein.<sup>[136]</sup> Crosslinking of proteins by genipin follows a two-step reaction with the primary amino groups of the proteins, resulting in a blue colour.<sup>[26]</sup> Tgase catalyses the

crosslinking of the amino acids glutamine and lysine. The ability of Tgase to react with whey proteins has already been shown in several studies.<sup>[8][146][176]</sup>

The OPA method was used to determine the number of primary amino groups present,<sup>[27]</sup> which was expected to decrease when genipin or Tgase reacted with the wet gel particles or the whey proteins in the whey protein isolate (WPI) dispersion. Fig. 8A and B show that the primary amino groups decreased with increased concentration (genipin) and incubation time (Tgase). Furthermore, the addition of Tgase after mixing resulted in MPs with the highest content of primary amino groups, whereas the MPs to which Tgase was added before mixing had the lowest content of primary amino groups—comparing the most extreme cases. This suggests that the crosslink density of MPs treated with Tgase before mixing was greater than that of MPs treated with genipin, which was, in turn, greater than that of MPs treated with Tgase after mixing.

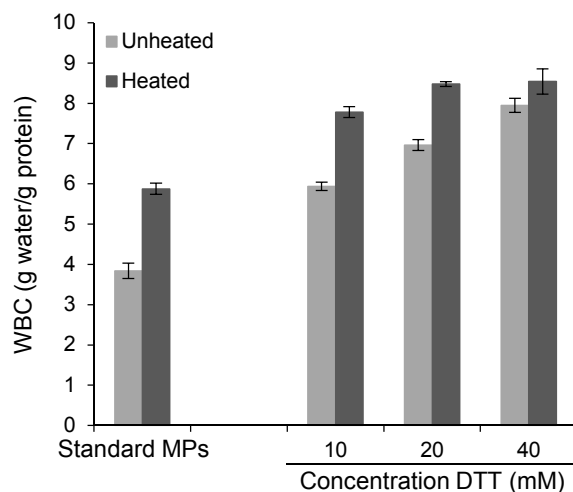


**Fig. 8.** The concentration of primary amino groups ( $\mu\text{mol/g protein}$ ) present in the standard whey protein microparticles (MPs) (0 mM or 0 h) and MPs incubated (A) in solutions with various concentrations of genipin or (B) for different times in a transglutaminase (Tgase) solution before mixing (bm) or after mixing (am). The bars show the standard deviation.

### 3.2 WATER-BINDING CAPACITY OF THE WHEY PROTEIN MICROPARTICLES

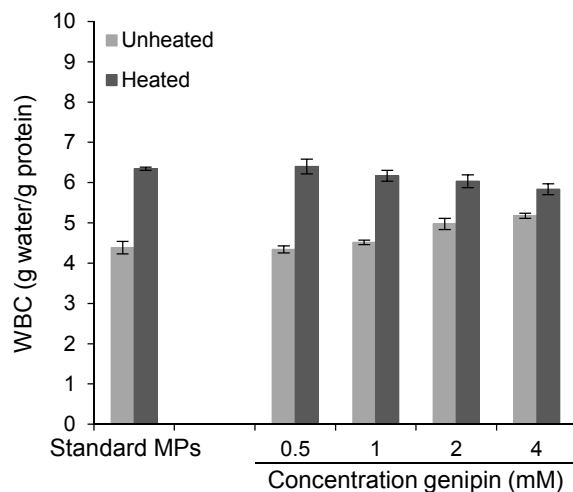
Fig. 9 shows that the treatment with DTT resulted in an increased water-binding capacity (WBC) for both the unheated and heated MPs. In addition, the WBC of the heated MPs was larger than the WBC of the unheated MPs, for all concentrations tested. This difference decreased with the addition of DTT.





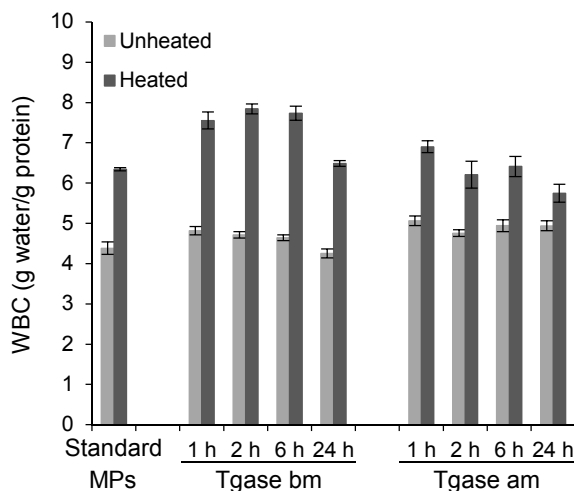
**Fig. 9.** The effect of incubating whey protein microparticles (MPs) after mixing in solutions with several concentrations of dithiothreitol (DTT) on the water-binding capacity (WBC) (g water/g protein) of unheated and heated MPs. The bars show the standard deviation.

The treatment with genipin resulted in an increase in the WBC of the unheated MPs (Fig. 10), which was unexpected. The WBC of the heated MPs decreased slightly when more genipin was used. Therefore, at concentrations of genipin higher than 0.5 mM, the effect of heating diminished with the crosslinking by genipin.



**Fig. 10.** The effect of incubating whey protein microparticles (MPs) after mixing in solutions with several concentrations of genipin on the water-binding capacity (WBC) (g water/g protein) of unheated and heated MPs. The bars show the standard deviation.

The addition of Tgase to the WPI dispersion before mixing resulted in a slight increase in the WBC of the unheated MPs after 1 h of incubation, and in a decrease of the WBC with longer incubation times (Fig. 11, before mixing). The WBC of the heated MPs increased initially as well, but decreased after 2 h of incubation.



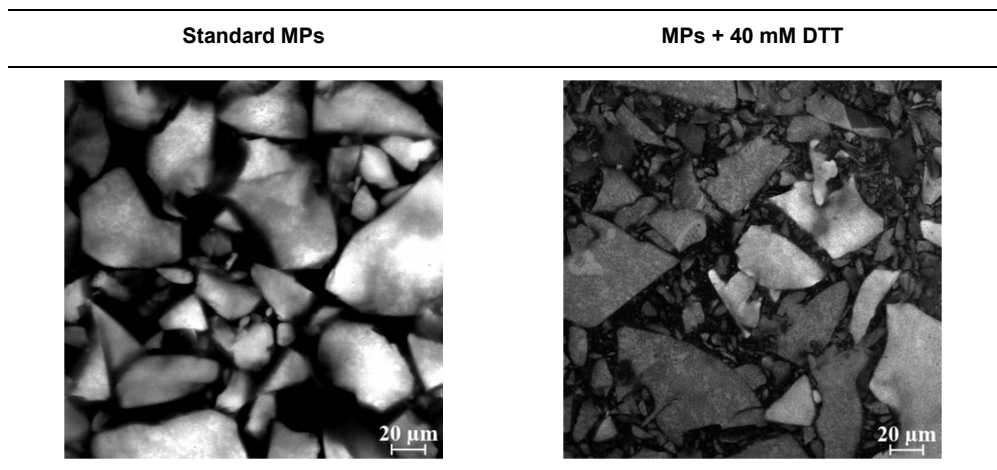
**Fig. 11.** The effect of incubating a whey protein isolate (WPI) solution before mixing (bm) and wet gel particles after mixing (am) in a transglutaminase (Tgase) solution for several incubation times on the water-binding capacity (WBC) (g water/g protein) of unheated and heated whey protein microparticles (MPs). The bars show the standard deviation.

Wet gel particles were incubated in a Tgase solution for different durations. This resulted in a slight increase in the WBC of the unheated MPs, which remained constant at all other incubation times tested (Fig. 11, after mixing). The WBC of the heated MPs, however, was increased after incubation for 1 h, and decreased again with longer incubation times. The WBC of heated MPs incubated for 24 h in a Tgase solution after mixing was even smaller than the WBC of the heated standard MPs.

### 3.3 MICROSCOPIC OBSERVATION OF THE PELLETS

The WBC values of the MPs were calculated, based on the amount of water bound by the pellet obtained after centrifugation. However, the pellet consists of the water inside the MPs and water between the MPs. The confocal laser scanning microscopy (CLSM) images show that the pellets of standard MPs and of the MPs treated with 40 mM DTT may contain a substantial amount of water between the MPs, visible as black space in Fig. 12. In addition, Fig. 12 shows that the pellets of MPs treated with DTT contained smaller particles,

probably due to breakage of larger particles. Those smaller particles were also present in the pellet of the standard MPs, although they are not visible here.



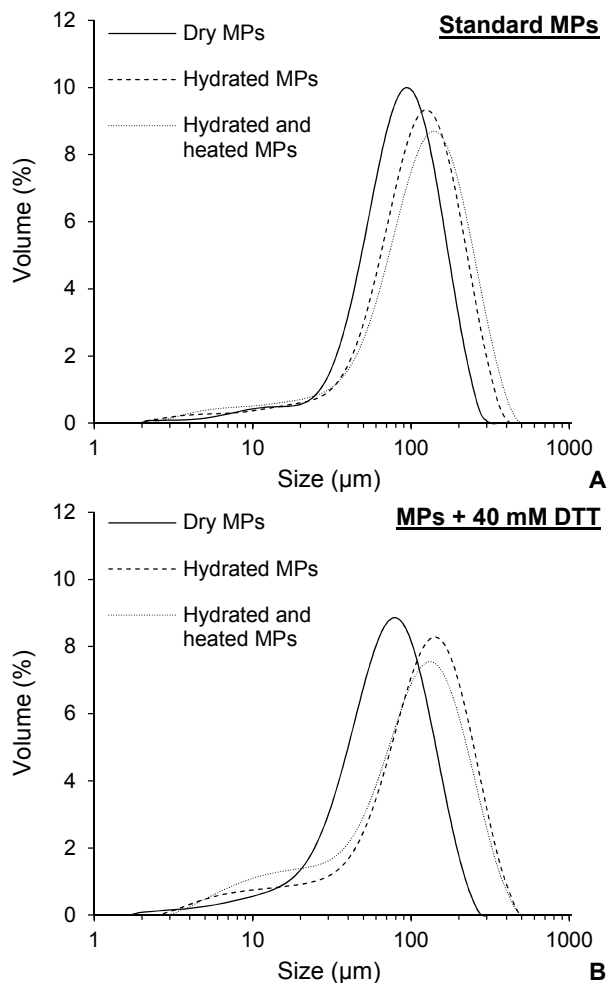
**Fig. 12.** The morphology of the pellets of standard whey protein microparticles (MPs) and MPs treated with 40 mM dithiothreitol (DTT) obtained after centrifugation during the water-binding capacity experiment.

### 3.4 SWELLING OF THE WHEY PROTEIN MICROPARTICLES

Light scattering was used to investigate the swelling of the MPs. The data should be interpreted with caution, because the MPs were assumed to be spherical to calculate the curves, which is not true; as can be seen in Fig. 12. Fig. 13 indicates that both the standard MPs and the MPs treated with 40 mM DTT swelled, when they were incubated in water for 3 h. Heating the MP suspensions caused slight further swelling in the standard MPs and the smaller sized ( $< 80 \mu\text{m}$ ) MPs treated with DTT.

The light scattering data can be used to estimate the swelling of the MPs and the importance of the water around the MPs, even though those values might not be completely quantitative given the non-spherical nature of the MPs. Table 2 shows the diameters of the hydrated, and the hydrated and heated MPs, when water-binding was caused by particle swelling only; as calculated from the average diameter ( $d_{4,3}$ ) of dry MPs and their WBC. These calculated values were higher than the values obtained from the light scattering data, which suggests that the swelling is less than expected from the WBC of the pellet; leading to the conclusion that a relevant amount of water was present between the MPs. The swelling of the unheated and heated MPs was also calculated from the average diameter obtained from their size distribution (Table 2). These values indicate that the treatment with DTT only had an effect on the swelling of the unheated MPs. Table 2 further shows the

ratio of water in the MPs and between the MPs, which indicates the importance of water present between the MPs.



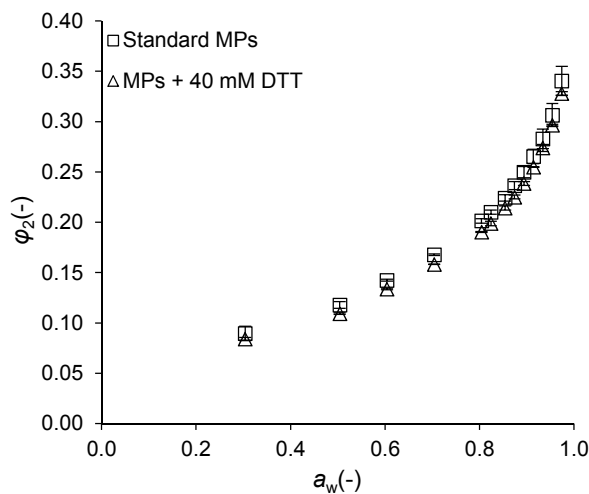
**Fig. 13.** The particle size distribution of dry whey protein microparticles (MPs), MPs hydrated for 3 h, and MPs hydrated for 3 h and heated of (A) standard MPs, (B) MPs treated with 40 mM dithiothreitol (DTT).

**Table 2.** The average diameter ( $d_{4,3}$ ) of the dry, hydrated, and hydrated and heated standard whey protein microparticles (MPs), and MPs treated with 40 mM dithiothreitol (DTT); the diameter when water-binding was caused by swelling of MPs only; the swelling of the MPs (g water/g particle); and the calculated ratio of water in the MPs to water between the MPs.

	Average diameter, $d_{4,3}$ ( $\mu\text{m}$ )			Calculated diameter of MPs when water was bound by swelling of MPs only ( $\mu\text{m}$ )		Swelling (g water/g particle)		Water in MPs : Water between MPs	
	Dry	Hydrated	Hydrated and heated	Hydrated	Hydrated and heated	Hydrated	Hydrated and heated	Hydrated	Hydrated and heated
Standard MPs	88 (5)	114 (7)	124 (6)	160	181	0.9	1.4	1.0 : 3.2	1.0 : 3.3
MPs + 40 mM DTT	73 (4)	122 (2)	111 (4)	161	166	2.8	1.9	1.0 : 1.7	1.0 : 3.3

### 3.5 SORPTION ISOTHERMS OF THE WHEY PROTEIN MICROPARTICLES

To see the effect of the crosslink density on the swelling behaviour of the MPs, water vapour sorption isotherms were constructed for the standard particles and the MPs treated with 40 mM DTT. From these isotherms (Fig. 14), it can be seen that they were nearly identical. This might indicate that the crosslink density was only decreased to a very small extent, and that the hydrophilicity did not change. Another possibility is that the effect of the crosslink density on the swelling was counteracted by a change in the hydrophilicity.



**Fig. 14.** The isotherms of standard whey protein microparticles (MPs) (squares) and MPs treated with 40 mM dithiothreitol (DTT) (triangles), where  $\phi_2$  is the volume fraction of water and  $a_w$  is the water-activity. The bars show the standard deviation.

## 4 DISCUSSION

Dithiothreitol (DTT), genipin and transglutaminase (Tgase) were used to alter the crosslink density in order to affect the water-binding capacity (WBC) of whey protein microparticles (MPs). The purpose of using those ingredients was to gain further understanding about the role of crosslinking on water-binding of MPs. For direct application in food products, DTT and probably genipin will have to be replaced by food-grade alternatives.

Genipin and Tgase were expected to increase the crosslink density. In both cases, the number of primary amino groups decreased (Fig. 8A and B). DTT was used to reduce the number of disulphide bridges in the MPs, so that the crosslink density of the MPs would decrease. Reducing the number of disulphide bridges is known to cause solubilisation of aggregated whey proteins.<sup>[134]</sup> Here, the solubility of MPs did increase; the remaining supernatant after incubation had a protein content of  $2.5 \pm 0.4\%$  (10 mM DTT),  $3.9 \pm 0.6\%$  (20 mM DTT) and  $6.3 \pm 0.5\%$  (40 mM DTT), which made the supernatants more opaque and viscous with increased addition of DTT. DTT also increased the concentration of sulphhydryl groups on the surface of the MPs (Fig. 7). It was expected that the number of sulphhydryl groups that was measured belonged not only to the proteins that formed the particle network, but also to the whey proteins that were detached from the network by DTT; remained around the MPs during drying; and solubilized during the measurement. The MPs treated with 40 mM DTT almost reached the maximum amount of sulphhydryl groups that can be present in whey protein isolate (WPI) when all disulphide bridges have been reduced; that is,  $248 \mu\text{mol/g}$  protein (according to the amino acid analysis done by the manufacturer).<sup>[36]</sup> Such a decrease in the amount of disulphide bridges could have led to solubilisation of the MPs, although MPs were still found in the pellet (Fig. 12). This outcome suggests the importance of non-covalent interactions present between the proteins in the MPs.

The treatment with DTT resulted in an increase in the WBC of both the unheated and heated MPs (Fig. 9). This increase in WBC was expected, and might be caused by a reduction in the elastic modulus of the MPs. A reduction in the elastic modulus should result in greater swelling as indicated by the Flory–Rehner model (Equations 1 and 3). It was found in earlier studies on MPs that heat can increase the swelling or WBC of MPs even further without aggregation of the MPs.<sup>[115][116][128][129]</sup> The increase in WBC in the heated MPs might be caused by the formation of a slightly more open network, with more space for water, due to heat-enhanced rearrangements of the non-covalent and covalent bonds.

Genipin and Tgase increased the crosslink density, although this did not result in a clear decrease in the WBC of the MPs (Fig. 10 and Fig. 11). Increasing the crosslink density after the formation of wet gel particles had barely any effect on the WBC of the unheated MPs made with Tgase; it even resulted in a slight increase in the WBC of the unheated MPs treated with genipin. The WBC of the heated MPs, however, decreased

in both cases with concentration (genipin) or incubation time (Tgase). This slight effect might be caused by a limited diffusion of genipin and Tgase into the MPs. Both crosslinking agents are relatively large molecules<sup>[121][182]</sup> and might have diffused slowly into the MPs. In addition, new crosslinks on the outside of the particles might have hindered further diffusion of the chemicals, as a result of which the bulk of the MPs remained unchanged.

The addition of Tgase before mixing resulted in the largest decrease in primary amino groups. However, the WBC of the unheated MPs was barely affected, whereas the WBC of the heated MPs was increased, compared with the standard MPs (except after incubation for 24 h). During crosslinking before mixing, relatively more intramolecular crosslinks may have been created; during crosslinking after mixing, more intermolecular crosslinks may have been formed. The formation of intramolecular crosslinks might have resulted in a slightly weaker network that could swell more, because the proteins could no longer unfold and link to each other so much.<sup>[146][174][176]</sup> We therefore conclude that not only the amount of crosslinks is important but also the position of the crosslinks.

Regarding the effect of the crosslink density on the swelling of the MPs, the Flory–Rehner model states that a change in the crosslink density has almost no effect on swelling at low crosslink densities, but a more pronounced effect at high crosslink densities. We expect that the crosslink density of the MPs is relatively high, because whey proteins are small polymers, compared with most of the synthetic polymers used to develop the Flory–Rehner model. The main proteins in WPI have a molecular weight of 18 kDa ( $\beta$ -lactoglobulin)<sup>[169]</sup> and 14 kDa ( $\alpha$ -lactalbumin)<sup>[169]</sup> and consist of 162 amino acids ( $\beta$ -lactoglobulin)<sup>[2][142]</sup> or 123 amino acids ( $\alpha$ -lactalbumin).<sup>[142]</sup> Synthetic polymers frequently have a molecular weight of 100 kDa or more. Thus, per kilogram of protein, many crosslinks have to be formed to incorporate all proteins in the MPs. Therefore, a small change in the crosslink density of the MPs should result in a noticeable change in swelling. However, a change in crosslink density had only a minor effect on the WBC of the MPs, except when DTT was used. Rough calculations on the sizes of the standard MPs and MPs treated with 40 mM DTT after swelling showed that, even with DTT, the MPs were not always clearly more swollen (Table 2). Besides, the sorption isotherm of the MPs with DTT was barely changed, compared with that of the standard MPs (Fig. 14), which implies that the effective crosslink density was not changed remarkably. These results suggest that the decrease and increase in crosslink density for all MPs was relatively small, compared with the total amount of non-covalent and covalent interactions present in the MPs. In addition, it might be that disulphide bridges are just a minor type of crosslinks present in whey gels, as previously suggested for whey protein concentrate gels.<sup>[66]</sup>

As a consequence, the increase in the WBC of the pellet of MPs treated with DTT could not only be ascribed to an increase in swelling of the MPs. Fig. 12 shows that, within the pellet, water was present between the MPs, and a rough calculation showed the



importance of this fraction (Table 2). It is not completely clear why the amount of water between the particles was so high and why it could not be removed by increasing the centrifugation speed (a speed of 12,000 rpm barely decreased the value of the WBC). A possible explanation could be that the water between the MPs contained either small protein particles—which were not visible by confocal laser scanning microscope and light scattering—or dissolved proteins. Those small or dissolved proteins might have enhanced water-binding by binding the water themselves, and it is also possible that they introduced extra repulsive interactions, creating more space for water. Overall, it can be concluded that the WBC, measured using the centrifugation method, might not always be representative of the WBC of MPs. Complete understanding of the WBC of MPs requires further investigation.

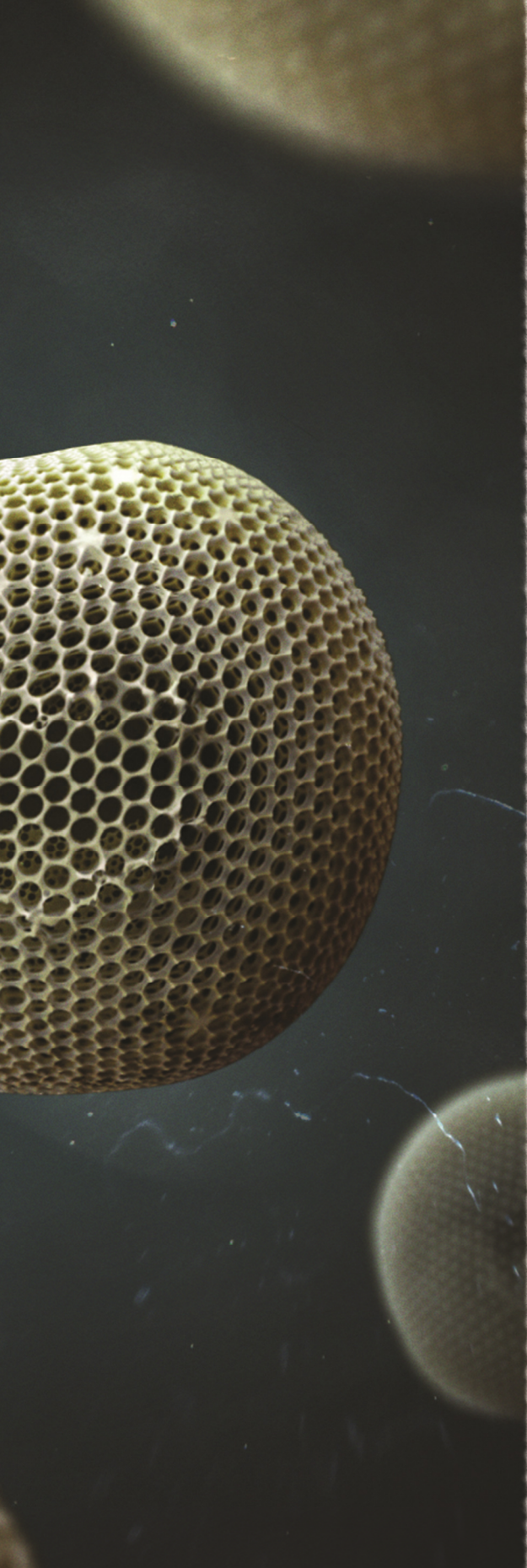
## 5 CONCLUSIONS

This study shows the effect of the crosslink density on the water-binding capacity (WBC) of whey protein microparticles (MPs). The crosslink density of MPs was altered with dithiothreitol (DTT), transglutaminase and genipin. Only the incubation of MPs in DTT led to a significant change in the WBC of MPs, which increased up to 9 g water/g protein. Further analysis showed, however, that these MPs were not always noticeably more swollen. It may be that the swelling of MPs was not influenced significantly by changing the crosslink density, because the changes in crosslink density were relatively small, compared with the total amount of interactions present in MPs. Because the WBC of the pellet could not be attributed to the WBC of the MPs only, it has to be concluded that water between the MPs also played an important role during the formation of the pellets.

## ACKNOWLEDGEMENTS

The authors would like to thank FrieslandCampina and NanoNextNL, a consortium of the Netherlands government and 130 partners, for financial support of this research.





### *Chapter 3*

**TIME DOMAIN NUCLEAR  
MAGNETIC RESONANCE  
AS A METHOD TO DETERMINE  
AND CHARACTERISE THE  
WATER-BINDING CAPACITY  
OF WHEY PROTEIN  
MICROPARTICLES**

## ABSTRACT

Water-binding capacity (WBC) is commonly measured with a centrifugation method, in which a sample is hydrated in excess water, and the pellet weight after centrifugation defines the WBC. When a dispersion is being analysed—here containing whey protein microparticles (MPs)—the pellet consists of swollen particles and water between the particles. These two water domains in MP pellets were distinguished using time domain nuclear magnetic resonance (TD NMR). This distinction showed that an increase in WBC from 2 to 5.5 g water/g dry matter was mainly due to an increase in water between the MPs. Besides, it was found that TD NMR-measurements could be used to provide accurate values of the amount of water in both water domains in MP pellets. This makes TD NMR therefore a more accurate method to determine the WBC of the whole pellet than weighing the pellet after centrifugation.

### THIS CHAPTER IS PUBLISHED AS:

Peters, J. P. C. M., Vergeldt, F. J., Van As, H., Luyten, H., Boom, R. M., van der Goot, A. J. (2016). Time domain nuclear magnetic resonance as a method to determine and characterize the water-binding capacity of whey protein microparticles. *Food hydrocolloids 54 Part A*, 170–178.

# 1 INTRODUCTION

An important functional property of proteins is their ability to bind water. Unfortunately, this property is not well defined; various definitions and terms are used in the literature.<sup>[52][84][185]</sup> Here, we use the term water-binding capacity (WBC) to describe *the ability of a protein sample, present in excess water, to bind water when subjected to an external force*. Several methods can be used to determine the WBC of a protein sample, but commonly a centrifugation method is used in which the obtained pellet weight determines the WBC. In this method, the protein sample is first placed in excess water to hydrate, and then surplus water is separated from the proteins by centrifugation. The WBC is then calculated using the following equation:

$$\text{WBC (g water/g dry matter)} = \frac{(M_{\text{wet\_pellet}} - M_{\text{dry\_matter}})}{M_{\text{dry\_matter}}} \quad (5)$$

where  $M_{\text{wet\_pellet}}$  is the pellet weight after centrifugation and  $M_{\text{dry\_matter}}$  is the weight of the dry matter of the particles.

In this study, water-binding of whey protein microparticles (MPs) is investigated to better understand the contribution of swelling of MPs and the water between MPs on the WBC. Previous research with MPs (**Chapter 2**) suggested that the amount of water bound by the pellet is not necessarily a measure of the amount of water bound by the MPs, because a certain amount of water is bound between the MPs. Therefore, more insight is required into the ratio of water inside and between MPs. Because the pellet weight obtained after centrifugation is used for other dispersions as well to determine the WBC,<sup>[1][15][76][143][183]</sup> the results of this study will have broader applicability and consequences.

Time domain nuclear magnetic resonance (TD NMR) or relaxometry seemed to be a promising method to gain a better understanding of WBC for MP pellets.<sup>[60][69][70][96][158]</sup> TD NMR is a non-destructive method and is used to determine, inter alia, the transverse relaxation time ( $T_2$ ) of water via the transverse relaxation of  $^1\text{H}$  protons.<sup>[96]</sup>  $T_2$  and the transverse relaxation rate  $R_2$  ( $R_2 = 1/T_2$ ) of every water fraction provide insight into the degree of exchange of either water protons with protein protons; or the exchange of water between water fractions, such as bulk water with the immobile water fraction around the proteins.<sup>[91]</sup> Since several mechanisms, such as diffusive and chemical exchange, and cross-relaxation, affect the  $T_2$  at the same time, a direct interpretation of the TD NMR results is difficult.<sup>[91]</sup> However, these mechanisms also cause the  $T_2$  of water in a protein sample to be related to the local protein and water concentrations, and the nano- and microstructure (e.g., pores and capillaries) of the protein network.<sup>[91][104][105]</sup> Because both

the protein concentration and the protein network structure are different inside and between the MPs in a pellet (**Chapter 2**), we hypothesize that TD NMR can be used to distinguish between these two water domains.

Several studies on meat<sup>[17][18][21][141]</sup> investigated the applicability of TD NMR to measure and gain insight into the WBC and WHC (i.e., the ability of meat to hold water under gravitational force). A good correlation was found between  $T_2$  of the water fraction assigned to the weakest bound water in meat and its WBC or WHC. In addition, the amplitude of this water fraction had a good correlation with the WBC or WHC. Therefore, it was concluded that TD NMR is a suitable method to gain insight into the WBC and WHC of meat. In addition to meat, TD NMR was found to be useful to examine the WHC of fresh cheeses,<sup>[69]</sup> carrageenan gels and solutions, whey gels, and yogurt.<sup>[70]</sup> Although, to our knowledge, pellets obtained with the frequently used method of centrifuging protein dispersions to measure the WBC of those proteins have not been investigated yet.

In this study, several modified MPs with different WBCs were made. The WBC of these MPs was determined through centrifugation of a dispersion of MPs and determining the pellet weight. The MPs and the pellet formed after centrifugation were further characterised with light scattering and TD NMR. These results were related to the WBC of the pellets to better understand the relationship between the swelling capacity of the MPs, the amount of water between the MPs, and the WBC of the pellets of MPs. In addition, a method is shown how TD NMR can be used to determine the WBC of MP pellets.

## 2 MATERIALS AND METHODS

### 2.1 MATERIALS

Whey protein isolate (WPI; BiPRO, lot no. JE 034-7-440, Davisco Food International Inc., Le Sueur, MN) was used to produce whey protein microparticles (MPs), gels, and solutions. WPI has a reported protein content of 97.7% on a dry basis. The water-binding capacity (WBC) of the MPs was changed by treatment with dithiothreitol (DTT), *N*-ethylmaleimide (NEM), genipin (all from Sigma–Aldrich, Germany), HCl, or microbial  $\text{Ca}^{2+}$ -independent transglutaminase (Tgase; Activa WM; activity of 81–135 units  $\text{g}^{-1}$  according to the manufacturer) derived from *Streptovercillium mobaraense* (Barentz Raw Materials, the Netherlands). Isopropanol Emplura (Merck, Germany) was used as a carrier fluid in static light scattering measurements. Potassium acetate ( $\text{CH}_3\text{CO}_2\text{K}$ ), potassium carbonate ( $\text{K}_2\text{CO}_3$ ), and potassium sulphate ( $\text{K}_2\text{SO}_4$ ) (synthesis grade; Sigma–Aldrich, Germany) were used to make saturated salt solutions. Milli-Q water was used (resistivity of 18.2  $\text{M}\Omega\text{ cm}$  at 25 °C, total oxidisable carbon <10 ppb; Merck Millipore, France) in all experiments, unless stated otherwise.

### 2.2 METHODS

#### 2.2.1 FORMATION OF STANDARD WHEY PROTEIN MICROPARTICLES

Standard MPs were made as described in **Chapter 2**. WPI was dissolved in water to obtain a 40% w/w solution. This solution was mixed using an overhead mixer at 100 rpm and room temperature for at least 2 h, and then mixed further with a magnetic stirrer at 4 °C overnight. The solution was centrifuged at 1000 rpm and 20 °C for 10 min. After removing the foam layer manually, the solution was mixed in a bowl mixer (type W50) connected to a Brabender Do-corder E330 (Brabender OHG, Duisburg, Germany). The mixer was heated with water at 95 °C using a water bath. The mixer settings were as follows: 5 min at 0 rpm, 5 min at 5 rpm, and 40 min at 200 rpm. After mixing, the mixer was cooled with water from a 4 °C water bath for approximately 5 min. The wet gel particles were taken out of the mixer and placed in an oven at 50 °C for 2 days. The dried gels were milled with an ultracentrifuge mill (Retsch ZM 1000) equipped with a 24-tooth stainless steel rotor. An 80- $\mu\text{m}$  sieve was attached to the rotor, which operated at 15,000 rpm for 120 s. The particles obtained after milling were the standard MPs.



### 2.2.2 FORMATION OF WHEY PROTEIN MICROPARTICLES WITH ALTERED WATER-BINDING CAPACITIES

MPs with an altered WBC were made by adapting the standard procedure (Section 2.2.1). MPs treated with DTT, a combination of DTT and NEM, or genipin were made by adding 25 g of wet gel particles to a 50-mL solution containing the chemicals. Concentrations of 10, 20, or 40 mM DTT were used with or without 15 mM NEM, or 0.5, 1, 2, or 4 mM of genipin. The dispersions were incubated and mixed at 20 °C for 24 h. Part of the wet gel particles with DTT were washed after incubation by placing the particles under running tap water for 3 min, followed by a washing step using approximately 1 L of Milli-Q water. All wet gel particles incubated in DTT and NEM were washed in the same way. After those treatments, the wet gel particles were oven dried and milled as described above (Section 2.2.1).

MPs treated with Tgase were made as follows. A 20% w/w Tgase solution was prepared and placed in a fridge at 4 °C for 1 week. Before use, the Tgase solution was mixed for 10 min and filtered over a 0.45- $\mu$ m filter. Tgase was added either to the WPI solution used to make the MPs or to the wet gel particles. In both cases, an enzyme to protein ratio of 1:5 was used. When added to the WPI solution, the Tgase solution was first incubated at 50 °C for 10 min and then mixed with the WPI solution. Subsequently, the solution was incubated at 50 °C for 1, 2, 6, or 24 h. After incubation, the protein samples were heated and mixed in a bowl mixer, oven dried, and milled as described for the standard MPs (Section 2.2.1). To obtain MPs incubated in a Tgase solution after mixing, 25 g of wet gel particles was added to 50 mL of Tgase solution (preheated for 10 min at 50 °C). This dispersion was further mixed at 50 °C for 1, 2, 6, or 24 h, and then oven dried and milled as described in Section 2.2.1.

The pH of the WPI solution was lowered before mixing with 1 M HCl, to obtain MPs made at pH 5.8. The WPI solution was then heated and mixed, oven dried, and milled as described above for the standard MPs (Section 2.2.1).

### 2.2.3 FORMATION OF WHEY PROTEIN MACRO GELS

WPI macro gels and heated WPI solutions (Section 2.2.4) were made using similar conditions to those of the MPs as much as possible. The macro gels were regarded as a model material for the MPs (i.e., the gel was considered as a large MP), because MPs were obtained by drying small gel particles. Drying and rehydrating the macro gels would have mimicked the MPs even better, though then we would not have a large homogenous sample. The macro gels were used to create a calibration curve that related the dry matter content to the transverse relaxation rate  $R_2$ , so the dry matter content present in each water fraction of the MP pellet could be estimated. To obtain WPI macro gels, solutions of various WPI concentrations were made as described in Section 2.2.1. Then, the solutions were centrifuged to remove air bubbles and carefully transferred to Teflon tubes

(diameter 20 mm, length 100 mm). The tubes were heated at 95 °C for 50 min, after which they were cooled with running tap water for 5 min. The gels obtained were wrapped in plastic foil and placed in the fridge prior to analysis, which was done within 24 h.

WPI macro gels were also made at pH 5.8 and some of the gels were incubated in a DTT solution. The same procedure was used as for the standard WPI macro gels, with some small modifications. To obtain gels made at pH 5.8, the pH of the solutions was lowered with 1 M HCl before heating. Gels that had reacted with DTT were made by cutting the gels into pieces of 20 mm in diameter and weighing approximately 2 g. The gels were placed in 25 mL of a 40 mM DTT solution and incubated at 20 °C for 24 h.

#### 2.2.4 FORMATION OF UNHEATED AND HEATED WHEY PROTEIN SOLUTIONS

A 10% w/w solution of WPI was made by dissolving WPI in water and mixing the solution at room temperature for 1 h. This solution was then diluted with water to obtain unheated WPI solutions at various concentrations, which were analysed further. Heated whey protein solutions were made from the unheated WPI solutions, by keeping the unheated solutions at 4 °C overnight, and heating them in a water bath at 95 °C for 50 min the next day. Subsequently, the samples were cooled using running tap water for 5 min, and analysed when they were at room temperature.

Heated WPI solutions at pH 5.8 were made using a 10% w/w solution, prepared as described in Section 2.2.1. The pH of the solution was brought to pH 5.8 with 1 M HCl, after which the solution was further diluted with water to obtain WPI solutions at various concentrations, and centrifuged to remove the air bubbles. After dilution, the pH of the solutions was still 5.8. The solutions were heated at 95 °C for 50 min, cooled under running tap water for 5 min, and placed in the fridge until they were analysed within 24 h.

#### 2.2.5 THE WATER-BINDING CAPACITY OF WHEY PROTEIN MICROPARTICLES

The WBC of MPs was determined by preparing 10% w/w dispersions of the MPs. These dispersions were mixed with a vortex until the MPs were hydrated and then mixed with a rotator at a speed of 16 rpm at 25 °C for 3 h. Every 15 min, the dispersions were mixed with a vortex again. After hydration, the dispersions were centrifuged at 3000 rpm and 25 °C for 20 min to obtain a pellet and supernatant. The supernatant was decanted from the pellet; the weight of the pellet was determined and the WBC of the pellets was calculated using Equation 5. The average dry matter content of the MPs (95%) was used to calculate the dry matter weight of the MPs.

In addition, the MPs were reheated to create pellets with altered WBCs by reheating the dispersions after hydration at 90 °C for 30 min. Subsequently, the dispersions were cooled in ice water for 10 min and equilibrated at room temperature for an additional 10 min. Then, the dispersions were centrifuged as described for the unheated MP pellets.

The WBC of the pellets used for the calculations on swelling (Section 2.2.7) was measured in triplicate. The WBC of the pellets used for TD NMR analysis (Section 2.2.8.1) was measured once because the results were shown to be reproducible.

### 2.2.6 BINDING OF WATER WITHIN THE WHEY MICROPARTICLES

MPs were placed in desiccators for equilibration at various relative humidities (RHs). Saturated salt solutions were made from  $\text{CH}_3\text{CO}_2\text{K}$ ,  $\text{K}_2\text{CO}_3$ , and  $\text{K}_2\text{SO}_4$ . Approximately 0.2 g of MPs were spread over a plate and placed in the desiccator. The desiccator was set under a vacuum and the samples were kept there for 12 days before they were analysed. The water-activity ( $a_w$ ) of the samples in the desiccator with a  $\text{CH}_3\text{CO}_2\text{K}$  saturated salt solution was 0.25 (25 °C), 0.46 (25 °C) in a  $\text{K}_2\text{CO}_3$  saturated salt solution, and 0.95 (25 °C) in a  $\text{K}_2\text{SO}_4$  saturated salt solution. This was measured with an Aqualab 4 TE water-activity meter (Decagon Devices Inc., Pullman, WA).

### 2.2.7 SWELLING EXPERIMENTS

The swelling of MPs in water was determined for hydrated MPs, and hydrated and reheated MPs, prepared as described in Section 2.2.5. After hydration, or hydration and reheating, the size of the MPs was determined with static light scattering (Mastersizer 2000, Malvern Instruments). Also the size of the unhydrated MPs (i.e., MPs obtained after oven drying and milling and referred to as dry MPs) was determined. Therefore, a 10% w/w dispersion was made with isopropanol, a solvent in which the MPs do not swell. During the measurements, water was used as a carrier fluid for the hydrated MPs and isopropanol for the dry MPs. The rotation speed of the vessel of the carrier fluid was set at 1200 rpm. Refractive indices of 1.545 (MPs), 1.33 (water), and 1.39 (isopropanol) and an absorption of 0.001 (MPs) were used for the calculations.<sup>[164]</sup> The measurements were done for three dispersions per type of MP; the size distribution was measured in quintuplicate. The size of the dry MPs was measured in triplicate. From the measurements, the average particle diameter  $d_{4,3}$  (volume mean diameter) was calculated assuming that the MPs were spherical. The average diameter ( $d_{4,3}$ ) was used to calculate the average volume of the dry MPs and the volume increase when hydrated, or hydrated and reheated. The amount of water inside and between the MPs was calculated from the WBC of the pellets, assuming that the proteins did not dissolve, that the density of dry MPs<sup>[119]</sup> was  $1.3 \text{ g cm}^{-3}$ , and that the density of water was  $1 \text{ g cm}^{-3}$ .

### 2.2.8 <sup>1</sup>H RELAXOMETRY

<sup>1</sup>H relaxometry was performed with a Maran Ultra NMR spectrometer (at 30.7 MHz proton resonance frequency; Resonance Instruments Ltd., Witney, United Kingdom).  $T_2$ -relaxation decay curves were recorded by means of a standard Carr–Purcell–Meiboom–Gill (CPMG) pulse sequence. The CPMG decay train consisted of 16,384 echoes with an echo time of 1 ms. Experiments were averaged over 16 scans with a repetition time of 30 s.

$T_2$ -spectra of relative intensity as a function of  $T_2$  were determined by numerical inverse Laplace transformation of the data, as implemented in CONTIN.<sup>[113]</sup> The regularization parameter in CONTIN was set to the same, rather conservative, value for all spectra, to facilitate comparison of the results. This is justified by the fact that the signal-to-noise ratio was comparable for all measurements.  $T_2$ -spectra were subsequently analysed by determining peak positions (the top of the peaks was used to determine the  $T_2$ -values of the various water fractions in the samples) and areas to determine the relative area using IDL (ITT Visual Information Solution, Boulder, CO).

For decays with a clear mono-exponential character, the Levenberg–Marquardt non-linear least squares algorithm, implemented in SPLMOD,<sup>[114]</sup> was used to analyse the data. These decays were measured to obtain  $T_2$ -values for calibration purposes. The rationale for using SPLMOD instead of CONTIN in those cases is that SPLMOD fits both the amplitude and  $T_2$ -relaxation time of a discrete sum of exponentials. CONTIN, on the other hand, determines amplitudes given a distribution of fixed  $T_2$ -values. In the latter, an extra unnecessary step is needed to obtain average  $T_2$ -values.

Every sample was measured once because extra experiments performed on a number of samples showed good reproducibility. This allowed us to measure a broader range of samples.

#### 2.2.8.1 <sup>1</sup>H RELAXOMETRY OF WHEY PROTEIN MICROPARTICLE PELLETS

Pellets were made as described in Section 2.2.5. After decanting the supernatant from the pellet, the bottoms of the Eppendorf tubes were cut off so the samples were disturbed as little as possible before analysis (scooping the pellet from the tube affected the results). The tips of the tubes were used for further analysis. The resulting transverse decay curves were all multi-exponential and analysed with CONTIN.

To estimate the absolute amount of water present inside and between the MPs, the amount of water present, according to the WBC of the pellets, was divided over those two fractions according to the ratio of these areas in the CONTIN  $T_2$ -spectra. Using the  $T_2$ -values for the top of the two fractions, the dry matter content inside and between all the various MP pellets was calculated from the standard calibration curves (Appendix A-Fig. S1A). The calibration curve, obtained for solutions and gels made at

pH 5.8 (**Appendix A-Fig. S1A**), was used only for the MPs made at pH 5.8. From the amount of dry matter that was present between the MPs, the percentage of dry matter dissolved from the MPs was calculated. Although, if the mass balance was used, the solubility would be lower or larger than calculated via the WBC,  $T_2$ -values and the calibration curves. The relative area under the peaks was determined by dividing either the area of the peak attributed to water inside the MPs, or between the MPs, over the sum of the total area.

#### **2.2.8.2 $^1\text{H}$ RELAXOMETRY OF SUPERNATANTS**

The spectra of the supernatant of standard MPs, unwashed MPs incubated in 40 mM DTT, and MPs made at pH 5.8, were obtained by making pellets and supernatants first, as described in Section 2.2.5. After decanting the supernatant from the pellet, 125  $\mu\text{L}$  was added to the NMR tube and analysed. The resulting transverse decay curves were assumed to be mono-exponential and analysed with SPLMOD.

The SPLMOD results for the supernatants were used to calculate the dry matter content of the supernatants. For that, only the solution part of the calibration curve was used (**Appendix A-Fig. S1B**). For the supernatant of the standard MPs and the unwashed MPs incubated in 40 mM DTT, the calibration curve of the standard solutions was used; for the MPs made at pH 5.8, the curve for the solutions made at pH 5.8 was used.

#### **2.2.8.3 $^1\text{H}$ RELAXOMETRY OF MACRO GELS**

After the formation of the macro gels, as described in Section 2.2.3, the gels were cut with a biopsy punch into small cylinders and analysed. The curves obtained were all assumed to be mono-exponential and analysed with SPLMOD.

#### **2.2.8.4 $^1\text{H}$ RELAXOMETRY OF UNHEATED AND HEATED WHEY PROTEIN ISOLATE SOLUTIONS**

Unheated and heated WPI solutions, which were made according to Section 2.2.4, were analysed using TD NMR by pipetting 125  $\mu\text{L}$  of the solution into the NMR tubes. The resulting curves were analysed with SPLMOD because of the mono-exponential character of the decay curves.

#### **2.2.8.5 $^1\text{H}$ RELAXOMETRY OF WHEY PROTEIN MICROPARTICLES HYDRATED IN DESICCATORS**

After hydration of the MPs in the desiccators (Section 2.2.6), the hydrated MPs were placed in an NMR tube and analysed. The curves obtained were assumed to be mono-exponential and analysed with SPLMOD.

### **2.2.9 DRY MATTER CONTENT**

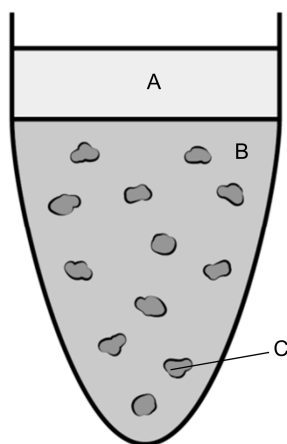
The dry matter content of the gels, solutions, and MPs was determined by drying the samples in an oven at 105 °C for 24 h.

### 3 RESULTS AND DISCUSSION

The following sections describe the steps that were taken to gain insight into the water-binding capacity (WBC) of whey protein microparticles (MPs). First, the WBC of the MPs was determined, and then the value was compared to the swelling of the MPs as calculated from the light scattering data. Subsequently, the pellets were analysed with time domain nuclear magnetic resonance (TD NMR). To be able to further interpret these TD NMR results, swollen MPs were mimicked by MPs subjected to certain relative humidities (RHs) and whey protein gels, and also analysed with TD NMR. In addition, the dry matter and water concentrations in both water fractions were calculated and compared with the light scattering results. Finally, the water fractions obtained were assigned to the two water domains in the MP pellets (water inside and between the MPs), and the contribution of both water domains to the WBC of the pellet was investigated.

#### 3.1 ANALYSIS OF THE SWELLING OF WHEY PROTEIN MICROPARTICLES IN A PELLET WITH LIGHT SCATTERING

To determine the WBC of MPs, the MPs were hydrated in excess water, after which the dispersions were centrifuged to obtain a pellet and supernatant (Fig. 15). The pellet, containing swollen MPs and water between the MPs, was weighed to determine the WBC, assuming that the amount of water between the MPs was negligible as an initial hypothesis. However, the importance of water between the MPs is investigated in this study. That is why the term WBC-P (WBC of the pellet) is introduced to distinguish the WBC of the MPs themselves (WBC-MPs) from the WBC of the pellet that includes water between the MPs as well.



**Fig. 15.** The various water domains formed after centrifuging whey protein microparticles (MPs) that were hydrated in an excess amount of water: (A) supernatant, (B) water between the MPs, and (C) water inside the MPs.

The WBC-P of the unwashed MPs treated with 40 mM DTT and the MPs made at pH 5.8 differed most from the WBC-P of standard MPs from all tested MPs. Therefore, those three types of MPs were analysed in more detail. The unwashed MPs treated with 40 mM DTT had a much larger WBC-P than the standard MPs, whereas MPs made at pH 5.8 had a much lower WBC-P (Table 3). However, it is not clear whether this WBC-P can be translated to the WBC-MPs directly or that the water between the MPs contributed to the WBC-P as well. A first route to estimate the relative importance of water inside and between the MPs is to consider the swelling of the MPs. Calculations based on the average particle diameter  $d_{4,3}$  (volume mean diameter) of these MPs (see Section 2.2.7) suggested that the unheated MPs treated with DTT contained more water than the standard MPs, whereas both the unheated and reheated MPs made at pH 5.8 contained less water than the standard MPs (Table 3). Although these results are merely indicative (among other reasons, because the particles were not spherical (**Chapter 2**)), they strongly suggest that swelling of the MPs only cannot explain the WBC-P. In all cases, the water content inside the swollen MPs was significantly lower than the total amount of water present in the pellets (WBC-P). This implies that a certain amount of water was present between the MPs since the pellet consists of water inside and between the MPs. The WBC-MPs is therefore most probably lower than the WBC-P.



**Table 3.** The water-binding capacity (WBC) of the unheated and reheated pellets (g water/g dry matter) of standard (ST) whey protein microparticles (MPs), unwashed MPs treated with 40 mM dithiothreitol (DTT MPs) and MPs made at pH 5.8 (pH MPs), the average size of the dry, hydrated, and hydrated and reheated MPs ( $\mu\text{m}$ ) ( $d_{4,3}$ ), and the calculated water content (g water/g dry matter) and dry matter content (%) inside the unheated and reheated swollen MPs.

	WBC pellets (g water/g dry matter)		Average size MPs ( $d_{4,3}$ ) ( $\mu\text{m}$ )			Calculated water content inside swollen MPs (g water/g dry matter)		Calculated dry matter content of swollen MPs (%)	
	Unheated	Reheated	Dry	Hydrated	Hydrated and reheated	Unheated	Reheated	Unheated	Reheated
ST MPs	3.7 (0.2)	5.4 (0.1)	79 (2)	110 (2)	127 (2)	1.3	2.4	43	29
DTT MPs	6.9 (0.2)	7.9 (0.0)	78 (2)	120 (3)	114 (3)	2.0	1.6	33	38
pH MPs	2.1 (0.2)	2.4 (0.1)	74 (3)	99 (4)	98 (2)	1.1	1.0	48	50

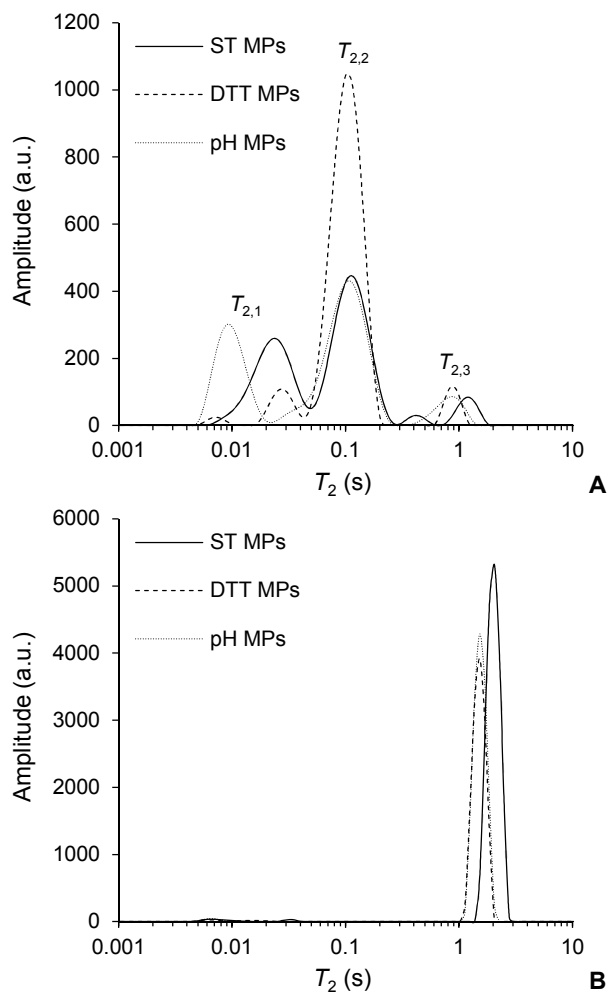
The standard deviations are given in parentheses.

### 3.2 ANALYSIS OF PELLETS OF WHEY PROTEIN MICROPARTICLES WITH TIME DOMAIN NUCLEAR MAGNETIC RESONANCE

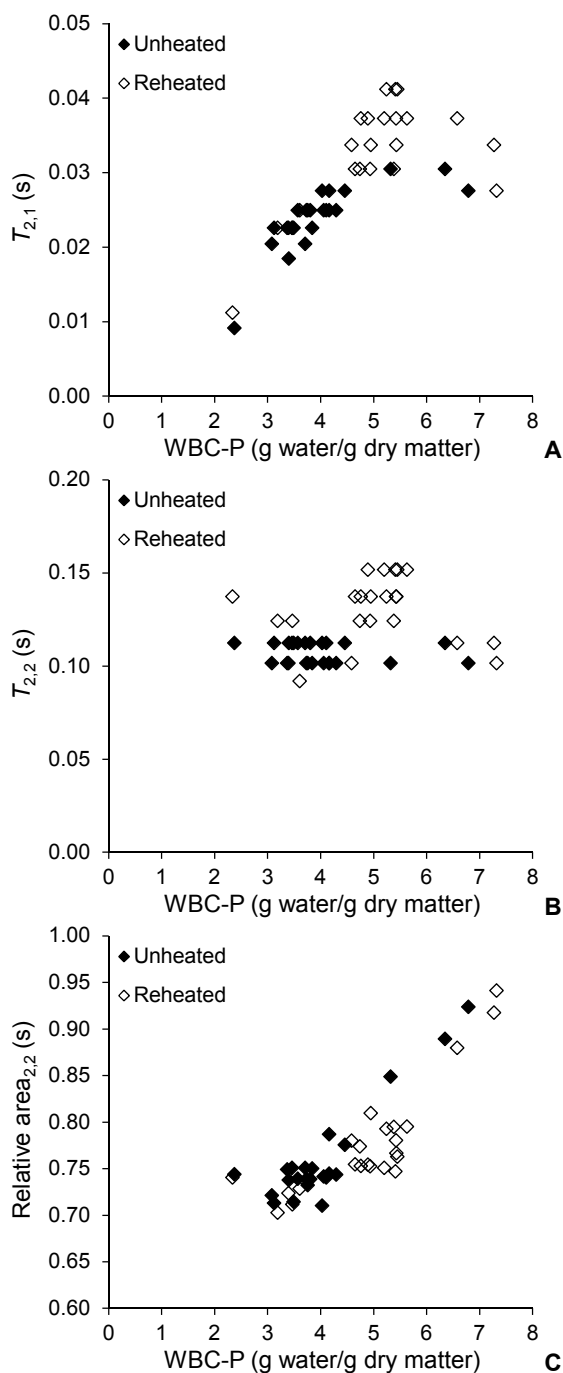
Time domain nuclear magnetic resonance (TD NMR) was used to further analyse the water distribution in the pellets. CONTIN transverse relaxation time ( $T_2$ )-spectra for the pellets of standard MPs, unwashed MPs treated with 40 mM DTT, and MPs made at pH 5.8 showed two main peaks and one small peak around  $T_2 = 1$  s (Fig. 16A), indicating the presence of three different water fractions. The fraction with the largest transverse relaxation time ( $T_{2,3}$ ) was assigned to expelled water that was present after cutting the tube with the pellet. This assignment was done based on the fact that the supernatant obtained after centrifugation (domain A in Fig. 15) also showed a  $T_2$ -fraction around 1 s (Fig. 16B). Therefore, the water fraction appearing around  $T_2 = 1$  s seems to be related to water that is not bound within the pellet. The  $T_2$ -value of both the supernatant and expelled water fraction was lower than the  $T_2$ -value of free water, which was measured to be around 2.4 to 2.7 s, suggesting the presence of proteins in the supernatant and expelled water.

The other two fractions are therefore ascribed to water present inside the pellets. The  $T_2$ -values of the fractions with the smallest transverse relaxation time ( $T_{2,1}$ ) were different for the three samples. A smaller WBC corresponded to a smaller  $T_{2,1}$ -value, suggesting a larger dry matter content in that water fraction. The second fraction ( $T_{2,2}$ ) had a  $T_2$ -value around 0.1 s, which was similar for all three pellets. The ratio of the areas of the  $T_{2,1}$  and  $T_{2,2}$  peaks differed between the pellets, as depicted in Fig. 16A. The unwashed MPs treated with 40 mM DTT had a larger area for the  $T_{2,2}$ -fraction than for the  $T_{2,1}$ -fraction; the areas for these fractions were nearly the same for the MPs made at pH 5.8.

For further insight into the WBC-P, the pellets of all the other MPs (MPs treated with DTT, washed and unwashed; MPs treated with DTT and *N*-ethylmaleimide; MPs treated with genipin; and MPs treated with transglutaminase (Tgase) by addition of Tgase to the WPI solution or the wet gel particles), both unheated and reheated, were analysed with TD NMR. The CONTIN  $T_2$ -spectra of all MP pellets showed at least the two water fractions  $T_{2,1}$  and  $T_{2,2}$ . Fig. 17A shows that  $T_{2,1}$  increased from WBC-P 2 to 5.5 g water/g dry matter, after which it tends to deviate from the trend. No clear relationship was found between  $T_{2,2}$  and the WBC-P (Fig. 17B), because all pellets had a  $T_{2,2}$ -value around 0.12 ( $\pm 0.02$ ). The relative area<sub>2,2</sub> was almost linearly related to the WBC-P (Fig. 17C). Therefore, these results suggest that an increase in WBC-P is caused by both an increase in the amount of water in water fraction  $T_{2,1}$  ( $T_{2,1}$  increased with an increase in the WBC implying an increase in the water content), and in water fraction  $T_{2,2}$  (the relative area<sub>2,2</sub> increased with an increase in WBC).



**Fig. 16.** The CONTIN  $T_2$ -spectra of (A) pellets and (B) supernatant formed during the water-binding experiment with standard whey protein microparticles (ST MPs) (solid line), unwashed MPs treated with 40 mM DTT (DTT MPs) (dashed line), and MPs made at pH 5.8 (pH MPs) (dotted line).

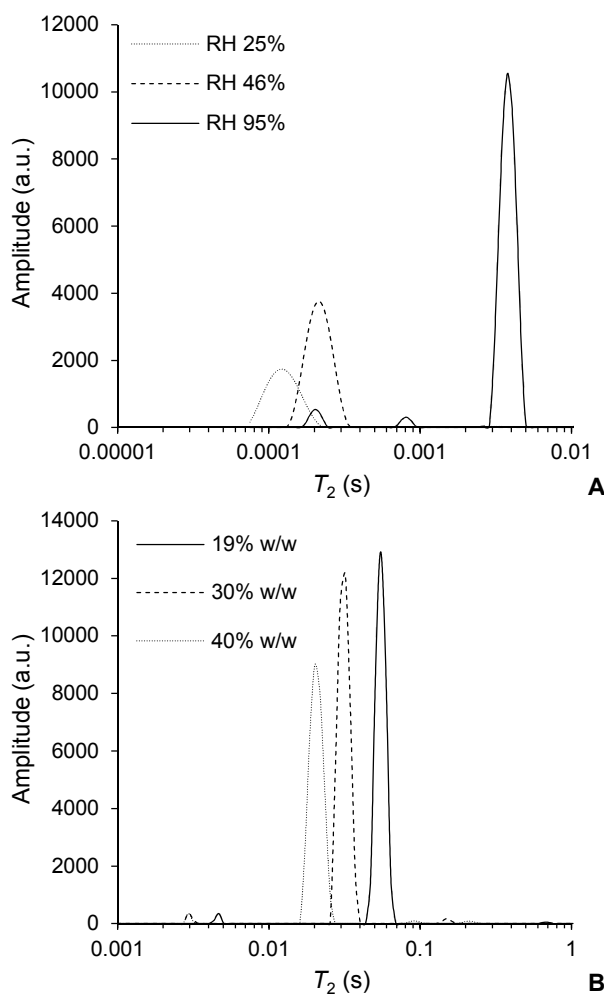


**Fig. 17.** Relationship between the water-binding capacity (WBC-P) (g water/g dry matter) of the unheated (filled diamond) and reheated (open diamond) pellets and (A)  $T_{2,1}$  (s), (B)  $T_{2,2}$  (s), and (C) the relative area<sub>2,2</sub> (-).

### 3.3 ASSIGNMENT OF WATER FRACTIONS OBTAINED WITH TIME DOMAIN NUCLEAR MAGNETIC RESONANCE TO THE WATER DOMAINS IN WHEY PROTEIN MICROPARTICLE PELLETS

It is likely that  $T_{2,1}$  and  $T_{2,2}$  can be assigned to the two water domains within the pellet: the swollen MPs and water between the MPs. The exchange rate of protons and the water/protein ratio are probably larger inside the MPs (domain C in Fig. 15) than between the MPs (domain B in Fig. 15). Therefore, it can be hypothesized that  $T_{2,1}$  represents water inside the MPs and  $T_{2,2}$  the water between the MPs. However, from the TD NMR results of the pellets only it is not clear if this assignment can be done instantly, or that water in the pellet was divided over two water peaks for other reasons. Therefore, it would be the best to analyse swollen MPs and water between the MPs separately. Since it would be hard to separate both fractions from the pellet, here it was tried to mimic swollen MPs to get to know if  $T_{2,1}$  could be assigned to this water domain.

To get hydrated MPs without water between the MPs, MPs were placed in a desiccator with controlled RHs for 12 days. A TD NMR analysis of those MPs resulted in spectra with mainly one fraction, as illustrated in Fig. 18A for the standard MPs. Smaller  $T_2$ -values were found when less water was present. The  $T_2$ -value of the MPs at RH 95% was still one order smaller than the  $T_{2,1}$ -value of the pellet spectra. This relatively large difference corresponds to the isotherm of these MPs, which shows a strong increase in moisture content from  $a_w$  0.95 to 1 (**Chapter 2**).



**Fig. 18.** The CONTIN  $T_2$ -spectra of (A) the standard microparticles incubated in a desiccator with RH 25% (dotted line), 46% (dashed line), and 95% (solid line); and (B) whey protein isolate (WPI) gels with a WPI concentration (w/w) of 19% (solid line), 30% (dashed line), and 39% (dotted line).

In addition, whey protein isolate (WPI) macro gels were analysed with TD NMR, because macro gels were considered as a model material for MPs without surrounding water but with a large moisture content. Fig. 18B shows that all the spectra for WPI macro gels contained one main fraction in the same range as the  $T_{2,1}$ -fraction of the pellets (Fig. 16A). Mono-exponential behaviour for WPI and whey protein concentrate gels with a protein concentration of 6 to 36% w/w has also been found by others.<sup>[33][87][109]</sup> As expected, the  $T_2$ -value of the gels decreased when the WPI concentration of the gel increased (Fig. 18B), because an increase in the protein content increases the total interaction with

water and reduces the transverse relaxation time.<sup>[105]</sup> The spectra of the WPI macro gels and MPs hydrated in a desiccator both suggest that one fraction ( $T_{2,1}$ ) within the pellet spectra is associated with water inside the MPs, and that therefore  $T_{2,2}$  can be assigned to water between the MPs.

Another method to check whether  $T_{2,1}$  can be assigned to water inside the MPs and  $T_{2,2}$  to water between the MPs, is by calculating the water and dry matter concentrations within those domains, and comparing those concentrations to the light scattering data. Therefore, a standard calibration curve relating the dry matter content to the transverse relaxation rate  $R_2$  ( $R_2 = 1/T_2$ ) was drawn (**Appendix A-Fig. S1A**).<sup>[33][87][104][105]</sup> A separate calibration curve was made for the MPs at pH 5.8, because those samples showed a different relationship between  $R_2$  and the dry matter content (**Appendix A-Fig. S1A**). The dry matter content in the supernatant of the standard MPs and MPs made at pH 5.8 could be estimated well (Table 4), indicating the validity of the calibration curves. The supernatant values obtained for the MPs treated with 40 mM DTT show some discrepancy between the measured and calculated dry matter content. These samples seem to be a special case, as they also deviate from the trend in Fig. 17A. The dry matter content inside the MPs estimated from the TD NMR data and the calibration curves (Table 4) compares well with the light scattering data for the standard MPs, the unwashed MPs incubated in 40 mM DTT, and the MPs made at pH 5.8 (Table 3). So, it was concluded that  $T_{2,1}$  can be assigned to water inside the MPs and  $T_{2,2}$  to water between the MPs.

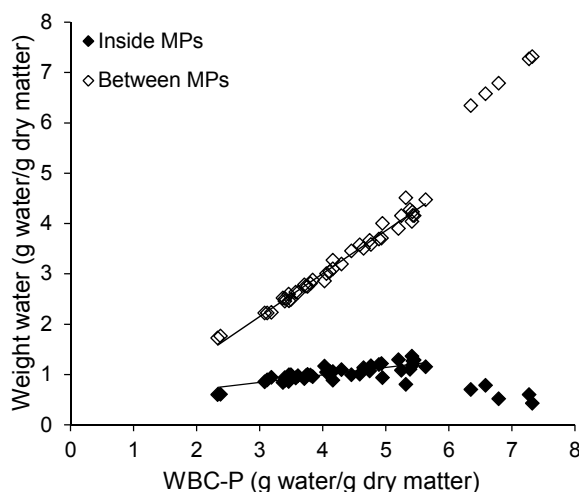
**Table 4.** The measured dry matter content (%) (standard deviation) and calculated dry matter content (%) with the calibration curves in the supernatants of the unheated and reheated standard (ST) whey protein microparticles (MPs), unwashed MPs treated with 40 mM DTT (DTT MPs), and MPs made at pH 5.8 (pH MPs), and the calculated dry matter content (%) and solubility of these MPs (%) in the unheated and reheated pellets.

	Supernatant			Pellet					
	Measured dry matter content (%)			Calculated dry matter content (%)			Solubility of MPs (%)		
	Unheated Reheated			Unheated Reheated			Unheated Reheated		
							Between MPs	Inside MPs	
ST MPs	0.6 (0.1)	0.6 (0.1)	0.7	0.9	12	35	9	25	33
DTT MPs	2.2 (0.5)	3.2 (0.5)	1.2	2.1	12	31	12	27	89
pH MPs	0.5 (0.1)	0.5 (0.1)	0.4	0.4	12	59	8	60	23



### 3.4 CONTRIBUTION OF WATER INSIDE AND BETWEEN THE WHEY PROTEIN MICROPARTICLES TO THE WATER-BINDING CAPACITY OF THE PELLETS

The next step is to estimate the contribution of water inside and between the MPs to the WBC-P. Therefore, the total amount of water present in the pellets is divided into two water fractions, according to the ratio between the areas under the curve of those two fractions. This division shows that the amount of water present inside the MPs increased slightly in the WBC-P ranging from 2 to 5.5 g water/g dry matter (Fig. 19). It seems that the increase in  $T_{2,1}$  with increasing WBC-P was less important than the decrease in the relative area<sub>2,1</sub> with increasing WBC-P. The increase in the WBC-P appears to be mainly related to an increase in the amount of water between the MPs. A consequence of that reasoning is that the contribution of water between the MPs cannot be neglected in the WBC-P, and that the WBC-MPs cannot be determined via the WBC-P.



**Fig. 19.** Relationship between the water-binding capacity of the pellets (WBC-P) (g water/g dry matter) and the amount of water (g water/g dry matter) present inside (filled diamond) and between (open diamond) the whey protein microparticles (MPs).

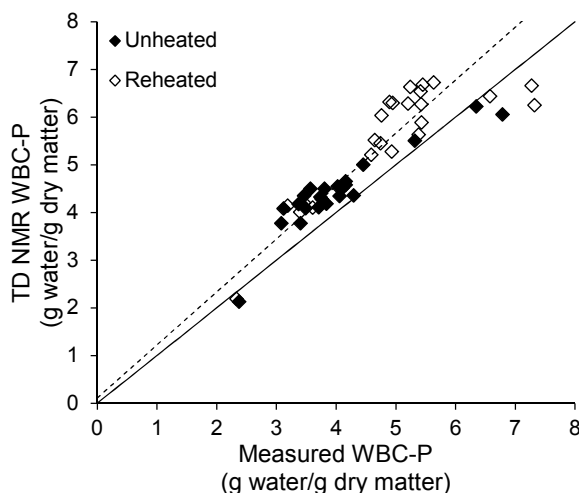
The contribution of water between the MPs to the WBC-P seems to be large. At a WBC of 5.5 g water/g dry matter, 80% of the water was present between the MPs, which implies that water-binding in this fraction in the pellet probably consisted of more than water inclusion by the MPs only. A remarkable observation for all MP pellets is that they had nearly the same  $T_{2,2}$  (Fig. 17B), which suggests a similar dry matter content between the MPs. Consequently, it seems that dissolved proteins originating from the MPs are a determining factor for the WBC-P. If it is assumed that the  $T_2$  of water is caused by

dissolved proteins only, the  $T_{2,2}$ -values suggest the presence of around 11 to 15% dry matter between the MPs. Although a certain amount of dry matter was expected due to the fact that the supernatant contains proteins as well (Fig. 16B and Table 4), this high dry matter content was unexpected. The suggested higher dry matter content between the MPs could be related to small, highly swollen protein aggregates that were dragged down upon centrifugation. The protein content suggested by the  $T_{2,2}$ -value could also explain the binding of water between the MPs, because this concentration might have led to the formation of a (particle) gel, or an increased viscosity at least, upon centrifugation. Without such effect, more water would be expelled during centrifugation. Rough calculations show that the volume fraction of standard MPs in a pellet is around 0.5 only, which is clearly lower than the maximum packing density of randomly packed monodisperse spheres (around 0.65), while polydisperse systems could have an even higher packing density.<sup>[166]</sup> Nevertheless, the possibility that  $T_{2,2}$  was influenced by other interactions and/or capillary pressures cannot be excluded. In that case, the actual protein concentration is somewhat lower than indicated by  $T_{2,2}$ , but still much larger than the protein content in the supernatant.

Fig. 19 also shows the different behaviour of the unwashed DTT treated particles (the particles with a WBC-P larger than 5.5 g water/g protein), compared to the other MPs. The differences are probably due to the fact that no clear distinction can be made between water inside and between those particular MPs, due to overlapping water peaks in the TD NMR spectra. This seems likely, because the area of  $T_{2,1}$  for the unwashed MPs incubated in 40 mM DTT was small compared with the area of  $T_{2,1}$  for the other MPs (Fig. 16A). It may be that those MPs incubated in 40 mM DTT partly solubilized, leading to a nearly equal dry matter and water content inside and between the MPs.

After the division of water according to the ratio of the areas, the WBC-P was calculated from the concentrations obtained via calibration curves. A comparison between the WBC-P calculated from the TD NMR data and the measured WBC-P shows that the WBC-P measured from the TD NMR data was mostly larger than the measured WBC-P (Fig. 20). This is probably caused by the way the WBC-P was determined when using the pellet weight after centrifugation. This method does not consider the solubilisation of dry matter, and therefore it can overestimate the dry matter content, and consequently underestimate the WBC. A 10% smaller dry matter content can explain the difference between the measured WBC-P and the calculated WBC-P from the TD NMR data, as shown in Fig. 20 with the dotted line. With TD NMR, on the other hand, the pellet obtained after centrifugation was used for analysis and the water concentration was obtained from measuring  $^1\text{H}$  protons. This has probably resulted in more accurate values for the dry matter and water concentrations within both water domains in the pellets, and a more accurate WBC-P.

Therefore, it can be concluded that with TD NMR a distinction between water present inside and between the MPs in a pellet can be made. In addition, TD NMR is a more exact method to determine the WBC-P and the dry matter and water concentrations in the water fractions of the pellet, than the use of the pellet weight obtained after centrifugation of a MP dispersion.



**Fig. 20.** The measured water-binding capacity of the pellets (WBC-P) (g water/g dry matter) and the WBC-P calculated from time domain nuclear magnetic resonance (TD NMR data) of the unheated (filled diamond) and reheated (open diamond) MPs. The WBC-P was calculated from the ratio between the areas of water inside ( $T_{2,1}$ ) and outside ( $T_{2,2}$ ) the MPs from the CONTIN  $T_2$ -spectra and the protein concentrations obtained from the calibration curves. The solid line shows the relation if the measured WBC-P was the same as the TD NMR WBC-P. The dashed line shows the relation in case the dry matter content of the pellets was actually 10% higher than used to calculate the measured WBC-P.

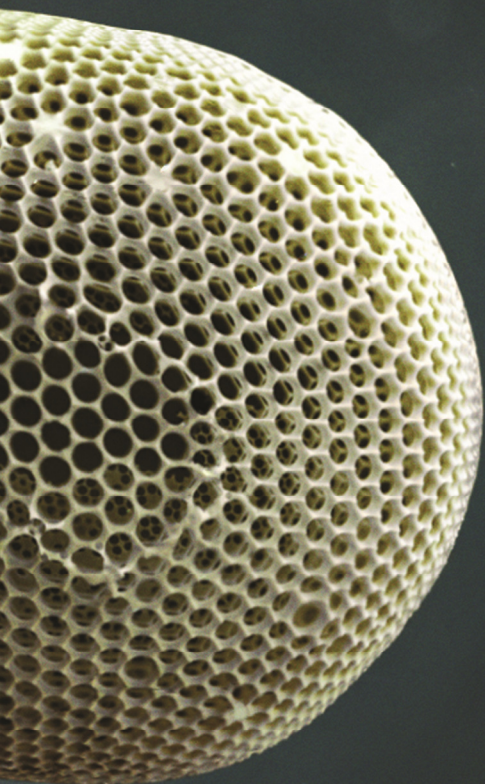
## 4 CONCLUSIONS

The water-binding capacity (WBC) of protein samples is frequently determined from the pellet weight obtained after centrifuging a dispersion of this sample, assuming that water between the sample particles can be neglected. However, we have demonstrated in this paper that the amount of water between the particles cannot be neglected. For pellets made of whey protein microparticle (MP) dispersions, with time domain nuclear magnetic resonance (TD NMR) a distinction was made between water inside and between the MPs. It was shown that an increase in WBC of the pellet (WBC-P) from 2 to 5.5 g water/g dry matter was partly caused by a slight increase in swelling of the MPs, but to a larger extent by an increase in the amount of water between the MPs. The latter could account for as much as 80% of the water being kept in a pellet with a WBC of 5.5 g water/g dry matter. Therefore, it is concluded that the WBC-P is not a measure for the WBC of MPs (WBC-MPs); the outcomes of the centrifugation method should be interpreted cautiously when used to determine the WBC-MPs. We hypothesize that this relatively large amount of water between the MPs could be present because small highly swollen protein structures co-sedimented between the MPs during centrifugation. The presence of such structures can also explain the remarkable result of a nearly constant  $T_2$ -value at all WBC-Ps, which suggest the presence of 11 to 15% of dry matter in the water fraction of water between the MPs. The results presented in this paper demonstrate that TD NMR is a better method to determine the WBC-MP, the amount of water between the MPs and the overall WBC-P, than using the pellet weight after centrifugation. We therefore conclude that TD NMR used in the manner proposed is a useful additional tool to understand WBC of a dispersed particle system.

## ACKNOWLEDGEMENTS

The authors would like to thank FrieslandCampina and NanoNextNL, a consortium of the government of the Netherlands and 130 partners, for their financial support of this research. In addition, we would like to thank Antoinette Toebe of FrieslandCampina for help with the TD NMR experiments and reading of the manuscript.





## *Chapter 4*

# **UNRAVELLING OF THE WATER-BINDING CAPACITY OF COLD-GELATED WHEY PROTEIN MICROPARTICLES**

## ABSTRACT

Whey protein microparticles (CG MPs) were made with a cold gelation method. Without shearing or mixing during gelation, spherical CG MPs formed, while shearing or mixing resulted in smaller irregularly shaped CG MPs. The water-binding capacity of pellets (WBC-P; comprising water within and between CG MPs) that was obtained after centrifugation of CG MP dispersions, was remarkably large (11 to 18 g water/g dry matter), but decreased at larger centrifugation speeds.

Microscopy images clearly showed the presence of two water domains, while just one main peak was found for all CG MPs in  $T_2$ -spectra: water had diffused from one water domain to the other within the measuring time. A fast two-state exchange model showed that, in most of the CG MPs pellets, a significant amount of water was present between the CG MPs. The amount of water that could be held between CG MPs seemed to be defined by the amount of particle–particle interactions that were present. Unsheared and unmixed CG MP pellets had a significantly smaller WBC-P than sheared and mixed CG MP pellets, because more water could be included between the smaller irregularly shaped CG MPs, due to increased particle–particle interactions. The significance of water inclusion for the WBC-P was also shown by blocking sulphhydryl groups on CG MPs, which resulted in less water inclusion and a lower WBC-P. This showed that water between CG MPs, and particle–particle interactions are important, if not determining, factors for the overall WBC-P of dispersed protein microparticles.

### THIS CHAPTER IS SUBMITTED AS:

Peters, J. P. C. M., Vergeldt, F. J., Van As, H., Luyten, H., Boom, R. M., van der Goot, A. J. Unravelling of the water-binding capacity of cold-gelated whey protein microparticles.

# 1 INTRODUCTION

The water-binding capacity (WBC; “the ability of a protein sample present in excess water to bind water when subjected to an external force” (**Chapter 3**)) of protein particles is an important property of the particles giving insight into the ability of the particles to interact with water. Often, the WBC is determined by centrifuging a particle dispersion and calculating the WBC from the pellet weight. This results in one value that shows both the ability of the particles to swell and to include water between them. It is hypothesized that the amount of water bound by the particles is governed by their internal network, while water inclusion between particles is determined by particle–particle interactions. Time domain nuclear magnetic resonance (TD NMR) was shown to be a useful tool to better understand the WBC of protein particle pellets (WBC-P), because a distinction could be made between water inside the particles and water between the particles, using TD NMR (**Chapter 3**).

Here, we studied the WBC-P of pellets, obtained from dispersions that contained whey protein microparticles made via cold gelation (CG MPs). Cold gelation is a two step-process. In the first step, whey proteins are turned into reactive aggregates by mildly heating a protein solution with a concentration lower than the critical gelation concentration (11–12%),<sup>[7][90]</sup> at low ionic strength; and a pH above or below its isoelectric point (pH 5.2–5.4).<sup>[58][147]</sup> This results in the formation of protein aggregates with a hydrodynamic diameter of about 80 nm.<sup>[5][6]</sup> Repulsive forces between the aggregates prevent further aggregation and gelation, yielding a stable solution of these aggregates. The second step in this process is therefore to induce gelation of the protein aggregate suspension, which can be accomplished by reducing the repulsive forces between the aggregates through reducing the pH. Often, glucono- $\delta$ -lactone (GDL) is used to form a regular gel by gradually decreasing the pH.<sup>[5]</sup> The addition of a polysaccharide prior to addition of GDL results in phase separation during gelation, and the creation of a water-in-water emulsion with protein being the dispersed phase, which may result in the formation of CG MPs.<sup>[39][40][159][160]</sup>

CG MPs are investigated because we hypothesize that CG MPs have the potential to swell to a larger extent than directly heat-gelated whey protein gels, which might lead to a larger and maybe distinct WBC-P range. This is suspected because a protein solution with a lower protein concentration was used during cold gelation than during heat gelation. Increased swelling of protein gels can be achieved by creating a gel with a reduced crosslink density,<sup>[63]</sup> by utilizing a lower protein concentration so there is less interaction between the proteins; i.e., covalently and non-covalently.<sup>[78]</sup>

In addition, CG MPs were investigated because previous research performed on CG MPs showed that the degree of particle–particle interactions could be influenced by the size and shape of the CG MPs.<sup>[159]</sup> Van Riemsdijk, et al. (2011)<sup>[159]</sup> changed the size and shape of CG MPs by applying a simple shear flow during gelation. Shear influences the



cold gelation process by affecting the stresses in the fluids. Using this, the tendency to phase separate can be enhanced, and anisotropy can be induced, which influences the size and the shape of the phases that are formed.<sup>[25]</sup> Wolf, Scirocco, Frith, & Norton (2000)<sup>[178]</sup> showed that the application of shear yielded spherical particles, long extended particles, thread-like particles or irregularly shaped particles (depending on the viscosity ratio between the two biopolymer phases and the shear applied). In case of CG MPs, smaller spherical particles were obtained at larger shear rates. A further increase of the shear rate ( $54 \text{ s}^{-1}$  and  $108 \text{ s}^{-1}$ ) resulted in smaller and irregularly shaped particles. The viscosity of dispersions of these CG MPs increased when the particle size was smaller. This was explained by increasing particle–particle interactions when the CG MPs became smaller and more irregular, resulting in more water inclusion between the particles and therefore a higher viscosity. Thus, by applying shear, the size and shape of CG MPs can be altered as well as the interaction with water, without changing the composition of the CG MPs. Another route van Riemsdijk et al. (2011)<sup>[159]</sup> utilized to control particle interaction was through the addition of a sulphhydryl blocking agent during gelation. It was found that the viscosity of the resulting dispersion of CG MPs was significantly lower than without the addition of the sulphhydryl blocking agent.

In this study, the effect of shearing and mixing on the size and shape of CG MPs and the water-binding properties is investigated. Therefore, the water-binding properties are studied by measuring the weight of the CG MP pellet obtained after centrifugation, and examining the pellets with microscopy and TD NMR. Then, the size and shape are linked to the ability of the CG MPs to bind water in a pellet, both within and between the CG MPs.

## 2 MATERIALS AND METHODS

### 2.1 MATERIALS

Whey protein isolate (WPI; BiPRO, lot no. JE 034-7-440 (Davisco Food International Inc., Le Sueur, MN) was used to prepare cold-gelated whey protein microparticles (CG MPs). WPI has a reported protein content of 97.7% on dry basis. In the preparation process of CG MPs, locust bean gum (LBG; Danisco Holland BV, The Netherlands) was used as polysaccharide, and glucono- $\delta$ -lactone (GDL; Sigma-Aldrich, Germany) was used as acidifier. *N*-ethylmaleimide (NEM; Fluka, The Netherlands) was used to block the sulphhydryl groups of the proteins and Rhodamine B (Sigma-Aldrich, Germany) was used to visualize the proteins with confocal laser scanning microscopy (CLSM). Milli-Q water (resistivity of 18.2 M $\Omega$  cm at 25 °C, total oxidisable carbon <10 ppb, Merck Millipore, France) was used in all experiments, unless stated otherwise.

### 2.2 METHODS

#### 2.2.1 PREPARATION OF COLD-GELATED WHEY PROTEIN MICROPARTICLES

For the preparation of the CG MPs the same method was used as described by van Riemsdijk et al. (2011)<sup>[159]</sup> with some additions. First, WPI- and LBG stock solutions were prepared. To make a WPI stock solution, 9% w/w WPI was dissolved in water and mixed with an overhead mixer at room temperature for at least 2 h. The solution was then heated at 68.5 °C for 2.5 h to obtain reactive aggregates. The aggregate solution was cooled under tap water for 2 to 3 min, placed in ice-water for 10 min, and further cooled at room temperature until it reached room temperature.

A LBG stock solution was made by dissolving 1% w/w LBG in water. This solution was heated in a water bath of 80 °C for 1 h. Then the solution was cooled in the same way as the WPI stock solution.

To prepare the CG MPs, the WPI stock solution; LBG stock solution; GDL; and water were added together, such that a 3% w/w WPI; 0.45% w/w LBG; and 0.2% w/w GDL solution was obtained, and subsequently mixed. Part of this solution was placed in an in-house made Couette shear device, while another part was placed in a mixing device. The Couette shear device has two cylinders: a stationary inner- and a rotating outer cylinder with diameters of respectively 40 and 42 mm. The bottom of the shear device has a cone/plate geometry with an angle of 2.75°. To mix the solution during incubation, a 200 mL double-walled glass vessel was used with an anchor stirrer. The vessel was closed with a clasp to prevent evaporation. During acidification and gelation in those two devices, the rotational speed of the cylinder and the stirrer was set at 0, 50, 100 or 300 rpm, corresponding to a shear rate in the Couette shear device of 0, 107, 215 or 644 s<sup>-1</sup> respectively, while the devices were heated with water of 25 °C from a water bath.

In addition, CG MPs were made in the Couette shear device at 25 rpm ( $54 \text{ s}^{-1}$ ). This was not done in the mixer due to a practical limitation: it cannot rotate at this speed. CG MPs formed at 0 rpm (static conditions) in the Couette shear device were called unsheared CG MPs, and CG MPs formed at 0 rpm in the mixing device were called unmixed CG MPs. Every kind of CG MP was made twice. The addition of GDL caused a gradual lowering of the pH from  $7.1 (\pm 0.0)$  to  $5.2 (\pm 0.0)$  after 16 h, for all samples.

After 16 h of incubation, the CG MP dispersion was diluted 1:1 and centrifuged at 2000 g for 15 min. The formed supernatant was discarded, while the pellet was re-dispersed in an amount of water equal to the amount of discarded supernatant, and centrifuged at 2000 g for another 15 min. Part of the pellet was then re-dispersed, resulting in a 6.5% w/w pellet dispersion. This dispersion and the rest of the pellet were analysed within one day.

To test the effect of blocking of the sulphhydryl groups on the size and shape of CG MPs and the water-binding capacity of a pellet of these CG MPs (WBC-P), the same procedure was used as described above, with the difference that 30 min before incubation, NEM was mixed into the reactive protein aggregates (2.25 mM). During incubation, the solution was sheared at 50 rpm.

### 2.2.2 SIZE AND SHAPE OF COLD-GELATED WHEY PROTEIN MICROPARTICLES AND PELLETS FORMED DURING THE WATER-BINDING CAPACITY EXPERIMENT

The size and shape of the CG MPs present in the dispersions obtained after gelation, the 6.5% w/w pellet dispersion of CG MPs, and the pellets of CG MPs obtained after the WBC-P test (Section 2.2.3) were examined with CLSM. To visualize the dispersions, 20  $\mu\text{L}$  of a  $2 \times 10^{-3}\%$  w/w Rhodamine B solution was added to a 780  $\mu\text{L}$  dispersion, and 500  $\mu\text{L}$  of this mixture was visualized with a LSM 510 microscope (Zeiss, Germany). To visualize the pellets, 200  $\mu\text{L}$  of water was replaced with a  $2 \times 10^{-3}\%$  w/w Rhodamine B solution. To induce fluorescent emission of Rhodamine B, a 543 nm laser was used for excitation and this was detected between 600 and 650 nm. The area fraction of the CG MPs and water between the CG MPs was determined with Image-J (ImageJ 1.49o, National Institute of Health, USA), using 5 images per treatment. The area fraction obtained from an image is assumed to be equal to the volume fraction,<sup>[126]</sup> so the area fraction was used to calculate the WBC (g water/g dry matter) of the CG MPs, assuming that the density of water was  $1000 \text{ kg m}^{-3}$  and that of the dry matter  $1300 \text{ kg m}^{-3}$ , and that no dry matter was present between the CG MPs.

### 2.2.3 WATER-BINDING CAPACITY OF COLD-GELATED WHEY PROTEIN MICROPARTICLE PELLETS

The WBC-P of CG MPs was determined by first adding 0.5 g of water to 0.5 g of pellet that was obtained after the last centrifugation step during washing of the CG MPs (Section 2.2.1), and mixing it with a vortex until a homogenous dispersion was obtained.

The dispersion was mixed with a rotator, rotating at 16 rpm at 25 °C for 30 min. After mixing, the dispersions were centrifuged at 1000, 3000, 6000 or 12,000 rpm at 25 °C for 20 min, which corresponds to 94, 845, 3381 or 13,523 g respectively. The supernatant was decanted from the pellet, and the pellet was weighed. Then the pellet was dried in an oven at 105 °C for 24 h and weighed again. From the weight difference between the dried and the wet pellet the WBC-P was calculated, using the following formula:

$$\text{WBC}_{\text{pellet}} (\text{g water/g dry\_matter}) = \frac{(W_{\text{wet\_pellet}} - W_{\text{dry\_pellet}})}{W_{\text{dry\_pellet}}} \quad (6)$$

with  $W_{\text{wet\_pellet}}$  as the weight of the pellet obtained after centrifugation and  $W_{\text{dry\_pellet}}$  as the dry matter weight of the pellet after drying in the oven. The WBC-P of the unsheared and sheared CG MPs was measured in duplicate per batch. The WBC-P of the unmixed and mixed CG MPs was determined in triplicate per batch. To calculate the WBC-P of each treatment, the average was taken from the two batches.

Furthermore, a dispersion of unsheared CG MPs was centrifuged at 12,000 rpm (13,523 g), the supernatant was discarded and the pellet was centrifuged again (every time for 20 min) until no additional supernatant was formed, to remove as much water as possible from between the CG MPs. In addition, a dispersion of unsheared CG MPs was centrifuged at 15,000 rpm (21,130 g) for 180 min to remove as much water as possible from between the CG MPs.

## 2.2.4 <sup>1</sup>H RELAXOMETRY

<sup>1</sup>H NMR measurements of the transverse relaxation time  $T_2$ , and the 2-dimensional correlated diffusion coefficient  $D$  and  $T_2$  were performed with a Maran Ultra NMR spectrometer (Resonance Instruments Ltd., Witney, United Kingdom) at 30.7 MHz proton resonance frequency.

### 2.2.4.1 <sup>1</sup>H RELAXOMETRY OF THE TRANSVERSE RELAXATION TIME

$T_2$ -relaxation decay curves were obtained by applying a standard Carr–Purcell–Meiboom–Gill (CPMG) pulse sequence.  $T_2$ -spectra of relative intensity as a function of  $T_2$  were determined by numerical inverse Laplace transformation of the data as implemented in CONTIN.<sup>[113]</sup> Relaxation decay curves of the CG MP pellets were obtained by first making pellets according to the method described in Section 2.2.3. Then, the tip of the tubes in which the pellets were present was cut off and placed in the NMR tube, as this method disturbed the pellets as little as possible (**Chapter 3**). A CPMG pulse was applied

that consisted of 2048 echoes, with an echo time  $TE$  of 1 ms and five data points each. Experiments were averaged over 16 scans with a repetition time  $TR$  of 15 s. From every batch two samples were analysed for the mixed CG MPs and one sample for the sheared CG MPs. The average  $T_2$ -value of the two batches of CG MPs made was used as the  $T_2$ -values of a certain treatment.

Relaxation decay curves of the supernatant of unsheared CG MP pellets obtained after the WBC-P-experiment (Section 2.2.3) and Milli-Q water were made by pipetting 125  $\mu$ L into the NMR tubes. A CPMG pulse was applied that consisted of 16,384 echoes, with an echo time  $TE$  of 1 ms and five data points each. Those experiments were averaged over 16 scans with a repetition time  $TR$  of 30 s. The spectrum for the supernatant was measured once and the spectra of Milli-Q water in triplicate.

#### 2.2.4.2 DIFFUSION COEFFICIENT IN THE PELLET OF COLD-GELATED WHEY PROTEIN MICROPARTICLES

The 2-dimensional correlated transverse relaxation time ( $T_2$ ) and diffusion coefficient ( $D$ ) measurement on an unsheared CG MP pellet centrifuged at 845 g consisted of a pulsed field gradient stimulated echo NMR pulse sequence (PFG-STE) to measure diffusion, combined with a CPMG pulse sequence<sup>[157]</sup> to measure  $T_2$ . This sequence is also referred to as DRCOSY (Diffusion Relaxation CORrelation Spectroscopy).<sup>[122]</sup> This sequence was analysed using a 2D numerical inverse Laplace transform 2D spectrum, showing the correlation between  $T_2$  and  $D$ .<sup>[74][137][162]</sup> Parameters related to the determination of  $D$  were a diffusion encoding time  $\Delta$  of 20 ms, and a PFG duration  $\delta$  of 2 ms. The experiment was repeated 22 times with different PFG gradient strengths ranging from 0 to 1.21 T/m with 32 repetitions to improve signal-to-noise, and a repetition time  $TR$  of 5 s, resulting in an experiment time of approximately 1.5 h. For the  $T_2$  determination, the CPMG echo train consisted of 4096 echoes with an echo time  $TE$  of 0.5 ms. The 2D datasets were processed in IDL (ITT Visual Information Solution, Boulder, CO USA) and analysed with MATLAB (The MathWorks, Inc., Natick, MA USA) to obtain DRCOSY spectra. This measurement was performed twice.

The diffusion coefficient ( $D$ ) from the DRCOSY spectra and the diffusion encoding time ( $\Delta$ ) were used to calculate the root-mean-square displacement of water with the Einstein-Smoluchowski equation for free diffusion in three dimensions:<sup>[32][79]</sup>

$$\langle x \rangle = \sqrt{6 D \Delta} \quad (7)$$

For this calculation it was assumed that water diffused isotopically with a Gaussian distribution.

### 3 RESULTS

#### 3.1 SIZE AND SHAPE OF COLD-GELATED WHEY PROTEIN MICROPARTICLES

Table 5 shows the size and shape of the cold-gelated whey protein microparticles (CG MPs) obtained after 16 h of incubation. Washing and centrifuging the CG MPs, and making a 6.5% w/w pellet dispersion of the pellets that were obtained after the second washing step, seemed to have barely affected the size and shape of the CG MPs (Table 5). Spherical unsheared and unmixed CG MPs were obtained when static conditions of 0 rpm were used. Shearing or mixing of the WPI–LBG–GDL (whey protein isolate aggregates–locust bean gum–glucono–delta–lactone)-solution during gelation, resulted in the formation of irregularly shaped CG MPs that were smaller than the spherical unsheared and unmixed CG MPs. Confocal laser scanning microscopy (CLSM) images of the CG MPs did not reveal clear differences in size and shape when the shearing or mixing rates were increased during incubation (Table 5). Size distributions of the 6.5% w/w CG MP pellet dispersions obtained with static light scattering showed a decrease in size of the main peak at larger shearing and mixing rates, with the exception of CG MPs that were sheared at 100 rpm during incubation (**Appendix B**-Fig. S2A and B). Differences in size, as measured with static light scattering, are caused by an actual difference in size between the CG MPs themselves, but might also be caused by a difference in ability to form clusters.<sup>[159]</sup> CLSM images of the CG MPs show small differences in size and shape between sheared and mixed CG MPs (Table 5). The unmixed CG MPs were noticeably larger than the unsheared CG MPs. Size distributions of the 6.5% w/w pellet dispersions of CG MPs showed that, on average, the sheared CG MPs were smaller than the mixed CG MPs (**Appendix B**-Fig. S2A and B). The difference between the sheared and mixed CG MPs was expected to be more explicit, because the forces applied to the dispersions were different. It is probable that the conditions during gelation were not dissimilar, as the forces applied in both cases were relatively large.

CLSM images of pellets obtained during the water-binding capacity experiment (Section 2.2.3) show differences in the effect of the centrifugation speed on the CG MPs (Table 5). In case of unsheared and unmixed CG MPs, an increased centrifugation speed forced the CG MPs together and to start to overlap, but they stayed intact. Sheared and mixed CG MPs tended to fuse when larger centrifugation speeds were used. However, the CG MPs were quite small, so it may also be that the CG MPs were pressed closer to each other.

Blocking the sulphhydryl groups before gelation with *N*-ethylmaleimide (NEM), resulted in a more even distribution of CG MPs over the dispersion and fewer particle clusters, when comparing to the 6.5% w/w pellet dispersions (Table 5). In addition, CLSM images show more dense particles within the 6.5% w/w pellet dispersions of CG MPs that were treated with NEM than in the dispersions of CG MPs for which that was not the case. Size distributions of the 6.5% w/w pellet dispersions revealed that the NEM treatment resulted in smaller particles, cluster sizes, or both (**Appendix B-Fig. S2C**).

**Table 5.** Size and shape of unsheared and unmixed (speed during incubation of 0 rpm); and sheared and mixed cold-gelated microparticle (CG MP) dispersions after incubation; 6.5% w/w CG MP pellet: dispersions after washing; and CG MP pellets formed during the water-binding capacity experiment at centrifugation speeds of 94, 845, 3381 and 13,523 g.

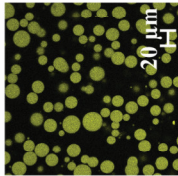
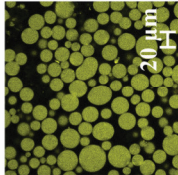
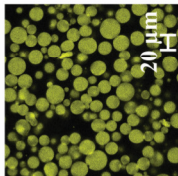
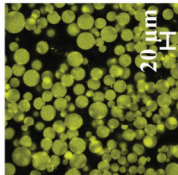
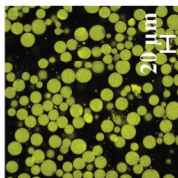
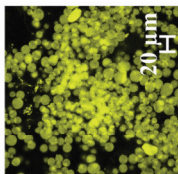
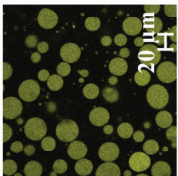
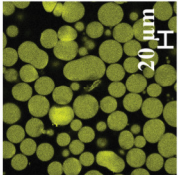
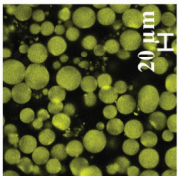
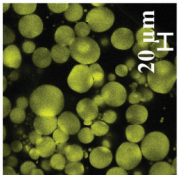
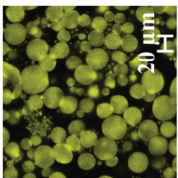
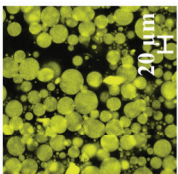
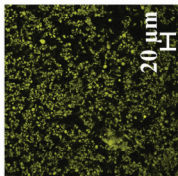
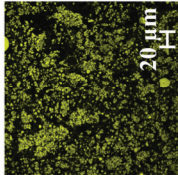
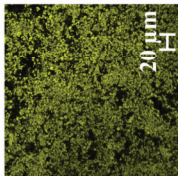
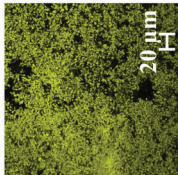
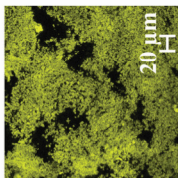
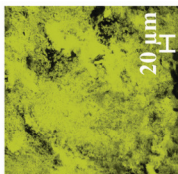
		Centrifugation speed (g)					
		Dispersion after incubation	6.5% w/w pellet dispersion after washing	94	845	3381	13,523
Speed during incubation (rpm)	0						
							
25	Sheared						



Table 5. (cont.)

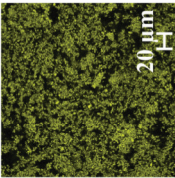
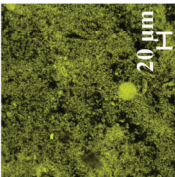
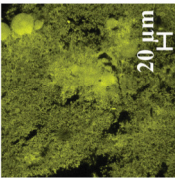
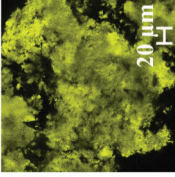
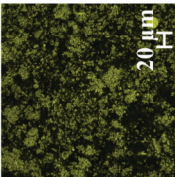
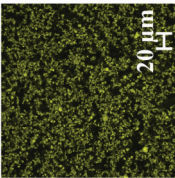
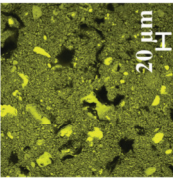
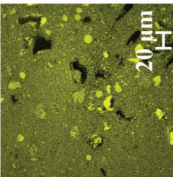

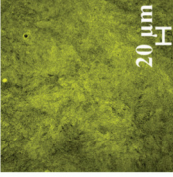
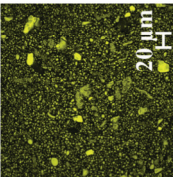
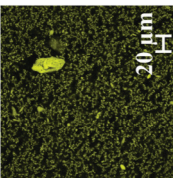
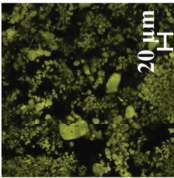
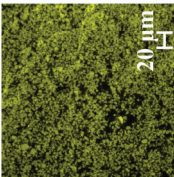
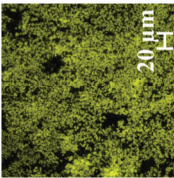
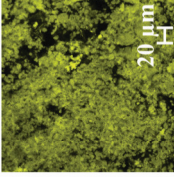
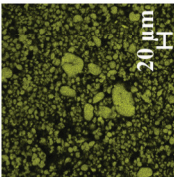
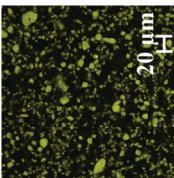
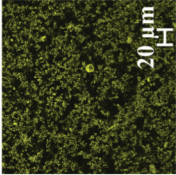
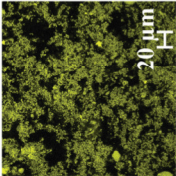
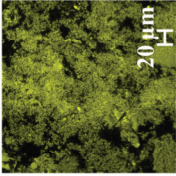
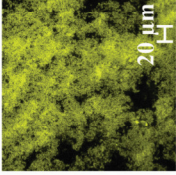
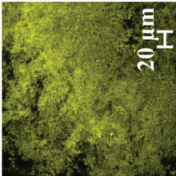
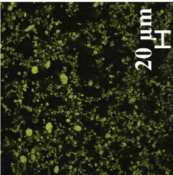
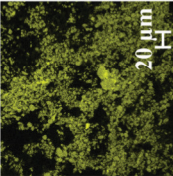
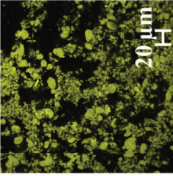
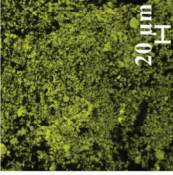
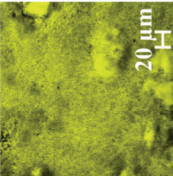
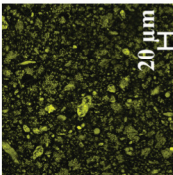
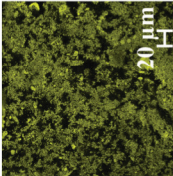
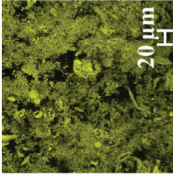
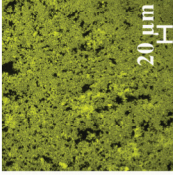
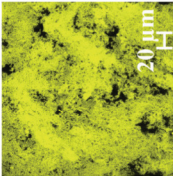
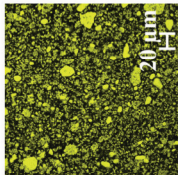
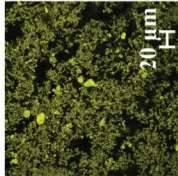
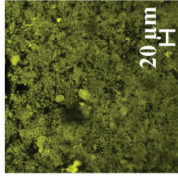
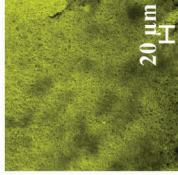
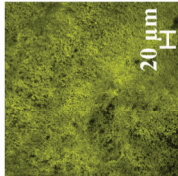
	Speed during incubation (rpm)	Centrifugation speed (g)				6.5% w/w pellet dispersion after washing	Dispersion after incubation
		94	845	3381	13,523		
50	Sheared						
	Sheared with NEM						
	Mixed						

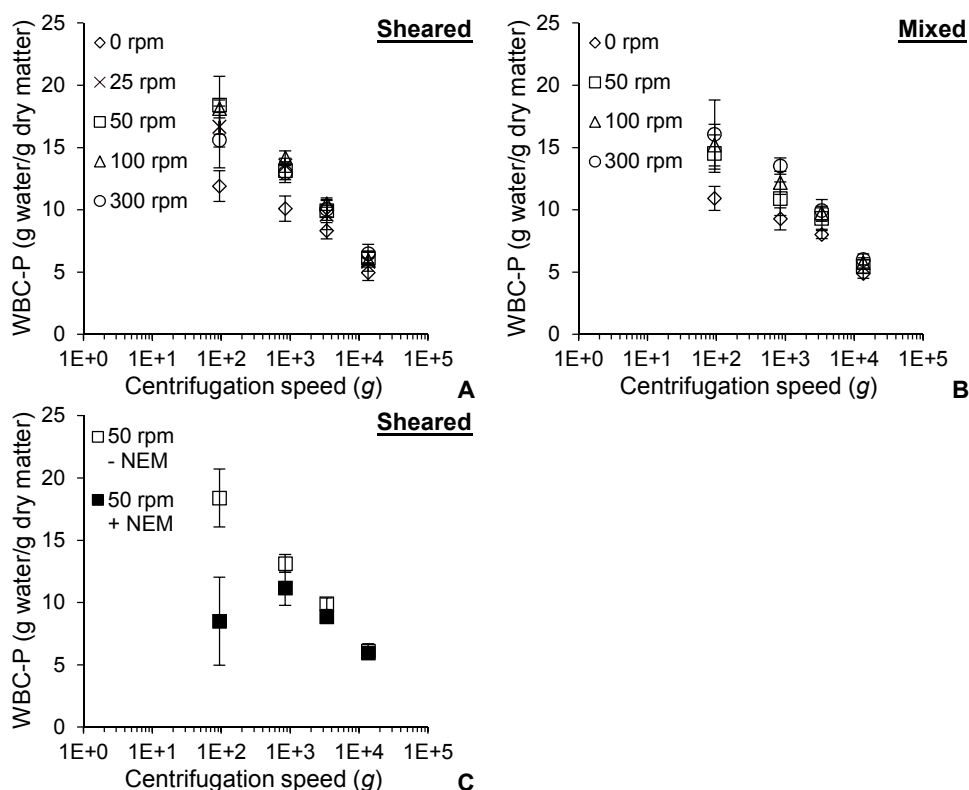
Table 5. (cont.)

	Dispersion after incubation	6.5% w/w pellet dispersion after washing	Centrifugation speed (g)			
			94	845	3381	13,523
Speed during incubation (rpm)	100					
	Mixed					
Speed during incubation (rpm)	300					
	Mixed					

### 3.2 THE WATER-BINDING CAPACITY OF PELLETS OF COLD GELATED WHEY PROTEIN MICROPARTICLES

The water-binding capacity of pellets (WBC-P) of CG MPs was remarkably large at 94 g, but decreased with larger centrifugation speeds (Fig. 21A and B). The WBC-P was similar for all CG MPs at a centrifugation speed of 13,523 g. All WBC-P-values taken together show that the sheared and mixed CG MP pellets had, on average, a larger WBC-P than the unsheared and unmixed CG MP pellets at centrifugal speeds of 94, 845 and 338 g. The sheared CG MPs had, on average, a slightly larger WBC-P than the mixed CG MPs.

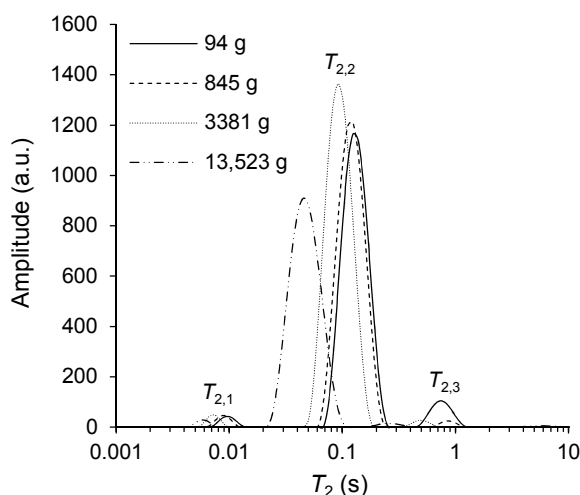
CG MPs treated with NEM had a significantly lower WBC-P at 94 g than CG MPs that were not treated with NEM (Fig. 21C). The average WBC-P of NEM-treated CG MPs became larger when centrifuged at 845 g, though the WBC-P was slightly lower than the WBC-P of CG MPs that were not treated with NEM. When the NEM-treated CG MP dispersions were centrifuged at higher speeds, their WBC-P decreased; at 3381 g their average WBC-P was smaller than the WBC-P of the regular CG MPs and they equalized at 13,523 g.



**Fig. 21.** The water-binding capacity (WBC-P) (g water/g dry matter) of (A) sheared and (B) mixed cold-gelated whey protein microparticle (CG MP) pellets made with a shearing or mixing speed during incubation of 0 (open diamond), 25 (cross), 50 (open square), 100 (open triangle) or 300 rpm (open circle) at various centrifugation speeds (g). (C) The WBC-P (g water/g dry matter) of CG MPs made with a shear rate of 50 rpm during incubation with (filled squares) and without (open squares) *N*-ethylmaleimide (NEM) at various centrifugation speeds (g). Error bars are based on the standard deviation of the WBC-P of two batches of CG MPs of which the WBC-P was measured two (sheared) or three (mixed) times per batch.

### 3.3 WATER DOMAINS IN COLD-GELATED WHEY PROTEIN MICROPARTICLE PELLETS

All CG MP pellets had at least two peaks in their CONTIN  $T_2$ -spectra. The peak with the lowest  $T_2$ -value, which was around 0.01 s, is labelled  $T_{2,1}$ . The second peak at around 0.1 s is labelled  $T_{2,2}$ . Some spectra also showed a small peak on the right side of peak  $T_{2,2}$ , which was labelled  $T_{2,3}$  (see Fig. 22 for an example of  $T_2$ -spectra). Probably, this latest peak relates to water present on the pellet after cutting the pellet, and it was therefore not taken into account for further analysis. For all CG MP pellets, the  $T_{2,2}$ -peak was predominant and the  $T_{2,1}$ -peak was minor.

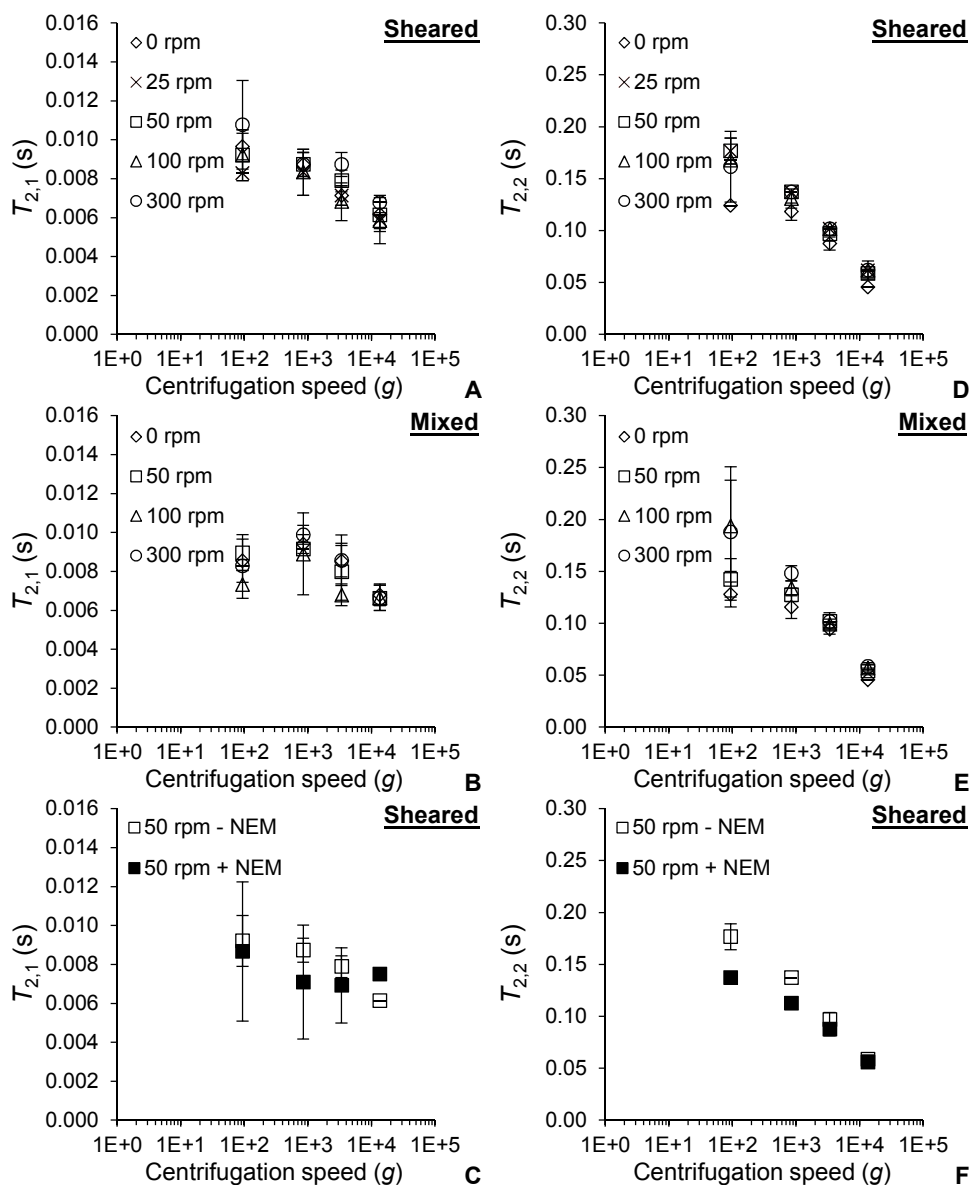


**Fig. 22.** CONTIN  $T_2$ -spectra of unsheared (0 rpm used during incubation) cold-gelated whey protein microparticle pellets centrifuged at 94 (solid black line), 845 (dashed line), 3381 (dotted line) and 13,523 g (dashed-dotted line).

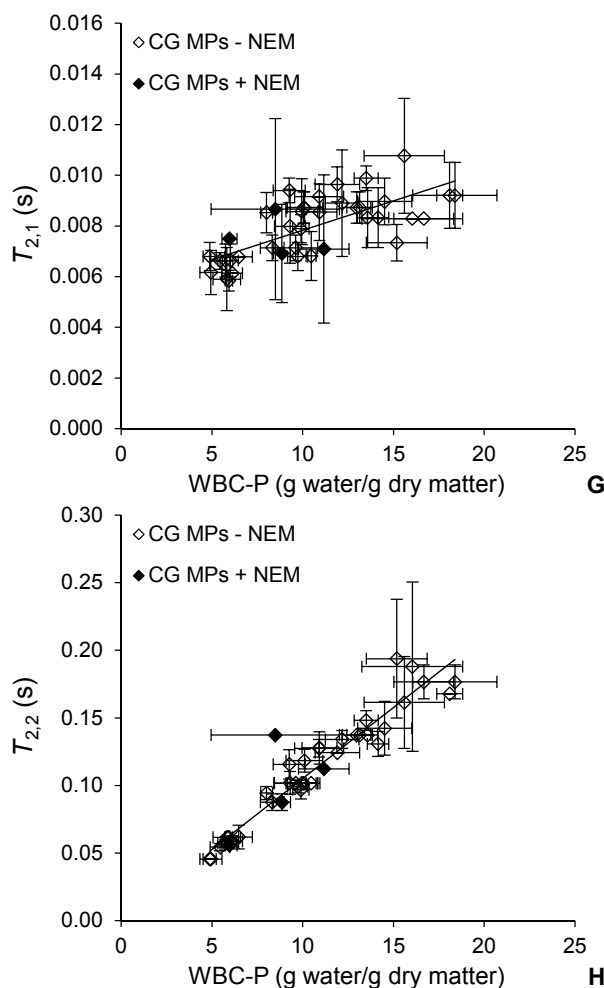
The  $T_{2,1}$ -value decreased when the centrifugation speed increased for sheared CG MP pellets (Fig. 23A). The  $T_{2,1}$ -values of mixed CG MP pellets showed a small increase in the  $T_{2,1}$ -value first, after which it decreased (Fig. 23B). There was no clear difference in the  $T_{2,1}$ -values between the unsheared and sheared, and unmixed and mixed CG MP pellets at all centrifugation speeds tested. The average  $T_{2,1}$ -values of CG MPs treated with NEM (Fig. 23C) were smaller than the values found for the CG MPs not treated with NEM. However,  $T_{2,1}$  was larger for the CG MPs treated with NEM than without NEM at the highest centrifugation speed. When the results of the TD NMR-measurements were compared to the WBC-P results, it was found that the  $T_{2,2}$  correlated better with the WBC-P than  $T_{2,1}$  (Fig. 23G and H). However, the WBC-P is the water-binding capacity of the total

pellet, while the  $T_2$  is related to a specific water domain within this pellet. These two values do not necessarily have to show the same trends, because the characteristics of the smallest water domain within the pellet might shrink into insignificance compared to those of the larger water domain, which therefore dominate the total water-binding capacity of the pellet.

The unsheared and unmixed CG MPs, as well as the sheared and mixed CG MPs, show a decrease in their  $T_{2,2}$ -values upon increasing the centrifugation speed (Fig. 23D and E). In most cases, the CG MPs made under static conditions featured the smallest average  $T_{2,2}$ -value. The  $T_{2,2}$ -values of the pellets of CG MPs made with different shearing or mixing rates became nearly equal at higher centrifugation speeds. NEM-treated CG MPs had smaller average  $T_{2,2}$ -values than the CG MPs without NEM treatment up to 3381 g, but were similar when a centrifugation speed of 13,523 g was used (Fig. 23F). This all contributed to a linear relation between  $T_{2,2}$  and the WBC-P (Fig. 23H), which can be used to determine the WBC-P via the  $T_{2,2}$  of CG MP pellets.



**Fig. 23.** The relaxation time  $T_{2,1}$  (s) of sheared (A) and mixed (B) cold-gelated whey protein microparticle (CG MP) pellets made at various centrifugation speeds (g) and (C) pellets of sheared CG MPs made with (closed square) and without (open square) *N*-ethylmaleimide (NEM) at 50 rpm. The relaxation time  $T_{2,2}$  (s) of sheared (D) and mixed (E) CG MP pellets made at various centrifugation speeds (g) and (F) pellets of sheared CG MPs made with and without NEM at 50 rpm. Error bars are based on the standard deviation of the  $T_2$ -values of two batches of which the  $T_2$ -values were measured once (sheared) or twice (mixed) per batch.



**Fig. 23.** (cont.) The relaxation times  $T_{2,1}$  (s) (G) and  $T_{2,2}$  (s) (H) correlated to the water-binding capacity of the pellets (WBC-P) (g water/g dry matter) of the various CG MPs made without NEM (open diamonds) and with NEM (closed diamonds). The relation of  $T_{2,1}$  without the CG MPs made with NEM is  $y = 0.0002x + 0.0055$  and  $R^2$  is 0.5186; and the relation of  $T_{2,2}$  is  $y = 0.0105x + 7E^{-5}$  and  $R^2$  is 0.9335. Error bars are based on the standard deviation of the  $T_2$ -values of two batches of which the  $T_2$ -values were measured once (sheared) or twice (mixed) per batch, and the standard deviation of the WBC-P of two batches of CG MPs of which the WBC-P was measured two (sheared) or three (mixed) times per batch.



## 4 DISCUSSION

### 4.1 WATER-BINDING CAPACITY OF COLD-GELATED WHEY PROTEIN MICROPARTICLE PELLETS

Cold-gelated whey protein microparticles (CG MPs) were made according to the two-step process as described above. Water-binding capacities of pellets (WBC-Ps) of all various CG MPs were measured by re-dispersing CG MPs in excess water and subsequently centrifuging these dispersions. The weight of these pellets was used to calculate the WBC-P. The WBC-P of CG MPs was remarkably large compared to the WBC-P of, for example, heat-gelated whey protein isolate (WPI) microparticles and the WBC of a heat-gelated WPI macro gel: 11 to 14 g water/g dry matter (Fig. 21A and B) at 845 g for CG MPs, compared to 3.7 g water/g dry matter and around 5 g water/g protein at 845 g for heat-gelated WPI microparticle pellets and a heat-gelated WPI gel respectively (**Chapters 2 and 3**).<sup>[85]</sup> Most likely, this is related to the protein concentration used during preparation and the resulting crosslink density of the gels. Remarkably, the protein concentration inside CG MPs was, according to our rough calculations, above the gelation concentration (Table 6), despite the fact that the protein concentration of the solution used to make CG MPs was below the gelation concentration before gelation.

Fig. 21A and B also show that the WBC-P of all CG MPs decreased with larger centrifugation speeds. Furthermore, the WBC-P was almost equal at a centrifugation speed of 13,523 g for all CG MPs. This coincides with images made of the pellets with confocal laser scanning microscopy (CLSM) (Table 5). In case of unsheared and unmixed CG MPs, an increased centrifugation speed forced the CG MPs together and they started to overlap, but stayed intact. This probably led to the expulsion of water present between the CG MPs, but possibly also to water squeezing out of the CG MPs themselves. Some shrinkage of CG MPs seems to be visible in the pellets of both the unsheared and unmixed CG MPs (Table 5), and rough calculations based on their CLSM images seem to support this. These calculations showed that the fraction of water present between the CG MPs barely decreased for the pellets made at 94 to 3381 g, despite some decrease in WBC-P (Table 6). Notably, about 33% of the area still was water present between the CG MPs (black space in the images; Table 6) when the CG MP dispersions were centrifuged at 13,523 g. It is likely that part of this water was reabsorbed by the pellet just after removal of the centrifugal force, because a significant increase in the weight of the pellets was observed when the supernatant was not directly removed after centrifugation. However, those gaps might also be air pockets, because the handling of the pellets became more difficult at larger centrifugation speeds: the pellets were smaller, more brittle and could not be spread out well.

Faster centrifugation also decreased the WBC-P of sheared and mixed CG MPs (Fig. 21A and B). Here, it seems that CG MPs tended to fuse when larger centrifugation speeds were used, though it might also be that the CG MPs are pressed closer to each other (Table 5). In pellets of mixed and sheared CG MPs made at 13,523 g some gaps were found between the protein structures. Here too, it is unclear if these signify water or air pockets.

**Table 6.** The water-binding capacity (WBC-P) (g water/g dry matter) of pellets of unsheared and unmixd cold-gelated whey protein microparticles (CG MPs), made at various centrifugation speeds (*g*); the average area (%) covered by water between the CG MPs pellets, as calculated with Image-J from the confocal laser scanning microscopy pictures of CG MPs pellets; and the WBC (g water/g dry matter) and protein concentration (%) of the CG MPs, calculated from the WBC-P and the average area of water between the CG MPs.

	Centrifugation speed during pellet formation ( <i>g</i> )	WBC-P (g water/g dry matter)	Average area water between CG MPs (%)	WBC-CG MPs (g water/g dry matter)	Protein concentration of CG MPs (%)
Unsheared	94	11.9 (1.2)	46 (6)	6.1	14.0
	845	10.1 (1.0)	38 (7)	6.0	14.4
	3381	8.3 (0.6)	41 (13)	4.6	18.0
	13,523	4.9 (0.6)	33 (8)	3.0	24.8
Unmixd	94	10.9 (1.0)	46 (3)	5.6	15.2
	845	9.3 (0.9)	45 (5)	4.7	17.5
	3381	8.0 (0.3)	45 (4)	4.1	19.6
	13,523	4.9 (0.4)	34 (6)	3.0	25.2

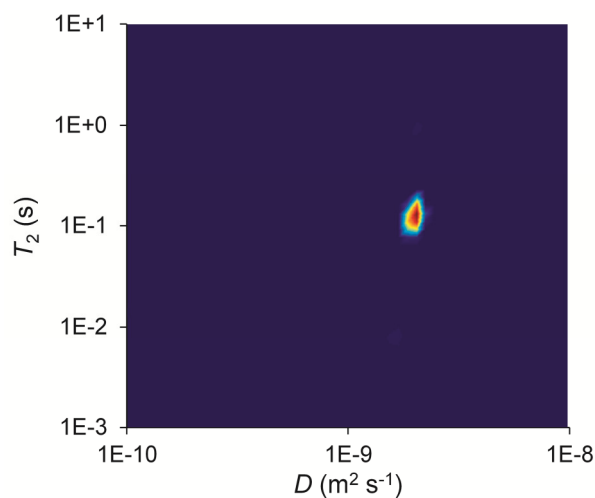
The standard deviation is given: within parentheses and is based on four (WBC-P unsheared), six (WBC-P unmixd) and five (area water in images) measurements.

## 4.2 CHARACTERISTICS OF WATER DOMAINS IN COLD-GELATED WHEY PROTEIN MICROPARTICLE PELLETS

Table 5 shows that pellets of CG MPs consisted of two water domains: water within and between CG MPs. However, with time domain nuclear magnetic resonance (TD NMR) only one main peak was found for all CG MP pellets, labelled  $T_{2,2}$  (see for an example Fig. 22). In a naive approach, the presence of one peak suggests that one predominant type of water was observed to be present in the pellet by TD NMR. Fast diffusional exchange of water between the water domains can explain the finding of just one peak. If the diffusivity ( $D$ ) is fast compared to the relaxation rate  $R_2$  ( $R_2 = 1/T_2$ ), the peaks of two water domains will average, leading to one peak in the  $T_2$ -spectrum.<sup>[92]</sup> The diffusional exchange is said to be fast when:

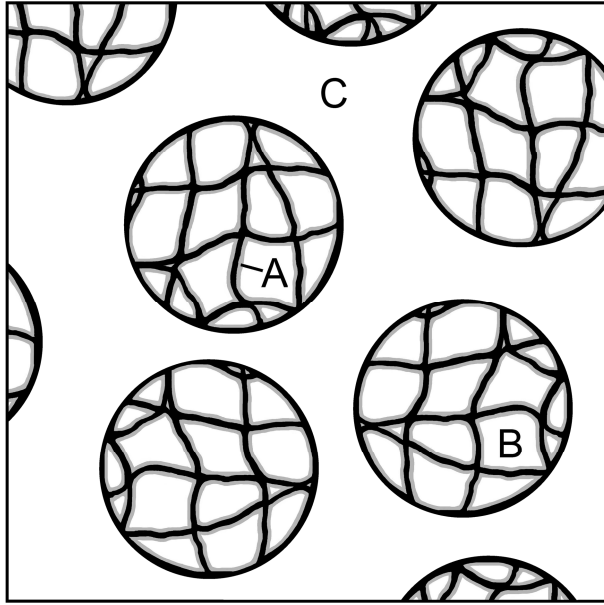
$$\frac{A^2 \Delta R_2}{D} \ll 1 \quad (8)$$

in which  $A$  is the size of the water domain, and  $\Delta R_2$  is the difference between the relaxation rates of the two domains. The pellet of unsheared CG MPs formed at 845 g showed a clear diffusivity peak that could be related to the  $T_{2,2}$ -peak in a DRCOSY measurement (Fig. 24), yielding a value for the diffusion coefficient of water of  $2 \times 10^{-9} \text{ m}^2 \text{ s}^{-1}$ . With this diffusivity coefficient, water is able to diffuse over a distance of approximately 15  $\mu\text{m}$  within the DRCOSY-measurement time. All sheared and mixed CG MPs were smaller than 15  $\mu\text{m}$ , and the unsheared and unmixed CG MPs had quite a lot of particles that were smaller than 15  $\mu\text{m}$  as well (Table 5). In conclusion, fast diffusion explains the presence of just one peak. In addition, the large diffusion coefficient of water suggests that the particles had a rather open particle structure.



**Fig. 24.** The relation between  $T_2$  (s) and the diffusion coefficient ( $D$ ) ( $\text{m}^2 \text{s}^{-1}$ ) of a pellet of unsheared cold-gelated whey protein microparticles made with a centrifugation speed of 845 g as measured with a DRCOSY experiment.

To explain the behaviour of water diffusivity and the water division within the CG MP pellets the following model is proposed. Within the pellet three types of structure–water interactions play a role (Fig. 25): (A) water bound to the aggregates (building blocks of the CG MPs; nanoscale), (B) water within the micro-pores of the CG MPs and (C) water included between the CG MPs due to the particle interactions between the CG MPs. The fast diffusion between water within and between the CG MPs shows that the CG MPs have a relatively open structure. The  $T_{2,2}$ -peak therefore probably is an average of the amount of water that is present within the CG MPs (B), and water that is present between the CG MPs (C). Water that is bound to the aggregates (A) might be represented by the  $T_{2,1}$ -peak (Fig. 22).



**Fig. 25.** Proposed representation for the water-protein (structure) interactions in a cold-gelated whey protein microparticle (CG MP) pellet. Herein, water is associated with the building blocks of the CG MPs (the aggregates) (A), water is present within the micro-pores of the CG MPs (B) and water is included between the CG MPs due to particle-particle interactions (C).

An estimation of the water division within and between the CG MPs can be obtained using a model for this system. Because water quickly diffuses between these two water domains (B and C), a fast exchange model can be used to determine the relative weight-fractions of water in the pellet, according to the following equation:<sup>[92]</sup>

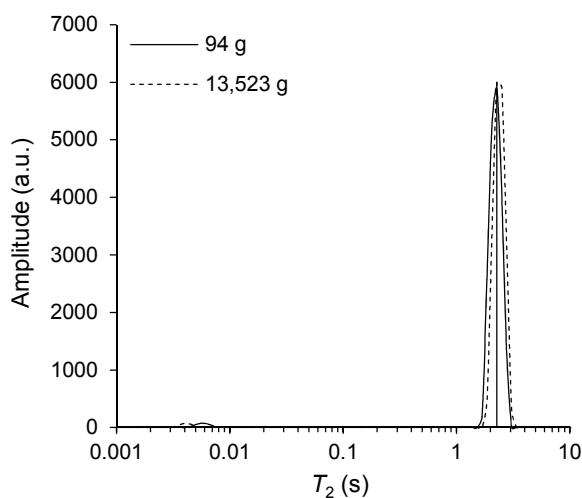
$$\frac{1}{T_{2,2\text{obs}}} = \frac{p_{2,2a}}{T_{2,2a}} + \frac{p_{2,2b}}{T_{2,2b}} \quad (9)$$

Here,  $T_{2,2\text{obs}}$  is the observed overall  $T_{2,2}$  of water within and between the CG MPs;  $p_{2,2a}$  is the weight-fraction of water within the CG MPs that has a  $T_2$ -value of  $T_{2,2a}$ ; and  $p_{2,2b}$  ( $p_{2,2b} = 1 - p_{2,2a}$ ) is the weight-fraction, representing water between the CG MPs that has a  $T_2$ -value of  $T_{2,2b}$ .

A  $T_2$ -value has to be estimated for each water domain, to calculate the weight-fraction of each of the two domains in every pellet measured. An initial assumption is that the amount of water bound within the MPs is independent of the centrifugation speed used. This was based on the fact that the application of a centrifugation speed of 13,523 g led to similar WBC-P-values for all CG MP pellets of around 5 to 6.5 g water/g dry matter. This value is interesting, because the WBC-P as reported for standard HG MP pellets also lies within this range (**Chapter 2**).<sup>[116][119]</sup> Therefore it seems that whey protein microparticle pellets have a general minimum WBC-P, irrespective of the process or conditions used. Similar conclusions were reported for soy aggregates.<sup>[149]</sup>

This WBC-P-value of the CG MPs could be decreased under more extreme conditions. When the CG MP dispersion of unsheared CG MPs was centrifuged at 21,130 g for 180 min, the WBC-P was further decreased to 4 g water/g dry matter ( $T_2 = 0.031$  s). A value of only 3 g water/g dry matter ( $T_2 = 0.025$  s) was achieved when CG MPs were centrifuged at 13,523 g and the supernatant was removed every 20 min until no additional supernatant was formed. This value is comparable with the WBC of the CG MPs, as roughly calculated from the CLSM images (Table 6). It is possible that these extreme centrifugation treatments resulted in a lower WBC than that would correspond to fully swollen intact CG MPs, because either water was squeezed out of the CG MPs, breakage or changes in pore structure inside the CG MPs occurred, or both, so less water could be bound.

The properties of water between the MPs were further analysed with the TD NMR response of the supernatants that were obtained after centrifuging a dispersion of CG MPs. The  $T_2$ -value of the supernatant obtained after centrifuging unsheared CG MPs at 94 g was equal to that of Milli-Q water (Fig. 26). A continued centrifugation at 13,523 g, of the pellet that belonged to the supernatant, resulted in a supernatant with the same  $T_2$ -value as Milli-Q water as well. It can therefore be postulated that water between the CG MPs does not contain any proteins, implying that all proteins are captured in the CG MPs. The WBC-P of CG MPs, represented by  $T_{2,2}$ , therefore comprises two water domains: water present within the network of the CG MPs and water without proteins between the CG MPs.

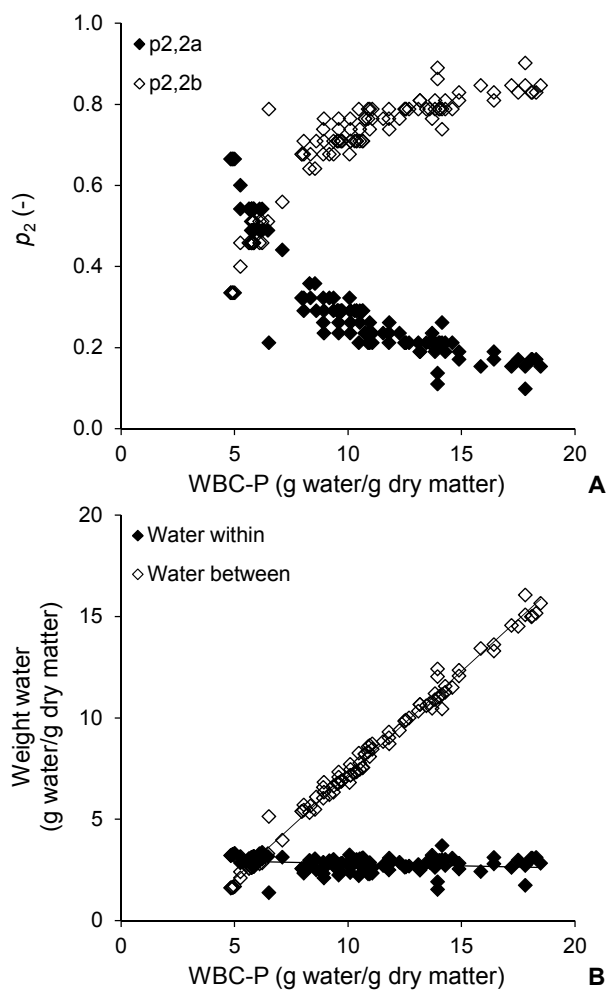


**Fig. 26.** CONTIN  $T_2$ -spectra of a supernatant obtained after centrifuging a dispersion of unsheared CG MPs at 94 g (solid line) and a supernatant obtained when the pellet was centrifuged further at 13,523 g (dashed line). The vertical line at  $T_2 = 2.28$  s is the  $T_2$ -value of Milli-Q water.

With the assumptions made as mentioned above,  $T_{2,2a}$  was chosen to be 0.031 s (the  $T_2$ -value of unsheared CG MPs centrifuged at 21,130 g for 180 min) and  $T_{2,2b}$  was deduced to be 2.28 s (the  $T_2$ -value of Milli-Q water). Subsequently, it was calculated that the fraction of water present between the CG MPs increased when the WBC-P increased from 5 to 10 g water/g dry matter, and levelled off at larger WBC-Ps (Fig. 27A). The fraction of water bound within the CG MPs decreased, when the WBC-P increased from 5 to 10 g water/g dry matter, and levelled off at larger WBC-Ps.

Overall, due to the assumptions made, the water division resulted in a nearly constant amount of water that was present within the CG MPs, of around 2.7 g water/g dry matter (Fig. 27B). It was expected that the centrifugation speed had an influence on the amount of water that was present within the CG MPs; however, this effect cannot be extracted from this data and model. Fig. 27B shows, furthermore, that in nearly all pellets the WBC-P was predominantly determined by the amount of water that was present between the CG MPs, which is related to the  $T_{2,2a}$ -value that was ascribed to the CG MPs themselves. The CLSM images of the pellets allow a similar conclusion, especially at lower centrifugation speeds. In conclusion, the amount of water between the CG MPs is very important, especially at high WBC-Ps, indicating that the WBC-P is not the same as the WBC of the CG MPs themselves.





**Fig. 27.** (A) The weight fraction of water within cold-gelated whey protein microparticles (CG MPs) ( $p_{2,2a}$ ) (closed diamond) and water between CG MPs ( $p_{2,2b}$ ) (open diamond), and (B) the resulting amount of water (g water/g dry matter) within (closed diamond) and between (open diamond) the CG MPs for CG MPs with various water-binding capacities of their pellets (WBC-P) (g water/g dry matter).

### 4.3 THE IMPORTANCE OF PARTICLE-PARTICLE INTERACTIONS ON THE WATER-BINDING CAPACITY OF PELLETS


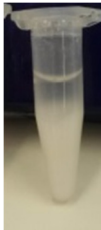
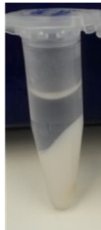
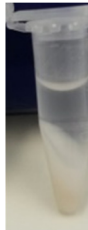
The amount of water between the CG MPs is an important factor for the overall WBC-P. We hypothesize that this is defined by the amount of particle–particle interactions, which affect water inclusion. All WBC-P-values taken together show that the sheared and mixed CG MP pellets had a larger WBC-P than the unsheared and unmixed CG MP pellets, at centrifugal speeds of 94, 845 and 3381 g (Fig. 21A and B). We hypothesized that sheared and mixed CG MPs had more particle–particle interactions, because they were smaller and more irregularly shaped (Table 5 and **Appendix B**-Fig. S2A and B), leading to higher water inclusion between the CG MPs. This corresponds to the finding of van Riemsdijk, et al. (2011),<sup>[159]</sup> who showed that dispersions of unsheared CG MPs had a lower viscosity compared to sheared CG MPs. The interactions between the particles were not very strong, because water could be easily expelled by applying a higher centrifugation speed (Fig. 21A and B).

The sheared CG MPs had, on average, a slightly larger WBC-P than the mixed CG MPs (Fig. 21A and B). This difference in WBC-P might be caused by the size of the CG MPs as well. The sheared CG MPs were somewhat smaller than the mixed CG MPs, according to their size distributions (**Appendix B**-Fig. S2A and B). Therefore, the sheared CG MPs possibly had a larger total surface area with which water and other CG MPs could interact, leading to greater water inclusion.

To further investigate the effect of particle–particle interactions on the WBC-P of the CG MPs, the sulphhydryl groups of the protein aggregates were blocked with *N*-ethylmaleimide (NEM). This affected both the amount of disulphide bridges within and between the CG MPs. The NEM treatment resulted in small irregularly shaped CG MPs, just like the CG MPs without the addition of NEM (Table 5). However, NEM-treated CG MPs showed less clustering of CG MPs (Table 5 and **Appendix B**-Fig. S2C). These observations suggest that there were fewer particle–particle interactions between the NEM-treated CG MPs than between the regular CG MPs. Fewer particle–particle interactions between NEM-treated CG MPs were also reported based on CLSM images made by van Riemsdijk, et al. (2011),<sup>[159]</sup> who additionally showed that the viscosity of a dispersion, containing CG MPs treated with NEM, was lower than a dispersion of CG MPs without NEM treatment. A reduced amount of particle–particle interactions between NEM-treated CG MPs might explain the lower water inclusion and, consequently, the lower WBC-P-values of NEM-treated CG MPs, as compared to the WBC-P of regular CG MPs (Fig. 21C). Less interaction between the NEM-treated CG MPs might also explain why a significant amount of material ended up in the supernatant after centrifugation, during the washing step of NEM-treated CG MPs. In addition, it was not possible to form a clear pellet and supernatant at 94 and 845 g; part of the CG MPs remained present in the supernatant (Table 7). NEM-treated CG MPs most likely behaved like separate CG MPs,

which required higher centrifugation speeds to sediment, while regular CG MPs, which form clusters, need a lower centrifugation speed.<sup>[168]</sup> Overall, it seems that the addition of NEM had limited effect on the particle formation process of CG MPs, but it did lead to a particle dispersion with reduced particle interaction and thus a lower water inclusion. Therefore, NEM-treated CG MP pellets confirmed that water between the CG MPs and particle–particle interactions are important, if not determining, factors for the overall WBC-P of dispersed protein microparticles.

**Table 7.** Pictures of the pellets and supernatants obtained after centrifuging dispersions of cold-gelated whey protein microparticles, treated with *N*-ethylmaleimide at 94, 845, 2281 and 13,523 g.

Centrifugation speed (g)			
94	845	3381	13,523
			

## 5 CONCLUSIONS

Cold-gelated whey protein microparticles (CG MPs) with different morphologies were made by shearing or mixing a WPI–LBG–GDL (whey protein isolate aggregates–locust bean gum–glucono–delta–lactone)-solution. Without shearing or mixing during gelation, spherical particles were formed, while shearing or mixing resulted in smaller irregularly shaped particles. Dispersions of these CG MPs were centrifuged, resulting in the formation of a pellet of CG MPs that was used to calculate the water-binding capacity of the pellets (WBC-P). The CG MP pellets had a remarkably large WBC-P, ranging from 11 to 18 g water/g dry matter when centrifuged at 94 g, which decreased when larger centrifugation speeds were used.

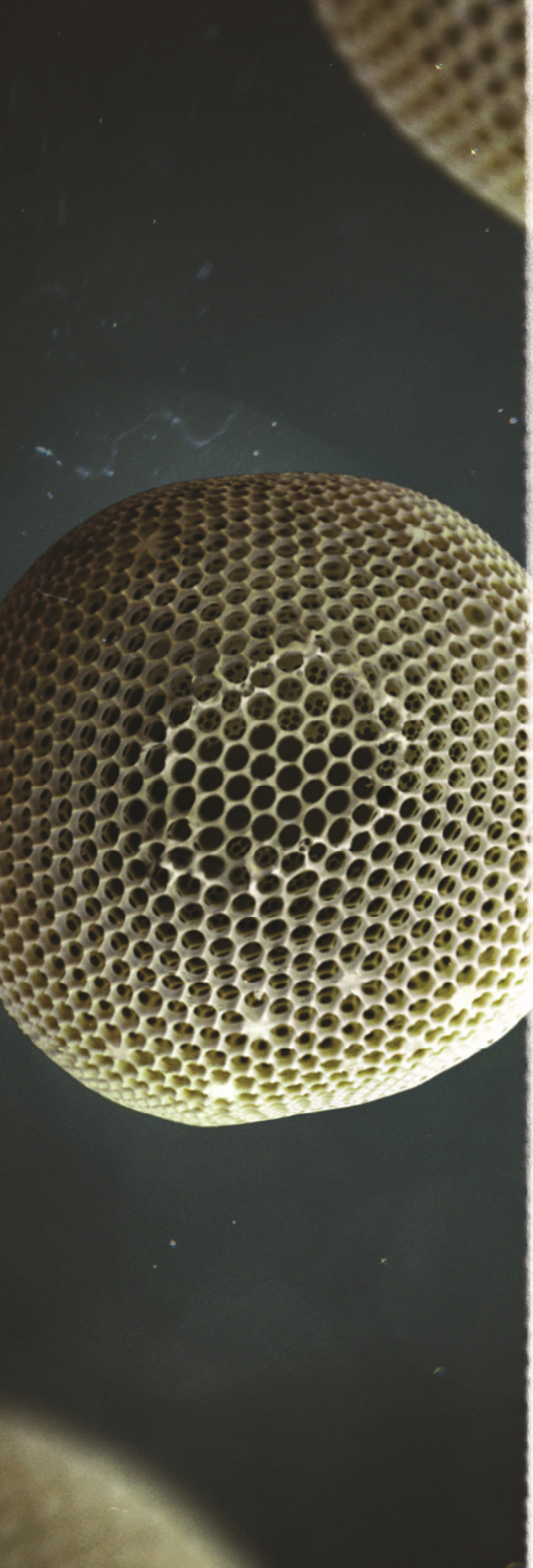
Confocal laser scanning microscopy (CLSM) images of the pellets showed that the pellets had two water domains (water within and between the CG MPs), though only one main water peak was found with time domain nuclear magnetic resonance (TD NMR). The presence of one main peak was caused by the fast diffusional exchange of water between both domains, suggesting that the CG MPs had a relatively open structure. In addition, using TD NMR we found that water that was present between the CG MPs did not contain any proteins; hence, all proteins had been captured in the CG MPs.

A fast two-state exchange model was used with this information, resulting in a division of water in the pellet, which implied that in most pellets the WBC-P was mainly determined by the amount of water between the CG MPs. This showed that the WBC-P was unequal to the WBC of the CG MPs themselves. The amount of water that could be held between the CG MPs seemed to be related to the amount of particle–particle interactions that were present. Smaller and more irregularly shaped CG MPs had larger WBC-Ps, which might have been caused by a greater number of particle–particle interactions, leading to the formation of more clusters in which water could be included. CG MPs treated with *N*-ethylmaleimide strengthened this hypothesis. Here, the disulphide bridge formation was inhibited, which seemed to result in less particle–particle interactions and a lower WBC-P. This implies that water between the CG MPs, driven by particle–particle interactions, is an important, if not determining factor for the overall WBC-P of dispersed protein microparticles.

## ACKNOWLEDGEMENTS

The authors would like to thank FrieslandCampina and NanoNextNL, a consortium of the government of the Netherlands and 130 partners, for their financial support of this research. We thank Wouter Perk for proofreading the manuscript.





## *Chapter 5*

# **WATER-BINDING CAPACITY OF PROTEIN-RICH PARTICLES**

## ABSTRACT

The water-binding capacities (WBCs) of pea protein isolate, soy protein isolate, lupin protein concentrate and vital wheat gluten particles were investigated by hydrating them in excess water, centrifuging these dispersions, and calculating the WBCs from the weight of the pellets. It was found that, except for pea proteins, the pellet consisted of protein structures with a noticeable amount of interstitial water between these structures. Additionally, in some cases a protein network was formed that did not represent the WBC of *particles* anymore. Consequently, it was concluded that the WBC of the pellet (WBC-P) differs from the WBC of the particles. Therefore, the characteristics of the particles and their pellets were further investigated with, among others, time domain nuclear magnetic resonance (TD NMR). TD NMR turned out to be a useful tool to do this, and has the potential to give an indication of the amount of water present in each water domain. From the information obtained about the characteristics of the particles and their pellets, it could be concluded that variations in the WBC-P were the result of differences in the toughness of the particles (i.e., their capabilities to swell and to withstand the centrifugal force, which are determined by their crosslink density and pores), and their ability to bind water interstitially.

### THIS CHAPTER IS SUBMITTED AS:

Peters, J. P. C. M., Vergeldt, F. J., Boom, R. M., van der Goot, A. J. Water-binding capacity of protein-rich particles.

# 1 INTRODUCTION

An important property of proteins is their ability to interact with water. This affects various functional properties such as their ability to gel, to dissolve, to swell, and to act as stabilizer in emulsions.<sup>[30][185]</sup> A way to describe the interaction of proteins with water is by their water-binding capacity (WBC). Unfortunately, not only are several definitions utilized for this term in literature, but other terms than the WBC are used as well.<sup>[185]</sup> A further complication is that various methods are utilized to determine the WBC. A frequently employed technique to determine the WBC of proteinaceous particles is to make a dispersion of the particles in excess water and centrifuge it.<sup>[15][75][175][183]</sup> The supernatant is then discarded and the WBC of the pellet (WBC-P) is determined via the weight of the pellet, with, for example, the following formula:

$$\text{WBC}_{\text{pellet}} (\text{g water/g dry matter}) = \frac{(M_{\text{wet\_pellet}} - M_{\text{dry\_pellet}})}{M_{\text{dry\_pellet}}} \quad (10)$$

in which  $M_{\text{wet\_pellet}}$  is the weight of the pellet obtained after centrifugation, and  $M_{\text{dry\_pellet}}$  the weight of the material after drying the pellet. In this way, the WBC is defined as *the ability of a protein sample to bind water when subjected to an external force*.

Previous research performed with whey protein microparticles showed that the weight of their pellets was a combination of water bound internally (within the particles) and interstitially (between the particles) (**Chapters 3 and 4**). Actually, measurements performed with time domain nuclear magnetic resonance (TD NMR) revealed that interstitial water was an important contributor to the WBC-P. This means that the WBC-P was unequal to the WBC of the particles themselves.

The results shown in **Chapters 3 and 4** may have consequences for interpreting the WBC of other proteinaceous powders as well. That is why the WBC-Ps of several protein-rich particles were investigated in this paper. These WBC-P values were compared to the values obtained via TD NMR data. In addition, swelling of the particles was studied and the morphology of the pellets examined with microscopy. These techniques allowed an estimation of the contribution of internal and interstitial water to the WBC-P. This information, together with the diffusivity of water in the pellet, was used to gain more insight into the microstructure–protein–water interactions in the pellets and to conclude whether water-binding by particles in pellets is governed by any general principles.



## 2 MATERIALS AND METHODS

### 2.1 MATERIALS

Pea protein isolate (PPI; Nutralys F85M, Roquette, Lestrem, France), soy protein isolate (SPI; Supro EX 37 IP, Solae, St. Louis, Missouri, USA), lupin protein concentrate (LPC; Fralu-Con, Barentz B.V., Hoofddorp, The Netherlands) and vital wheat gluten (VWG; Barentz B.V., Hoofddorp, The Netherlands) were used. These powders have a protein content of 72% ( $\pm 2$ ), 78% ( $\pm 2$ ), 41% ( $\pm 1$ ), and 70% ( $\pm 1$ ) respectively, according to Dumas analysis ( $N \times 5.7$ ). To visualize the proteins with a confocal laser scanning microscope (CLSM), Rhodamine B (Sigma–Aldrich, Germany) was used as a staining agent. Milli-Q water was used (resistivity of 18.2 M $\Omega$  cm at 25 °C, total oxidisable carbon <10 ppb, Merck Millipore, France) in all experiments.

### 2.2 METHODS

#### 2.2.1 WATER-BINDING CAPACITY OF PROTEIN-RICH PARTICLE PELLETS

The water-binding capacity of the protein-rich particle pellets (WBC-P) was measured using the following procedure. First, an excess amount of water was added to the particles, so a 10% w/w dispersion of each of the various materials was obtained in 1.5 mL Eppendorf tubes. The dispersion was mixed with a vortex until the sample was thoroughly wetted. Subsequently, the dispersion was mixed with a rotator at 16 rpm and 25 °C for 3 h (further referred to as hydrated for 3 h). Every 15 min, the dispersion was again mixed with the vortex. Next, the tube was centrifuged in an Eppendorf centrifuge at 3000 rpm (845 g) for 20 min. The supernatant was discarded and the pellet weighed. Afterwards, the pellet was dried in an oven at 105 °C for 24 h and weighed again. The weight difference between the wet and dried pellet was divided over the weight of the dry pellet to calculate the WBC-P, according to Equation 10.

The 10% w/w dispersion was also centrifuged immediately after thoroughly wetting (further referred to as hydrated for 0 h) to investigate the effect of the hydration time on the WBC-P of the sample. After centrifugation, the sample was weighed and dried in an oven at 105 °C for 24 h. For both hydration times, the WBC-P was measured in quadruplicate.

### 2.2.2 DISSOLUTION OF PROTEIN-RICH PARTICLES

The supernatants that were obtained after centrifuging the protein-rich particle dispersions after 0 h and 3 h of hydration (Section 2.2.1) were dried at 105 °C for 24 h, to determine the amount of material that dissolved during the WBC-P experiments. This was performed four times for each hydration time per material. The dry matter concentration of the supernatants was calculated with the following equation:

$$C_{\text{dm}_s} (\%) = \frac{M_{\text{dm}_s}}{M_s} 100 \quad (11)$$

in which  $M_{\text{dm}_s}$  is the weight of the remaining dry matter after drying the supernatant and  $M_s$  the weight of the amount of supernatant before drying. The solubility of the material was calculated using Equation 12:

$$\text{Solubility } (\%) = \frac{M_{\text{dm}_s}}{M_{\text{dpp}}} 100 \quad (12)$$

in which  $M_{\text{dpp}}$  is the weight of the material used to make a 10% w/w dispersion of the material (Section 2.2.1). The dry matter content of the supernatant and solubility of SPI hydrated at 0 h was not given, because the supernatant was enveloped by the pellet.

### 2.2.3 SIZE AND SHAPE OF DRY PROTEIN-RICH PARTICLES

The size and shape of the unhydrated protein-rich particles (further referred to as dry samples) were analysed with a high-resolution field emission scanning electron microscope (SEM; Phenom G2 Pure, Phenom-World BV, Eindhoven, the Netherlands). Carbon tabs were used to fix the samples on aluminium pin mounts.

In addition, the size of the dry particles was measured with static light scattering (Mastersizer 2000, Malvern Instruments). This was done with a Scirocco 2000 dry dispersion unit (Malvern Instruments, Malvern, UK), connected to the Mastersizer. From the measurements, the average particle diameter  $d_{4,3}$  (volume mean diameter) was calculated, whereby the assumption was made that the particles were spherical. The size of the dry particles was measured at least in triplicate.

## 2.2.4 SIZE AND SHAPE OF THE PROTEIN-RICH PARTICLES IN THEIR PELLETS

The size and shape of the protein-rich particles in their pellets were examined with CLSM, using pellets obtained after a hydration time of 3 h (Section 2.2.1). In this case, however, 200  $\mu\text{L}$  of Milli-Q water was replaced by 200  $\mu\text{L}$  of a  $2 \times 10^{-3}\%$  w/w Rhodamine B solution, and the samples were covered with aluminium during hydration. After centrifugation, the pellets were visualized with a LSM 510 microscope (Zeiss, Germany). Fluorescent emission of Rhodamine B was induced with a 543 nm laser for excitation and detected between 600 and 650 nm.

The area of water between the protein-rich particles in a pellet in the images was determined with Image-J (ImageJ 1.49o, National Institute of Health, USA), using 5 images per treatment. It is assumed that the area fraction obtained from an image is equal to the volume fraction.<sup>[126]</sup> To roughly calculate the WBC of the particles themselves, the volume of the pellet was first estimated with Equation S2 (**Appendix C**). Next, this volume was multiplied by the area fraction of the hydrated protein particles, to obtain the total volume of all hydrated protein particles. Subsequently, the amount of dry matter between the particles, the WBC of the particles themselves, and the ratio of water inside and between the protein particles were approximated with Equations S3, S4, and S5 (**Appendix C**). Then, the dry matter content of the hydrated particles was estimated with the WBC of the particles in the pellet. For these calculations, it was assumed that the density of proteins was  $1330 \text{ kg m}^{-3}$  and the density of water  $1000 \text{ kg m}^{-3}$ , and that the dry matter concentration within the supernatant was equal to the dry matter concentration between the particles.

## 2.2.5 DYNAMIC ADSORPTION ISOTHERMS

Dynamic water vapour adsorption isotherms for all four kinds of particles were obtained by using an automatic multi-sample moisture sorption analyser SPSx-11 $\mu$  (Projekt Messtechnik, Ulm, Germany). The relative humidity (RH) within the climate chamber of the moisture sorption analyser was controlled by mixing a dry nitrogen gas flow with a water-saturated gas flow. A dew point analyser and a microbalance (WXS206SDU Mettler–Toledo, Greifensee, Switzerland) were present in the moisture sorption analyser to monitor the RH and weight respectively. The variations in weight of a sample (measured at time intervals of at least 10 min), caused by the change in environmental RH, were measured to determine the water sorption.

Before the start of a dynamic water vapour sorption experiment, the samples were dried above  $\text{P}_2\text{O}_5$  for at least 3 days. The sorption measurement procedure started with initially drying at  $25^\circ\text{C}$  and RH 0% during 500 min, followed by an increase with steps of 10% from 0% up to 90% RH, and a final increase of 5% to 95% RH at  $25^\circ\text{C}$ . Equilibrium was assumed to be established when there was no weight change greater than 0.001% over a

period of 60 min, or when the sample was subjected to that RH for a maximum period of 50 h. Adsorption isotherms were made twice for every kind of material, and averaged.

The dynamic sorption isotherm can be analysed with various models, of which some result in values that have a physical meaning.<sup>[13]</sup> Here, the adsorption isotherms were evaluated in light of the underlying theory of the Flory–Rehner equation,<sup>[53][54]</sup> assuming that the role of ions was negligible:

$$a_{w\text{tot}} = a_{w\text{sorption}} a_{w\text{elastic}} \quad (13)$$

with  $a_{w\text{tot}}$  as the total water-activity,  $a_{w\text{sorption}}$  as the water-activity due to sorption, and  $a_{w\text{elastic}}$  as the water-activity due to the elastic contribution. In the Flory–Rehner equation, the sorption term is affected by the interaction between the proteins and water ( $\chi$ ), which is regulated by the hydrophilicity of the protein-rich particles. The elastic term is influenced by the molar weight of the polymeric units between the crosslinks ( $M_c$ ), or in other words, by the crosslink density. In studies on vegetables it was found that in the lower  $a_w$ -region ( $a_w < 0.8$ ), the hydrophilicity dominates, whereas the crosslink density dominates in the higher  $a_w$ -region ( $a_w > 0.8$ ).<sup>[111][156]</sup> The predominant effect of the crosslink density on swelling in the higher  $a_w$ -region was also derived from the equations (**Chapter 2**).

## 2.2.6 RELAXOMETRY BY <sup>1</sup>H TIME DOMAIN NUCLEAR MAGNETIC RESONANCE

A Maran Ultra NMR spectrometer (Resonance Instruments Ltd., Witney, United Kingdom) at 30.7 MHz proton resonance frequency was used for the <sup>1</sup>H NMR measurements of the transverse relaxation time  $T_2$  and the two-dimensional correlated diffusion coefficient  $D$  and  $T_2$ .

### 2.2.6.1 RELAXOMETRY BY <sup>1</sup>H TIME DOMAIN NUCLEAR MAGNETIC RESONANCE ON THE PELLETS AND PROTEIN-RICH PARTICLE DISPERSIONS

To obtain  $T_2$ -spectra of the protein-rich particle pellets, pellets of protein-rich particles were prepared first, according to Section 2.2.1. The tip of the Eppendorf tubes, in which the pellets were present, was cut off and placed in an NMR-tube, because this method least disturbed the samples (**Chapter 3**). A standard Carr–Purcell–Meiboom–Gill (CPMG) pulse sequence was applied to obtain  $T_2$ -relaxation decay curves of the pellets. This pulse consisted of 16,384 echoes, with an echo time of 1 ms (five data points each). In total, 16 scans were made with a repetition time of 30 s, and averaged. Then the data were subjected to a numerical inverse Laplace transformation, as implemented in CONTIN,<sup>[113]</sup>

to get  $T_2$ -spectra that showed the relative intensity as a function of  $T_2$ . Pellets of both conditions (hydrating for 0 h and 3 h) were analysed in duplicate. The average of the  $T_2$ -values of the peak of the highest curve was used in the calculations.

Curves, relating the relaxation rate ( $R_2 = 1/T_2$ ) to the dry matter content (further referred to as calibration curves), of PPI and LPC particles were made by first making particle dispersions with various concentrations. These dispersions were hydrated by mixing them at 100 rpm at room temperature, for at least 3 h. Dispersions that were too difficult to mix at 100 rpm were mixed at 200 rpm. Then, 125  $\mu$ l of the dispersions was placed in an NMR tube. Samples with a viscosity that was too high to be transferred to the NMR tubes by pipet were placed in a cut-off Eppendorf tip and subsequently in a NMR tube. Then,  $T_2$ -relaxation decay curves were obtained, using the same settings as for the pellets. Each concentration was measured at least in duplicate, and their dry matter content was determined in triplicate, by drying the dispersions in an oven at 105 °C for 24 h. For SPI and LPC, the  $T_2$ -relaxation decay curves of Dekkers et al. (2016)<sup>[41]</sup> were used. All these decay curves were analysed with CONTIN to obtain  $T_2$ -graphs. From those graphs the average  $T_2$ -values were calculated from the  $T_2$  values of the highest peak of the samples.

#### 2.2.6.2 DIFFUSION-RELAXATION CORRELATION SPECTROSCOPY ON THE PROTEIN-RICH PARTICLE PELLETS

Pellets of protein-rich particles were made by adding excess water and hydrating the particles for 3 h and centrifuging them (Section 2.2.1). These pellets were used for the 2-dimensional correlated transverse relaxation time ( $T_2$ ) and diffusion coefficient ( $D$ ) measurement. This measurement consisted of a pulsed field gradient stimulated echo NMR pulse sequence (PFG-STE) to measure diffusion, combined with a CPMG pulse sequence<sup>[157]</sup> to measure  $T_2$ ; also referred to as DRCOSY (Diffusion Relaxation COrrrelation Spectroscopy).<sup>[122]</sup> A 2D numerical inverse Laplace transform spectrum was used to analyse these sequences, resulting in a correlation between  $T_2$  and  $D$ .<sup>[74][137][162]</sup> For the  $D$ -measurement, a diffusion encoding time of 20 ms was used, and a 2 ms duration for the PFG sequence. The experiment was performed 22 times with varying PFG gradient strengths, ranging from 0 to 1.21 T/m, to improve the signal-to-noise ratio. Each PFG gradient strength was repeatedly applied 32 times, with a repetition time of 5 s. The CPMG pulse that was applied for the  $T_2$  determination consisted of 4096 echoes with an echo time of 0.5 ms. The 2D datasets were processed in IDL (ITT Visual Information Solution, Boulder, CO USA) and analysed with MATLAB (The MathWorks, Inc., Natick, MA USA) to obtain DRCOSY spectra. This measurement was performed twice for each kind of protein pellet.

## **3 RESULTS**

### **3.1 WATER-BINDING CAPACITY OF PROTEIN-RICH POWDER PELLETS VIA WEIGHING**

The water-binding capacities of pellets (WBC-P) of pea protein isolate (PPI), soy protein isolate (SPI), lupin protein concentrate (LPC), and vital wheat gluten (VWG), show that the WBC-P of SPI was the largest, followed by PPI, LPC, and VWG, for both hydration times (Table 8). We hypothesized that a longer hydration time could increase the swelling of the proteins, resulting in a larger WBC-P. However, this effect of time was not very clearly observed (Table 8), suggesting that all materials absorbed water quickly. A larger hydration time only caused a decrease in the WBC-P of SPI. This may have been caused by more effective packing of the particles and therefore less water being present between them, due to mixing during hydration.

**Table 8.** The water-binding capacity of the pellets (WPC-P) (g water/g dry matter) of pea protein isolate (PPI), soy protein isolate (SPI), lupin protein concentrate (LPC) and vital wheat gluten (VWG); measured via the pellet weight and time domain nuclear magnetic resonance (TD NMR), after hydrating the protein-rich particles for either 0 h or 3 h. In addition, the water-binding capacity of the structures (WBC-structures) (g water/g dry matter) and the ratio of water within and between the structures within these pellets; calculated via the area fraction of the proteins in the confocal laser scanning microscopy images.

Method → Material ↓	WBC-P (g water/g dry matter)				WBC-structures (g water/g dry matter)		Ratio in pellet water within : between structures	
	0 h		3 h		3 h		3 h	
	By pellet weight	Using TD NMR	By pellet weight	Using TD NMR	Using microscopy		Using microscopy	
PPI	5.5 (0.4)	3.9 (0.1)	5.6 (0.1)	4.3 (0.1)	5.6		1 : 0.0	
SPI	9.2 (0.2)	6.0 (0.1)	8.6 (0.2)	5.2 (0.1)	5.6		1 : 0.8	
LPC	2.8 (0.1)	2.7 (0.2)	3.0 (0.3)	3.3 (0.0)	1.6		1 : 1.0	
VWG	1.8 (0.0)	1.1 (0.0)	1.9 (0.0)	1.1 (0.0)	1.3		1 : 0.4	

The standard deviation is given within parentheses and is based on four measurements for the WBC-P, measured by the pellet weight; and two measurements for the WBC-P, calculated using TD NMR.

### 3.2 DISSOLUTION OF PROTEIN-RICH PARTICLES

During the WBC-P experiments, a certain amount of the material ended up in the supernatant, due to the partial dissolution of the material. Table 9 shows that VWG dissolved least, as calculated via either the solubility of the material or the amount of dry matter in the supernatant. Both calculations showed that PPI dissolved most after 3 h, and LPC after 0 h of hydration. Overall, a hydration time of 3 h resulted in more material in the supernatant and a larger solubility than a hydration time of 0 h.

**Table 9.** Comparison of the solubility (%) and amount of dry matter (%) in the supernatant of pea protein isolate (PPI), soy protein isolate (SPI), lupin protein concentrate (LPC) and vital wheat gluten (VWG) after the protein-rich particles were hydrated for 0 h or 3 h.

Material	Solubility material (%)		Dry matter content supernatant (%)	
	t = 0 h	t = 3 h	t = 0 h	t = 3 h
PPI	8.5 (2.4)	26.3 (0.6)	1.9 (0.5)	5.0 (0.2)
SPI	n.d.*	7.8 (1.1)	n.d.*	4.0 (0.3)
LPC	18.7 (0.2)	22.3 (0.2)	2.6 (0.1)	3.2 (0.1)
VWG	4.4 (0.1)	5.9 (0.2)	0.6 (0.0)	0.8 (0.0)

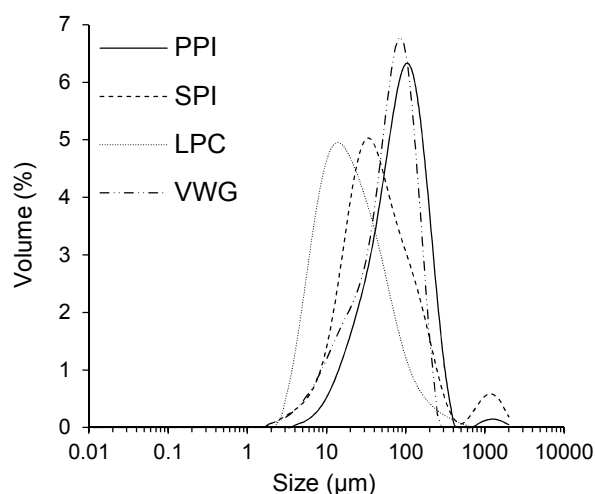
The standard deviation is given within parentheses and is based on four measurements.

\* not determined (as described in Section 2.2.2)

### 3.3 SIZE AND SHAPE OF PROTEIN-RICH PARTICLES AND THEIR PELLETS

All dry protein-rich particles were irregularly shaped and had a wide size distribution (Table 10 and Fig. 28). LPC consisted of the smallest particles. The size of the bulk volume of SPI particles was somewhat larger than that of LPC particles (Fig. 28). However, some particles had a remarkably larger volume, resulting in an average size ( $d_{4,3}$ ) comparable to that of PPI particles. The VWG particles had an average size ( $d_{4,3}$ ) that was smaller than the SPI particles, and the PPI particles were the largest (Fig. 28). Furthermore, the LPC and VWG particles were solid, whereas voids were frequently found within the SPI and PPI particles (Table 10). In addition, the surface of the SPI and PPI particles was coarser than that of the LPC and VWG particles (Table 10).

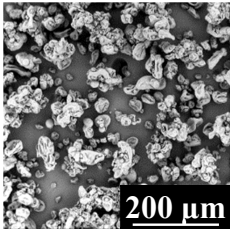
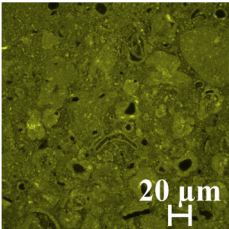
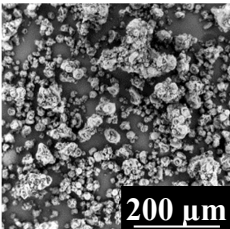
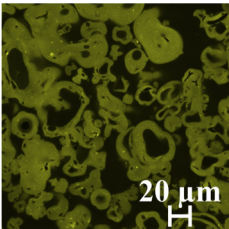
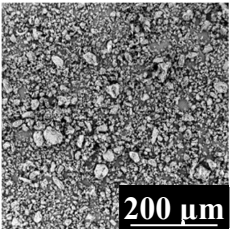
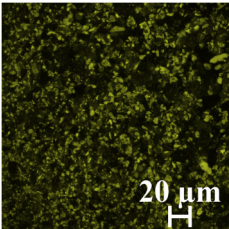
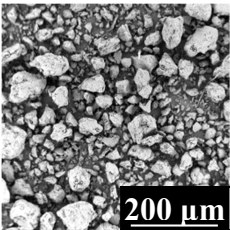
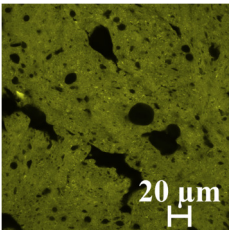




**Fig. 28.** Size distributions of the dry particles of (A) pea protein isolate (PPI) (solid line), (B) soy protein isolate (SPI) (dashed line), (C) lupin protein concentrate (LPC) (dotted line), and (D) vital wheat gluten (VWG) (dashed-dotted line).

Images of the pellets that were formed after centrifuging the hydrated protein-rich particles showed that not all water was removed upon centrifugation (Table 10; black space)—though we cannot exclude the possibility that part of the black space is air. With most pellets, the individual particles were no longer clearly visible. The one exception is in case of the LPC pellet. Therefore, we will use the term “protein structures” for all fully hydrated protein-rich materials. There are some differences between structures and particles, which we will elaborate on later in the discussion. Furthermore, it was found that these pellets exhibited, roughly speaking, two kinds of morphologies (Table 10): protein structures suspended in water, or a protein network with water bound in its pores. The PPI pellet consisted of a fully packed system of swollen protein structures with some pores. However, it may have also been a protein-rich continuous network with some pores and separate protein structures. The SPI pellet was made of swollen protein structures, surrounded by water. It may be that some structures were also aggregated, or that a semi-continuous network was formed. In addition, relatively large pores were found within the structures. In the LPC pellet, small protein structures were visible, surrounded by water. The VWG pellet was a continuous network, with suspended pores filled with water. In this network the VWG particles could no longer be distinguished, which was also found by Cumming & Tung (1975)<sup>[34]</sup> and Roccia, Ribotta, Pérez, & León (2009)<sup>[125]</sup> when they added water to VWG.

**Table 10.** The size and shape of the dry particles of pea protein isolate (PPI), soy protein isolate (SPI), lupin protein concentrate (LPC), and vital wheat gluten (VWG). In addition, the microstructure of pellets made from these particles, obtained after hydrating them for 3 h in an excess amount of water and subsequent centrifugation; the area fraction of protein-rich structures in these images of the pellets (-); and the resulting dry matter content in the protein-rich structures in the pellet (%).

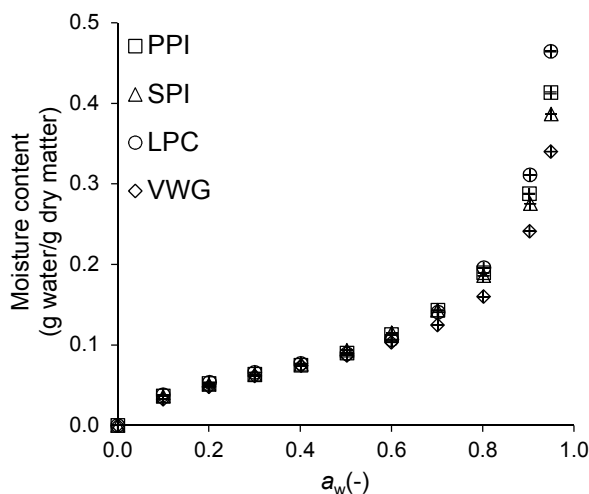
Material	Image particles	Image pellets	Area fraction protein-rich structures (-)	Dry matter content protein-rich structures (%)
PPI			0.98 (0.01)	15
SPI			0.57 (0.09)	15
LPC			0.59 (0.17)	39
VWG			0.78 (0.06)	43

The area fraction of water and the protein structures in the pellets was estimated from the images of the pellets (Table 10). With this information, the WBC of the protein-rich structures themselves was approximated (Table 8). This resulted in similar amounts of water being bound by the SPI and PPI protein structures, and by the LPC and VWG structures. The swelling of the structures was also estimated by determining the size of the structures after swelling (**Appendix C**). However, the curves seemed to be significantly affected by either dissolution of the material or by aggregation, or both, and are therefore not taken into account here.

### 3.4 DYNAMIC ADSORPTION ISOTHERMS

The dynamic adsorption isotherms of the protein particles (Fig. 29) show that until  $a_w = 0.6$ , the water sorption of all protein particles overlap. A possible explanation may be, based on the Flory–Rehner theory, that the differences in crosslink density and hydrophilicity of the various particles resulted in a similar water uptake. However, Paudel, et al. (2015)<sup>[111]</sup> state that the effect of crosslink density is negligible below  $a_w = 0.8$ . Therefore, this overlap may also mean that the protein–water interaction parameter  $\chi$  was similar for the various materials; in other words: the hydrophilicity of the materials was similar.

At  $a_w = 0.7$ , VWG started to deviate from the other materials, because it absorbed less water than the other particles (Fig. 29). At larger  $a_w$ -values, VWG also bound the least amount of water. Differences in the amount of water absorbed by the other particles were found at  $a_w = 0.9$  and  $0.95$  (Fig. 29). LPC absorbed the largest amount of water, followed by PPI and SPI. Differences in this region can be explained by differences in the crosslink density of the materials. The higher its crosslink density, the less water is absorbed by the material, and the less it is able to swell at high  $a_w$ -values. As a side note, the effect of pores on swelling is not taken into account with the Flory–Rehner theory. However, pores also affect the adsorption isotherm over the whole  $a_w$ -range (small pores at lower  $a_w$ -regions and larger pores in the larger  $a_w$ -regions).<sup>[80][86]</sup>



**Fig. 29.** Dynamic adsorption isotherms of pea protein isolate (PPI) (open square), soy protein isolate (SPI) (open triangle), lupin protein concentrate (LPC) (open circle), and vital wheat gluten (VWG) (open diamond). The standard deviation is based on two measurements.

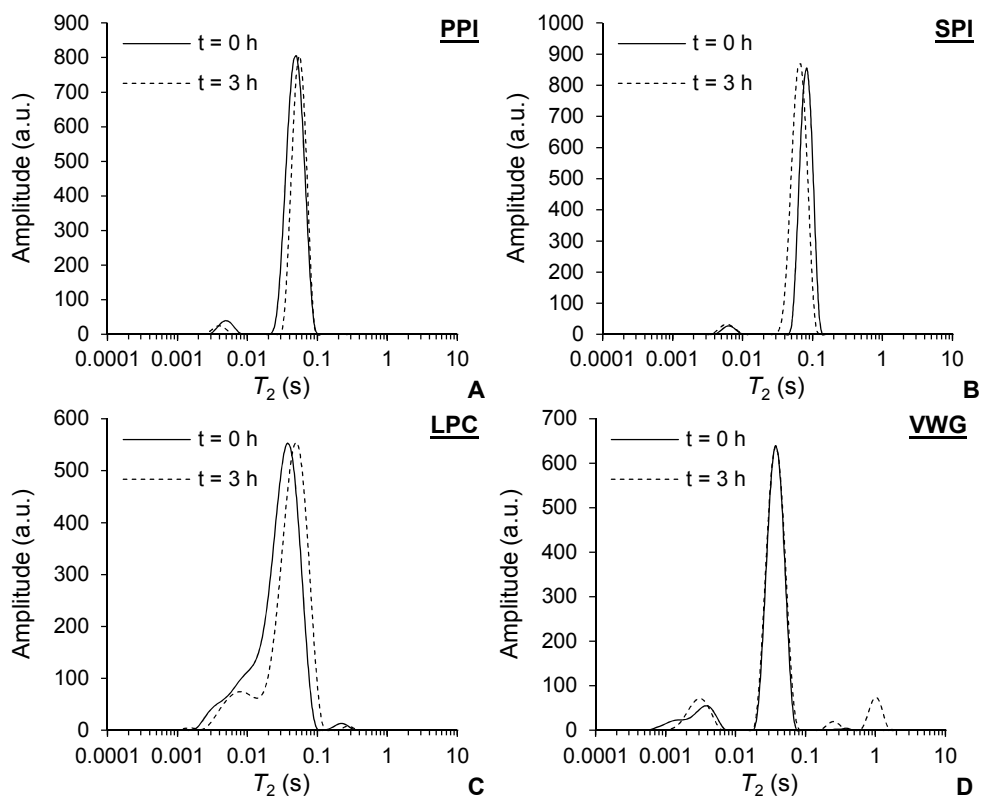
### 3.5 RELAXOMETRY BY $^1\text{H}$ TIME DOMAIN NUCLEAR MAGNETIC RESONANCE ON THE PELLETS OF PROTEIN-RICH PARTICLES

Pellets of the protein-rich particles were investigated with time domain nuclear magnetic resonance (TD NMR). PPI pellet spectra showed two peaks when hydrated for 0 h and 3 h (Fig. 30A): one main peak and a smaller peak to the left of the main peak. The pellets of the particles which were hydrated for 3 h had a narrower main peak with a slightly higher  $T_2$ -value, whereas the small peak had a slightly lower  $T_2$ -value.

SPI pellets showed a main peak and a smaller peak to its left (Fig. 30B). When SPI was hydrated for 3 h instead of for 0 h, the main peak shifted to the left, while the small peak did not change.

The LPC spectra show a main peak with a shoulder on its left when the proteins were hydrated for 0 h (Fig. 30C). This shoulder became more pronounced after 3 h of hydration. In addition, the main peak shifted to the right after 3 h of hydration.

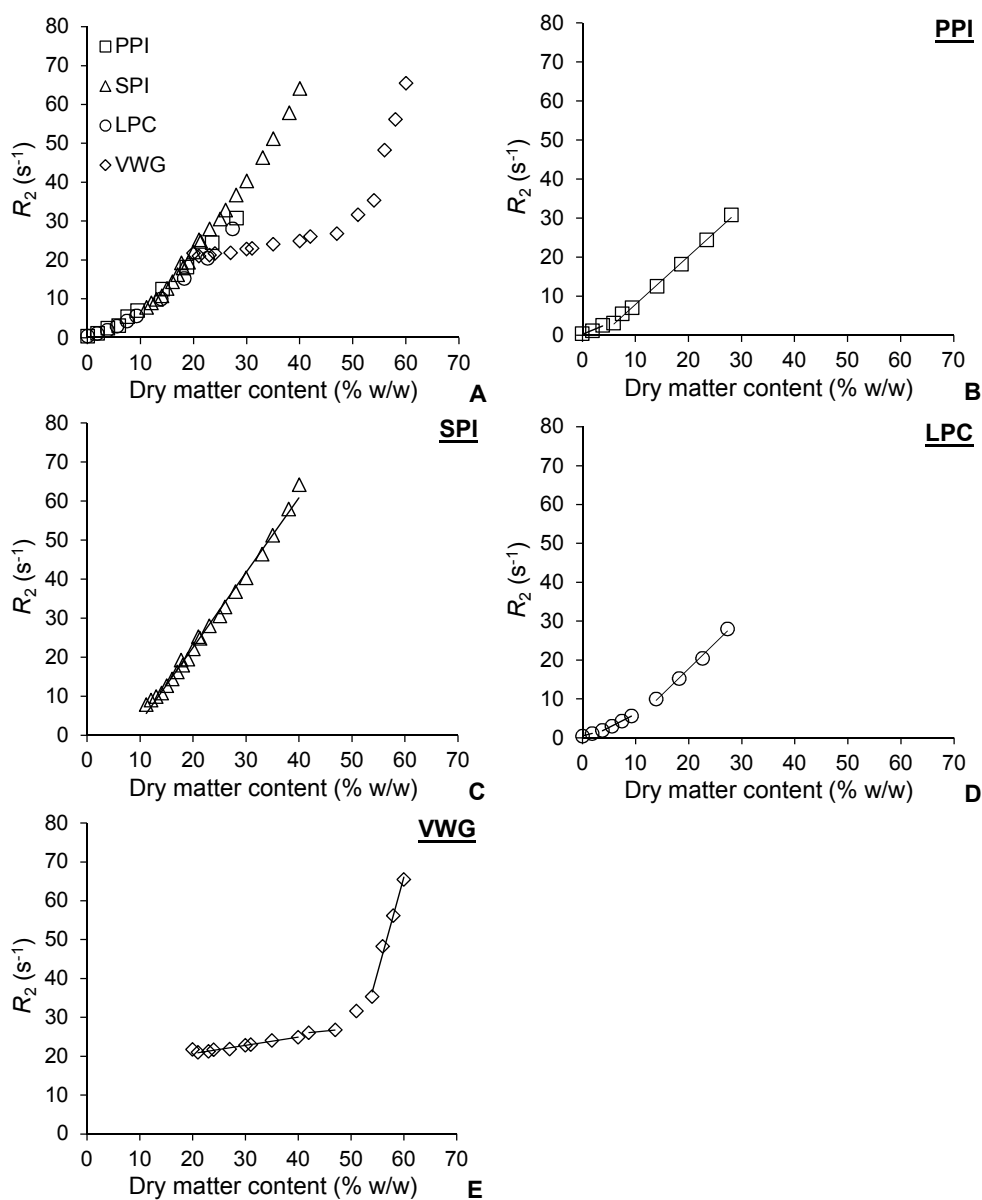
VWG pellet spectra also showed a main peak (Fig. 30D). In addition, a single smaller peak to the left of the main peak, with its own shoulder on its left, was present when gluten was hydrated for 0 h. The pellet, obtained from VWG that was hydrated for 3 h, showed a main peak and three smaller peaks: one peak on the left side of the main peak, and two peaks to the right. The  $T_2$ -value of the top of the main water peak did not change when hydrated for either 0 h or 3 h.



**Fig. 30.** The CONTIN  $T_2$ -spectra of pellets of (A) pea protein isolate (PPI), (B) soy protein isolate (SPI), (C) lupin protein concentrate (LPC), and (D) vital wheat gluten (VWG). Pellets were obtained from the water-binding capacity experiment, in which excess water was added to the protein-rich particles and the particles were hydrated for 0 h (solid line) and 3 h (dashed line).

### **3.6 RELAXOMETRY BY $^1\text{H}$ TIME DOMAIN NUCLEAR MAGNETIC RESONANCE ON PROTEIN-RICH PARTICLE DISPERSIONS**

Calibration curves were made from all protein-rich powders that relate  $R_2$  ( $R_2 = 1/T_2$ ) to the dry matter content, by using the largest peak in the  $T_2$ -spectra (Fig. 31A). For PPI, LPC and VWG, this calibration curve shows a non-linear correlation, while for SPI an almost linear correlation was obtained. A non-linear correlation between the dry matter concentration and  $R_2$  was also described for both undenatured and denatured bovine serum albumine dispersions (0 to 60% w/w dry matter).<sup>[104][105]</sup> Linear correlations were reported for whey protein concentrate, egg white powder, and soybean 7S globulin, in a concentration range of 6 to 18% w/v dry matter.<sup>[87]</sup> Linear correlations for our protein samples were also found in every calibration curve at certain concentration ranges, the length of which was dependent upon the material tested (Fig. 31B, C, D and E).



**Fig. 31.** (A) Calibration curves that correlate the relaxation rate  $R_2$  (s<sup>-1</sup>) with the dry matter content (% w/w) of pea protein isolate (PPI) (open square), soy protein isolate (SPI)\* (open triangle) lupin protein concentrate (LPC) (open circle), and vital wheat gluten (VWG)\* (open diamond). Calibration curves of PPI (B), SPI (C), LPC (D) and VWG (E) in which the linear regimes are denoted with a solid line.

\* Data obtained from Dekkers, et al. (2016)<sup>[41]</sup>

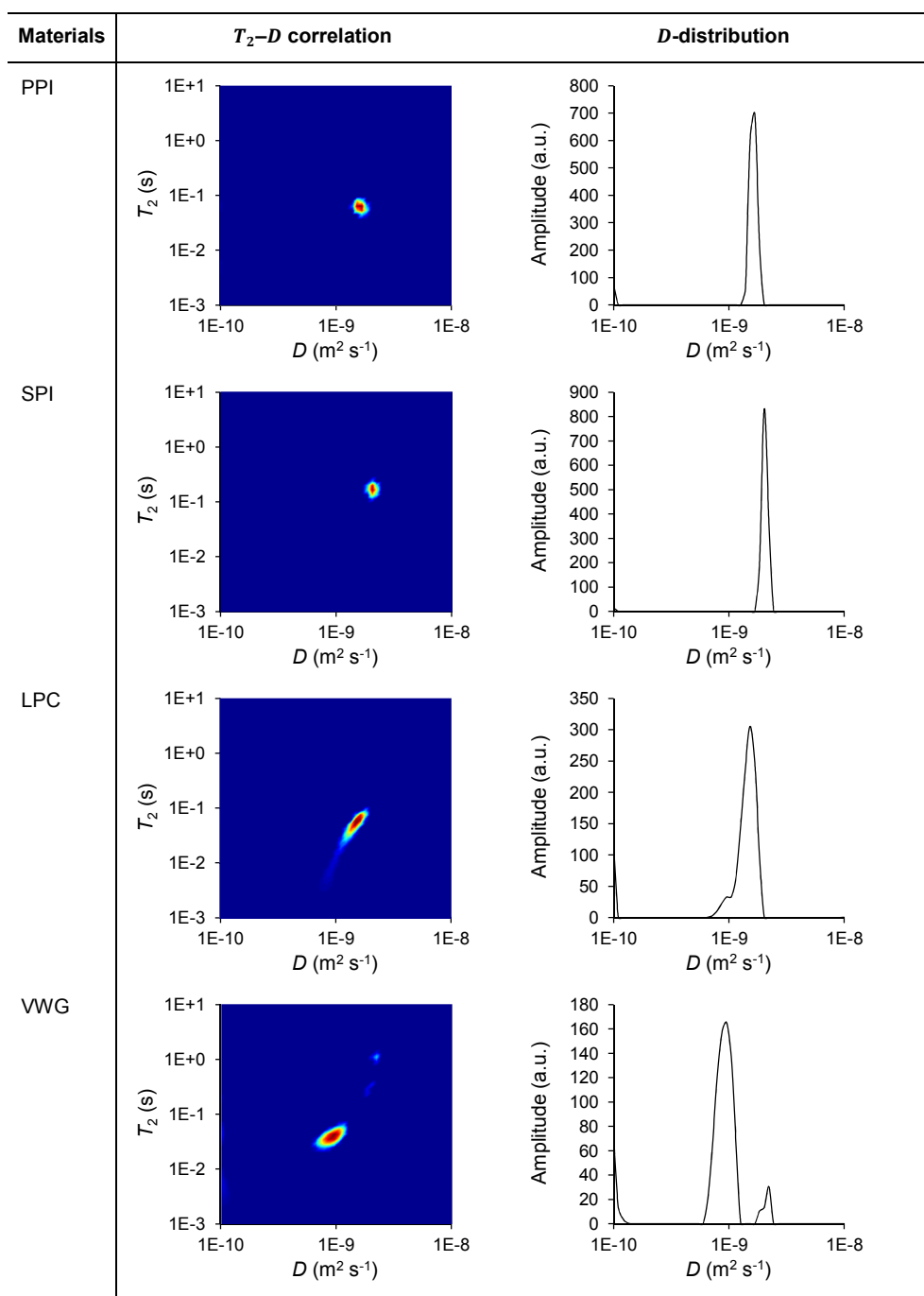
The calibration curves of PPI, SPI and LPC overlapped at low concentrations, up to approximately 15% w/w (Fig. 31A). At concentrations above 15% w/w, PPI and LPC showed similar behaviour; unlike SPI, whose  $R_2$ -dry matter content correlation increased more sharply. The VWG calibration curve could only be measured from 20% w/w onwards, because, at lower concentrations, water was no longer absorbed by the clumped gluten. The addition of extra water just added to the amount of bulk water (compare pouring water in a glass with a marble in it). The VWG calibration curve actually showed the same trend as PPI and LPC (i.e., a non-linear correlation), just starting at a higher  $R_2$ -value and dry matter content. However, the VWG calibration curve increased more gradually in the beginning of the curve than was found for the other materials.

The main peaks found in Fig. 30A, B, C, and D and the calibration curves of Fig. 31A, were used to calculate the WBC-P (Table 8). Remarkably, Table 8 shows that a significantly lower WBC-P was obtained when the WBC-P was calculated from the TD NMR data for PPI, SPI and VWG. The WBC-P of LPC was similar, regardless of when it was calculated from the weight of the pellet or from TD NMR.

### 3.7 DIFFUSION-RELAXATION CORRELATION SPECTROSCOPY ON THE PROTEIN-RICH PARTICLE PELLETS

Differences between the various samples were found when measuring the diffusivity of water in the pellet (Fig. 32). PPI and SPI pellets both showed one clear diffusion coefficient ( $D$ )-peak, with a slightly lower  $D$ -value for the PPI pellet. The LPC pellet had one main  $D$ -peak (which had a lower  $D$ -value than PPI) with a small shoulder on the left-hand side (thus indicating an even lower  $D$ -value). The VWG pellet showed a main diffusion coefficient peak, which had the lowest  $D$ -value among all pellets tested, as well as a smaller peak with a larger diffusion coefficient. Overall, a larger WBC-P correlated with a larger  $D$ -value of the main peak.

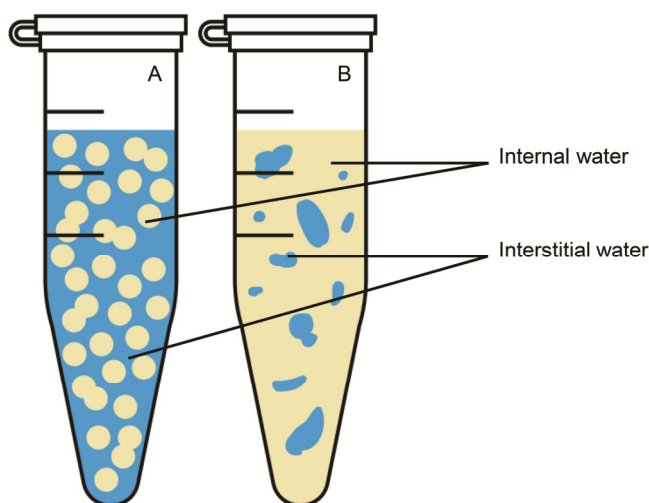




**Fig. 32.** The  $T_2$ - $D$  (diffusion coefficient) correlation and the  $D$ -distribution of pellets from pea protein isolate (PPI), soy protein isolate (SPI), lupin protein concentrate (LPC), and vital wheat gluten (VWG), as made by adding an excess amount of water and hydrating the protein-rich particles for 3 h.

## 4 DISCUSSION

In this research, we investigated the water-binding properties of pellets originating from four kinds of plant protein particles: pea protein isolate (PPI), soy protein isolate (SPI), lupin protein concentrate (LPC) and vital wheat gluten (VWG). To obtain pellets of these materials, excess water was first added to the particles. The resultant dispersion was hydrated and immediately centrifuged (referred to as hydrated for 0 h), or left for 3 h of hydration and then centrifuged. Centrifugation of the dispersions resulted in the formation of supernatant with some dissolved material (Table 9) and a pellet. Within the pellet, water was either bound internally (within the structures or network) or interstitially (between the structures or within the pores of the network) (Table 10; Fig. 33). To determine the general underpinnings of the water-binding by protein structures in pellets, the water-binding of each type of pellet will be discussed first. Thereafter, the general trends will be extracted from this information.



**Fig. 33.** The two kinds of pellet microstructures that can be obtained after centrifuging a dispersion of protein particles: (A) The pellet consists of protein structures that contain internal water. These structures are dispersed in interstitial water; (B) The pellet consists of a (semi-)continuous network that contains internal water. The network's micropores contain additional interstitial water.

### 4.1 WATER-BINDING IN PEA PROTEIN ISOLATE PELLETS

The PPI pellet consisted of swollen protein structures (or a network) with barely any interstitial water (Table 10). This coincides with the PPI pellets' *D*-distribution, which showed one *D*-peak with a *D*-value lower than that of bulk water (Fig. 32; *D*-value of

bulk water is approximately  $2.5 \times 10^{-9} \text{ m}^2 \text{ s}^{-1}$ ),<sup>[120][127]</sup> implying the presence of a homogeneous pellet structure in which water was slightly restricted in its mobility. In addition, only one main  $T_2$ -peak was found in the  $T_2$ -spectra of the pellet, which also points to the presence of a single water domain (Fig. 30A). The isotherm of PPI suggests that PPI can swell relatively well, because it contained the second largest amount of water at  $a_w > 0.8$  (Fig. 29). This all indicates that the WBC-P of PPI was predominately determined by the relatively large swelling capacity of PPI.

In addition, it seems that the PPI structures were weak and deformable, which may have caused interstitial water to be easily expelled and the structures to press together or even coalesce, resulting in a homogeneous structure after centrifugation (Table 10). This also seems to be a viable explanation for the discrepancy between the water-binding capacities of the pellets (WBC-Ps), as calculated via the weight of the pellet and TD NMR (Table 8). The only difference between the treatments of the samples used for the calibration curve and the pellets is the centrifugation step. This suggests that the interaction between the protein structures and water changed due to centrifugation. Both PPI and SPI particles contained large voids (Table 10) that may have weakened their structure, and showed a discrepancy in the WBC-Ps, as calculated via both methods (Table 8). In contrast, the LPC particles were more solid (Table 10), and their WBC-P was similar for both methods (Table 8). However, it is not completely clear from the images of the pellets whether coalescence, collapse, or both, of the PPI and SPI structures did indeed occur (Table 10). A second possibility is that air, present within the voids of the PPI and SPI particles, increased the  $T_2$ -values of the dispersions.<sup>[165]</sup> This air may have been removed from the sample during centrifugation, resulting in a lower  $T_2$ -value of the pellets as compared to that of a dispersion with the same concentration, and a lower WBC.

## 4.2 WATER-BINDING IN SOY PROTEIN ISOLATE PELLETS

The pellet of SPI contained the largest amount of water (Table 8): a combination of water bound within the SPI structures (and its pores), and between the structures (Table 10). Although two or three water domains were visible in the images of the SPI pellet (Table 10), only one main peak was found in the  $T_2$ -spectra (Fig. 30B). This discrepancy is thought to be caused by a fast exchange of water between the various domains; the  $D$ -value of water in the SPI pellet had a similar  $D$ -value to bulk water (Fig. 32), resulting in an average  $T_2$ -peak for the water domains.<sup>[92]</sup> We hypothesize that water exchanged quickly in the SPI pellet, because all structures were relatively open: the dry SPI particles comprised voids, and the SPI pellet contained large water domains outside, and sometimes within, the SPI structures (Table 10).

Swelling of the SPI structures seems to have played an important role on the overall water-binding by the pellet. The swollen SPI structures contained, according to rough

calculations based on the CLSM images, the same amount of water as the PPI structures (Table 8). In addition, a significant amount of water was visible between the protein structures and within the pores of the protein structures (Table 10). It is likely that this water contained proteins, either dissolved or as highly swollen structures, because the supernatant of SPI contained some dry matter (Table 9). Therefore it may be that interstitial water was bound by some highly swollen structures that were dragged down during centrifugation, or by dissolved proteins (as suggested for water-binding between heat-gelated whey protein microparticles (**Chapters 2 and 3**)). It also may be that interstitial water was bound due to capillary forces, or particle–particle interactions, or a combination thereof (as reported for cold-gelated whey protein microparticles (**Chapter 4**)).

We speculate that the difference in the manner of water-binding in the SPI pellet, compared to in the PPI pellet, may be partly caused by the strength of the swollen SPI structures. According to the isotherm of the SPI pellet, less water was bound by SPI than by PPI at the same water-activity (Fig. 29), suggesting that the SPI particles contained more crosslinks than the PPI particles did. Hence it is possible that the SPI particles and their pellet were less deformed by centrifugation and that less water was expelled.

### 4.3 WATER-BINDING IN LUPIN PROTEIN CONCENTRATE PELLETS

The LPC pellet had the second lowest WBC-P among the tested materials (Table 8). The following results suggest that the LPC structures were not able to swell much, which was also found for lupin protein isolate.<sup>[16]</sup> First of all, images of the LPC pellet show that the LPC structures were still relatively small (Table 10), resulting in a rather small WBC for the LPC structures themselves (Table 8). Secondly, it was expected that the LPC structures' small size would lead to one  $T_2$ -peak in their  $T_2$ -spectra, being an average of both internal and interstitial water. Averaging of the  $T_2$ -peaks will occur in case of a combination of small structures; small difference in relaxation rate ( $R_2$ ) between the domains; and fast diffusion of water between the domains.<sup>[92]</sup> However, a shoulder (at 0 h of hydration) and a smaller peak (at 3 h of hydration) were visible to the left of the main peak (Fig. 30C). This means that the difference in  $R_2$  ( $\Delta R_2$ ) between internal and interstitial water was rather large, or the diffusion in water was limited, or a combination of both caused a limited water exchange. A considerable amount of material is expected to be present within the interstitial water that increased the  $R_2$ -value, because the solubility of LPC was relatively large (Table 9). Therefore, to reach a sufficiently large difference between the  $R_2$ -values, the  $R_2$ -value of internal water must have been even larger. This could only have occurred when the LPC structures absorbed a limited amount of water. The  $D$ -distribution of the LPC pellet suggested the presence of two water domains, as shown by the main peak with shoulder (Fig. 32); which can be explained by the presence of dense LPC structures, and

interstitial water with a lower dry matter content. Only the isotherm of LPC is in contradiction with the idea that LPC particles did not swell much, because it showed that LPC particles contained the largest amount of water at  $a_w > 0.8$  among all tested particles (Fig. 29). This large water-binding may have been caused by the presence of carbohydrates in LPC. It is known that hygroscopic components like carbohydrates can bind a large amount of water in the higher  $a_w$ -region and may cause additional water-binding via liquid bridges.<sup>[112]</sup> However, the isotherm was not measured at  $a_w > 0.95$ , which is the expected  $a_w$  of structures when swollen. Up to  $a_w = 0.95$ , the total amount of bound water was only 0.46 g water/g dry matter (Fig. 29), which is an order of magnitude smaller than water-binding in excess water conditions (Table 8).

Besides swelling, the presence of interstitial water also seems to be a significant factor that contributes to the WBC-P, according to the ratio of water inside and between the protein structures (Table 8). The ability to calculate the WBC-P via the  $T_2$ -value of the main curve (Table 8), which is likely to be related to water between the LPC structures, also implies that interstitial water played a significant role. The manner in which water is bound between the LPC structures is not yet clear, though it is possible that inclusion is due to (a possible combination of) capillary forces, interactions between structures, the presence of highly swollen protein structures, or swollen proteins. Additionally, water may have been bound by carbohydrates.

#### 4.4 WATER-BINDING IN VITAL WHEAT GLUTEN PELLETS

VWG seems to be a special case in comparison with the other proteins that were tested. Its  $R_2$ -dry matter content calibration curve deviated significantly from the curves obtained by the other proteins (Fig. 31A). In addition, the  $T_2$ -spectra of the VWG pellet had one main peak and several smaller peaks (Fig. 30D). From our results it is not clear why VWG behaved so differently, though it is known that VWG has unique properties.<sup>[38]</sup>

It seems that the WBC-P of VWG was predominantly determined by the (relatively small) amount of water that could be bound by VWG, because the WBC-P was similar to the WBC of VWG (Table 8). This is remarkable, because interstitial water was present in the pellet (Table 10). However, this amount of water did not decrease the amount of water bound by VWG, because the amount of water in the pellet was relatively small; lowest among all materials tested (Table 8). The isotherm of VWG also showed that VWG swelled the least of all tested particles (Fig. 29). This may be caused by the hydrophobic nature of VWG.<sup>[38]</sup> However, its adsorption isotherm did not bear out that VWG is more hydrophobic than the other particles.

This hydrophobicity may also have caused the hydrophobic groups to drive water from their vicinity towards hydrophilic parts of VWG, resulting in a very strong water-binding by these parts: the  $D$ -value of the main peak is relatively small, suggesting water to be

rather restricted in its mobility (Fig. 32). The two peaks in the  $D$ -distribution (Fig. 32), as well as the main peak with several smaller peaks in the  $T_2$ -spectra (Fig. 30D), show that the VWG pellet is heterogeneous: water is bound in several distinct water domains; more than we could distinguish in the image of the pellet (Table 10). Previous research on gluten–water systems,<sup>[19]</sup> showed that the peaks were related to the  $-\text{CH}$ ,  $-\text{NH}$ ,  $-\text{OH}$  or  $-\text{SH}$  protons (peaks to the left of the main peak); gluten sheets (main peak) that reacted with water; and water expelled by gluten (peak to the right of the main peak). We consider this division in water domains plausible, even though these water-domains are not visible in the images of the pellet (Table 10).

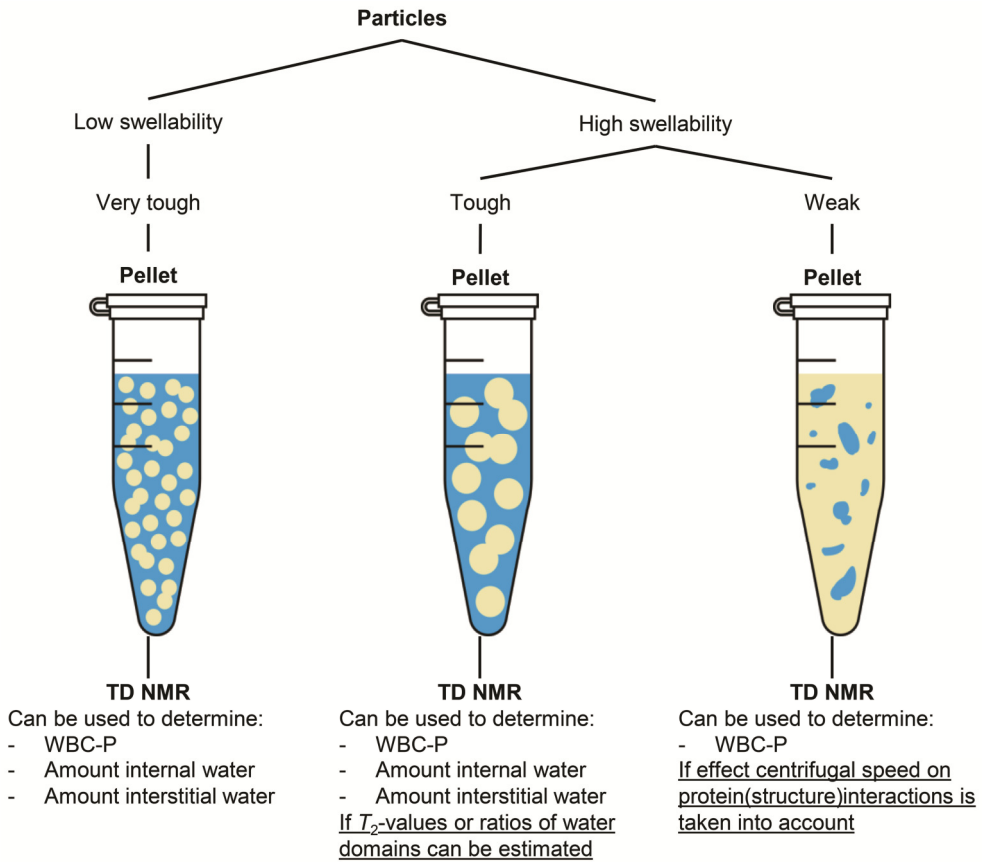
#### 4.5 WATER-BINDING CAPACITY OF PROTEIN-RICH PARTICLE PELLETS

The information above shows that there are some general principles that are valid when the WBC of protein particles is determined via their pellet, when the special case of VWG is not taken into account. First of all, images of the pellets show that both internal and interstitial water domains were present within the pellets (Table 10). Only the PPI pellet contained barely any interstitial water. Consequently, a lower WBC was found for the structures of SPI and LPC than for their pellets, when calculated from the protein area-fraction of the image of the pellet, whereas a similar WBC was found for PPI structures and pellets (Table 8). In addition, it may be that PPI formed a new network; and that SPI structures partly coalesced or formed a semi-continuous network, while determining the WBC-P (Table 10). Such pellets most likely no longer represent the interaction of *particles* with water, and may therefore be used to explain why the WBC-P was only partly correlated with the WBC of the constituent particles (Table 8), and why it could not be predicted from the sorption isotherms (Table 8 and Fig. 29). However, it may also be that swelling is not always the determinant factor for the WBC-P. In light of the above, we conclude that the WBC-P is unequal to the WBC of the particles themselves.

Furthermore, it can be surmised from the information in the previous sections that the amount of water that is bound within the pellets is determined by two factors: the toughness of the particles (i.e., their ability to swell and to resist disintegration and expulsion of water during centrifugation—which is likely to be influenced by the crosslink density of the particles and the presence of pores), and their ability to bind interstitial water (Fig. 34). This toughness determines which of the two roughly distinguished microstructures the pellet contains: that of particles suspended in water, or of a protein network with water inside its pores (there may also be an intermediate structure present: partly coalesced particles) (Fig. 33). This toughness also seems to determine in which way TD NMR can be used to provide information about the WBC-P and the amounts of water in the different domains (Fig. 34).

In case the particles are very tough (i.e., possessing a high crosslink density and a small amount of pores), as is the case with LPC particles and heat-gelated microparticles (**Chapter 3**), they are unable to absorb a large amount of water, and will remain present as particles in the pellet, surrounded by water. It is expected that the amount of water in both water domains, as well as the WBC-P, can be determined with TD NMR, due to the high density of the particles (Fig. 34).

When particles are able to swell sufficiently, they remain present as particles in their pellet, if they are also tough enough to withstand the centrifugal force (like SPI and cold-gelated microparticles (**Chapter 4**)). In that case water will, most likely, exchange quickly between the two water domains, allowing the use of a fast exchange model to estimate the water division in the pellet and the WBC-P (Fig. 34). However, if particles are too weak to withstand the centrifugal force, a new structure (network) will be created (as seems to be the case for PPI). This network will probably contain an insignificant amount of pores, since the proteins would not be able to maintain them. In this case, TD NMR may be used to determine the WBC-P directly from the pellet, if the effect of centrifugation on the protein–water interactions is known (Fig. 34).



**Fig. 34.** Schematic representation of the effect of the toughness of protein particles on the swellability of the particles; the microstructure of the formed pellet; and the ability to obtain more information about the pellet and its water domains, using time domain nuclear magnetic resonance (TD NMR).

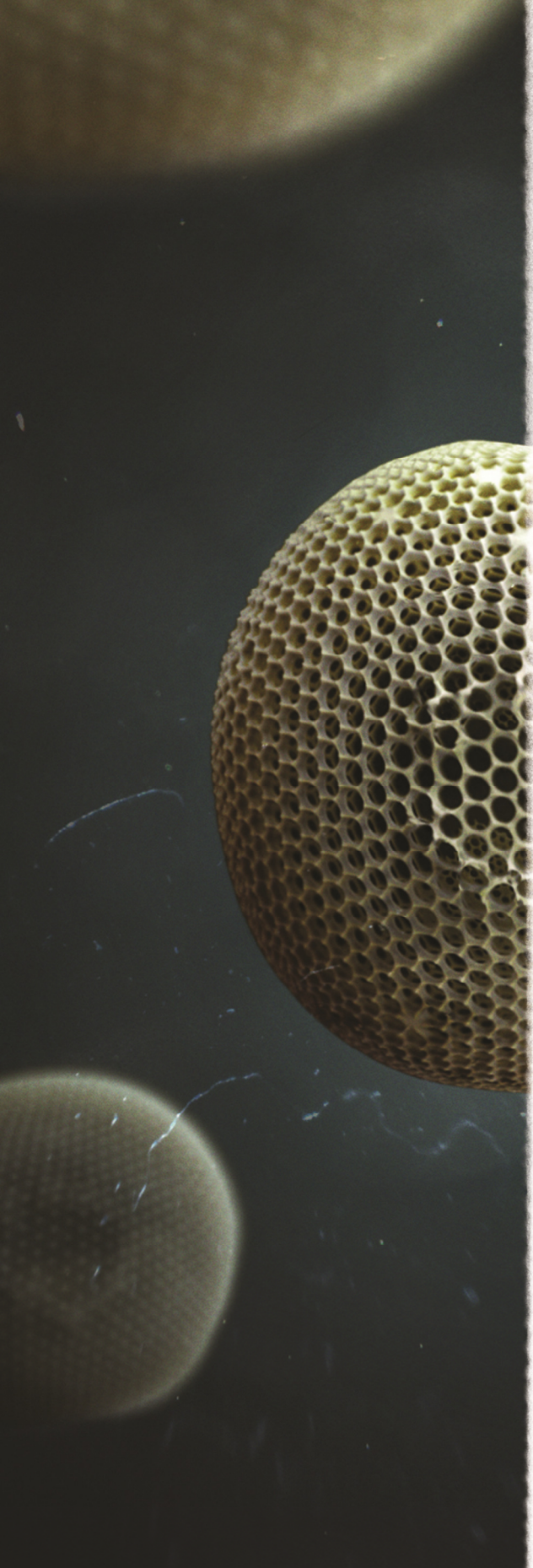


## 5 CONCLUSIONS

The water-binding capacity (WBC) of proteinaceous particles is commonly calculated from the pellet weight that is obtained after centrifuging a dispersion of these particles. Generally, it is not taken into account whether a significant amount of water is present between the particles. Soy, lupin, and gluten protein particles all formed a pellet that consisted of protein structures with a noticeable amount of interstitial water. Only the pea proteins formed a pellet that contained barely any interstitial water. In addition, it was found that the pellets formed, roughly speaking, two kinds of microstructures: particles suspended in water, or a protein network that additionally bound water in its pores. Such networks probably no longer represent the interaction of *particles* with water, resulting in other particle–water interactions. Consequently, the WBC of the pellet (WBC-P) differed from the WBC of the particles themselves. That is why the protein(structure)–water interactions of the protein particles and their pellets were further investigated with time domain nuclear magnetic resonance (TD NMR), among other tools. TD NMR turned out to be a good additional tool for this purpose, and has the potential to give an indication of the amount of water that is present in each water domain. From the information about the protein(structure)–water characteristics of the particles and their pellets, it was finally concluded that variations in the WBC-P were the result of differences in the toughness of the particles (i.e., their ability to swell and to resist disintegration and expulsion of water during centrifugation, which is likely influenced by the crosslink density of the particles and the presence of pores), and their ability to bind water interstitially.

## ACKNOWLEDGEMENTS

The authors would like to thank FrieslandCampina and NanoNextNL, a consortium of the government of the Netherlands and 130 partners, for their financial support of this research. In addition, we would like to thank Jarno Gieteling for his help with making the CLSM images; Wageningen light Microscopy Centre for the use of the CLSM; and Stefano Renzetti for measuring the isotherms. Furthermore, we would like to thank Wouter Perk for proofreading the manuscript.



*Chapter 6*

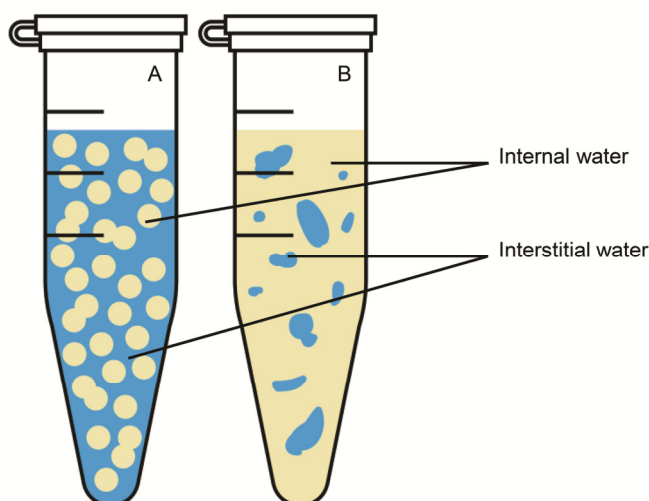
# GENERAL DISCUSSION

## 1 INTRODUCTION

The aim of this thesis is to gain a better understanding of the water-binding properties of protein microparticles (MPs). These are particles with a maximum size in the micro-range (1 to 1000  $\mu\text{m}$ ) that were obtained either by making them ourselves or via the industry. Insight in their water-binding properties is needed to eventually create protein particles that can absorb  $\geq 90\%$  w/w water and bind this water tightly. These particles can potentially be used in (dairy) products to decrease their caloric content, by increasing the total water content, without affecting sensory perception. Overall, we conclude that *pellets* of microparticles can indeed bind  $\geq 90\%$  w/w of water.

## 2 MAIN FINDINGS AND CONCLUSIONS

The water-binding capacity (WBC) is an important property of proteins, which quantifies the protein(structure)–water interactions. A frequently used method to determine the WBC of protein particles consists of first making a dispersion of the particles and centrifuging it, which leads to the formation of a pellet (i.e., a cake of protein particles) and supernatant. Pellets studied in this thesis had roughly two kinds of microstructures: that of particles suspended in water, or of a (semi-)continuous protein network with interstitial water in its pores (Fig. 35). The weight of the pellet is often considered as a good measure for the WBC of particles, thereby neglecting the amount of interstitial water.



**Fig. 35.** The two kinds of pellet microstructures that can be obtained after centrifuging a dispersion of protein particles. (A) The pellet consists of protein particles that contain internal water. These particles are dispersed in water (interstitial water). (B) The pellet consists of a (semi-)continuous network that contains internal water. The network's micropores contain additional interstitial water.

In this research we investigated the WBC of two types of whey protein MPs: heat-gelated whey protein microparticles (HG MPs) (**Chapters 2 and 3**) and cold-gelated MPs (CG MPs) (**Chapter 4**). In addition, the WBCs of pea protein isolate (PPI), soy protein isolate (SPI), lupin protein concentrate (LPC) and vital wheat gluten (VWG) particles were explored (**Chapter 5**). HG MPs were made by heating and simultaneously mixing a 40% w/w whey protein isolate (WPI) solution. The resulting broken gel pieces were dried and milled, providing HG MPs. CG MPs were made in a two-step process, of which the first step consisted of making aggregates by heating a 9% w/w WPI solution. Subsequently, an acidifier was added to reduce the charges on the aggregates, inducing gelation at

room temperature. A locust bean gum solution was added prior to gelation of the aggregates, which resulted in phase separation and the formation of CG MPs.

In **Chapter 2**, the Flory–Rehner model was used to ascertain which characteristics would increase the swelling capacity of MPs in water. This model showed that the crosslink density would be the most important factor for our research. To investigate this, the crosslink density of HG MPs was both increased and decreased (a type of nanostructuring). However, only a decrease in the crosslink density resulted in a significant change of the WBC of the pellet (WBC-P) (increasing from 6 to 9 g water/g dry matter). It is hypothesized that HG MPs already had a very high crosslink density; for that reason the *overall* crosslink density was not significantly affected by creating additional crosslinks. Although a decrease in the crosslink density resulted in a considerably increased WBC-P, the swelling of the individual HG MPs was not greatly enhanced. This implies that a significant amount of interstitial water remained between the HG MPs (Fig. 36; image pellet, and as in Fig. 35A), revealing that the WBC-P is not a measure for the WBC of HG MPs themselves.

To investigate the importance of internal and interstitial water to the overall WBC-P of HG MPs, their pellets were further analysed with time domain nuclear magnetic resonance (TD NMR) in **Chapter 3**. The resulting spectra showed two peaks that were related to internal and interstitial water (Fig. 36;  $T_2$ -spectrum), revealing that the WBC-P of HG MPs was primarily determined by the amount of interstitial water, and only to a small extent by the amount of internal water. This demonstrates that the WBC-P is unequal to the WBC of the HG MPs themselves. In addition, it was found that an increase in the WBC-P was predominantly caused by an increase in interstitial water. A very remarkable and not well understood observation was that the protein concentration of interstitial water was similar for all particles investigated. We theorized that this may have been caused by small, highly swollen protein aggregates that ended up between the HG MPs during centrifugation. Furthermore, this research revealed that the WBC-P could be accurately measured with TD NMR.

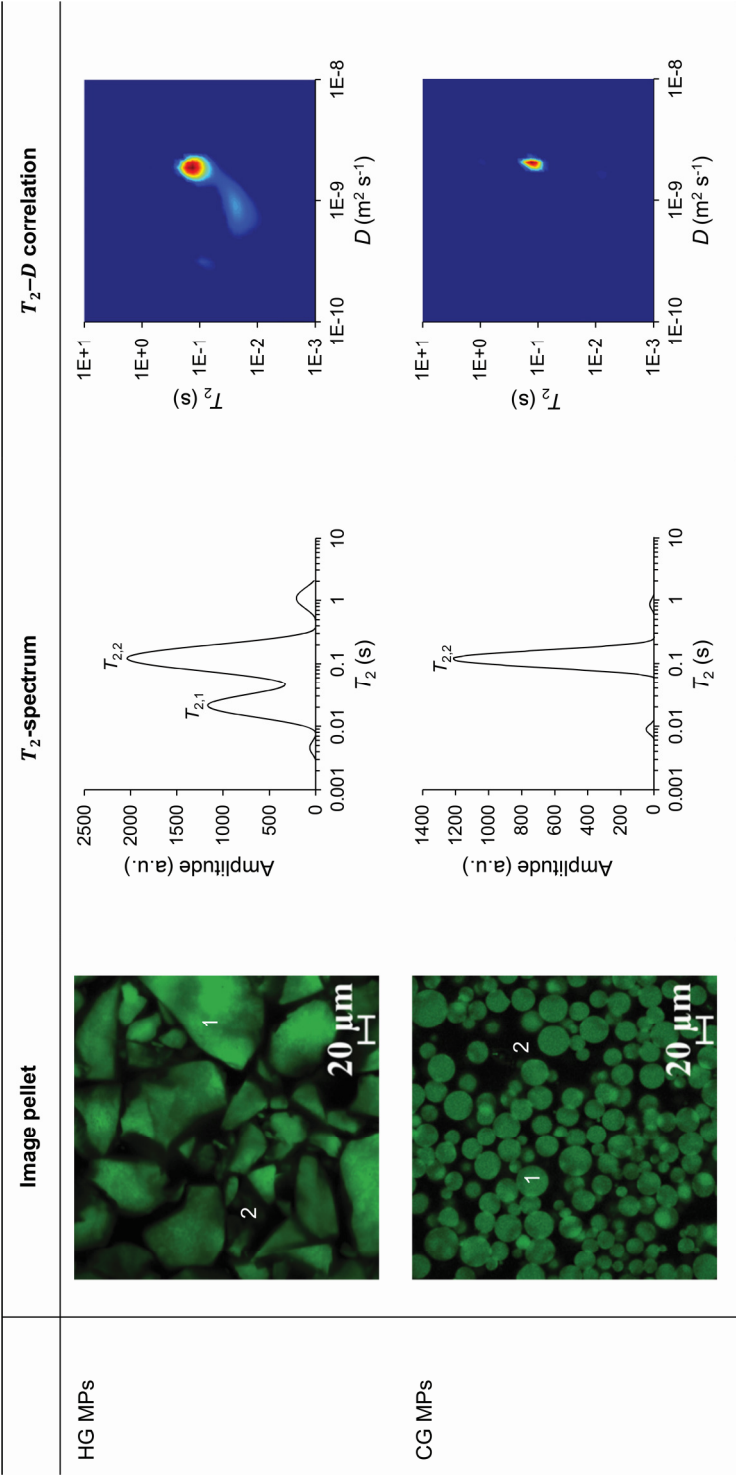
In **Chapter 4**, the WBC-P and WBC of CG MPs were investigated. We influenced the WBC-P by applying a shearing or mixing force during gelation, which resulted in a change in size and shape of the CG MPs. Spherical CG MPs were obtained when no shearing or mixing force was applied (unsheared and unmixed particles), while smaller irregularly shaped CG MPs were formed otherwise (sheared and mixed particles). All these MPs had a remarkably large WBC-P (ranging from 11 to 18 g water/g dry matter), with the largest WBC-P for the sheared and mixed CG MPs. This observation was explained by increased particle–particle interactions, resulting in more water inclusion between the smaller (sheared and mixed) CG MPs than between the larger (unsheared and unmixed) CG MPs. The significance of particle–particle interactions was confirmed by blocking the thiol groups of the CG MPs, which resulted in a lower WBC-P. This was ascribed to the presence of fewer particle–particle interactions.

TD NMR spectra of all the CG MP pellets showed one main peak (Fig. 36;  $T_2$ -spectrum), although the pellet images showed two water domains (internal and interstitial water, as in Fig. 35A and Fig. 36; image pellet). This was caused by fast diffusional exchange of water between these domains, implying that the CG MPs and their pellets had a more open structure than the HG MPs and their pellets (Fig. 36;  $T_2$ - $D$  correlation). A two-state fast diffusional exchange model was therefore used to estimate the amount of water present in each of the two water domains. We assumed that no proteins were present in the interstitial water, based on the observation that the supernatant, obtained after centrifuging the pellets, had a relaxation time equal to that of water without proteins. The model implied that the WBC-P was here mainly determined by the amount of interstitial water in the pellet as well.

The behaviour of MPs in a pellet suggested that water-binding by protein particles is based on a few general principles. That is why, in **Chapter 5**, we investigated the WBC-P of PPI, SPI, LPC and VWG particles. The pellets of these materials could be divided into the two kinds of pellet microstructures mentioned above (Fig. 35A and B). In all pellets, except for PPI, a significant amount of interstitial water was present. This reinforced the idea that the WBC-P is unequal to the WBC of the protein particles themselves; either because interstitial water was present between the particles, due to the formation of a new structure (i.e., a (semi-)continuous network), or both.

The WBC-Ps of pellets originating from these particles ranged from 1.5 to 9.2 g water/g dry matter, which was hypothesized to be caused by variations in toughness of the particles (i.e., their ability to swell and to resist disintegration and expulsion of water during centrifugation, which is influenced by the crosslink density of the particles and the presence of pores) and the ability to bind interstitial water. With a combination of TD NMR, microscopy and adsorption isotherms, we were able to gain a better understanding of the properties of these pellets and their constituent particles, providing information about the water-binding characteristics, the microstructure of the particles and pellets, and the diffusivity of water.

Overall, we found that it is possible to create pellets of protein particles that possess the required WBC of  $\geq 9$  water/g dry matter. However, the WBC-P is determined by the summation of the amounts of internal and interstitial water, and is therefore higher than the WBC of all individual protein particles together. In closing, we have found that TD NMR is a viable additional tool to improve the understanding of the WBC of the protein particles and their pellets.



**Fig. 36.** The confocal laser scanning microscopy images of pellets of heat-gelated microparticles (HG MPs) and unsheared cold-gelated microparticles (CG MPs), made with a centrifugation speed of 845 g, showing the two water domains in their pellet: internal (1) and interstitial (2) water. The CONTIN  $T_2$ -spectra, and the  $T_2$ -diffusion coefficient ( $D$ ) correlation, measured with a DR COSY experiment, of the HG MP and CG MP pellets. Within the  $T_2$ -spectra, the pellets comprising the HG MPs consisted of two water domains: internal ( $T_{2,1}$ ) and interstitial water ( $T_{2,2}$ ). The CG MPs pellet had one main water peak in its  $T_2$ -spectrum ( $T_{2,2}$ ) which is an average  $T_2$ -value for internal and interstitial water.

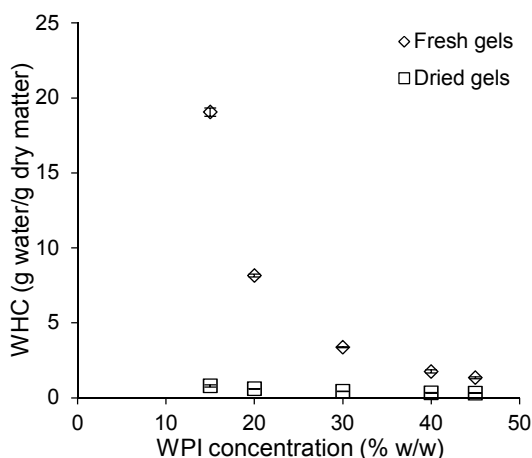
## 3 EVALUATION OF THE APPROACHES

### 3.1 MATERIAL

Whey proteins were used to make whey protein microparticles (MPs). For the purpose of reaching a better understanding of the water-binding properties of MPs, and for the flexibility of changing the micro- and nanostructure of the protein particle matrix, whey proteins were a good choice in case of dairy proteins. Just a simple heat treatment leads to novel structures in whey proteins on various length scales. Macroscopically, these changes can result in the formation of a gel. In addition, the micro- and nanostructure of this whey protein gel can quite easily be adapted by, for example, changing the pH or protein concentration.<sup>[23][55]</sup> Making new structures from the other main dairy protein group, caseins, is less straightforward, because they have little to no secondary and tertiary structure and can therefore barely be denatured.<sup>[169]</sup>

Two kinds of MPs were made from whey protein: HG MPs and CG MPs. To eventually produce HG MPs, we dried the heat-gelated gel pieces that were obtained after mixing and heating. For industrial-scale production, this is not a sustainable procedure when these MPs would subsequently be rehydrated and dispersed into a product. It would be better to omit the drying step and instead add wet HG MPs directly to the product. This might even be advantageous, because it is likely that a larger amount of water can be bound by the wet HG MPs. Drying frequently causes irreversible changes such as the collapse of (pores within) the structure, thereby resulting in a lower rehydration capacity.<sup>[93]</sup> Whey protein isolate (WPI) gels were found to hold more water when they were fresh compared to dried gels that were rehydrated (Fig. 37). An advantage of using dry particles is that this will give better control over particle size and storage stability, which facilitates doing experiments and industrial application.



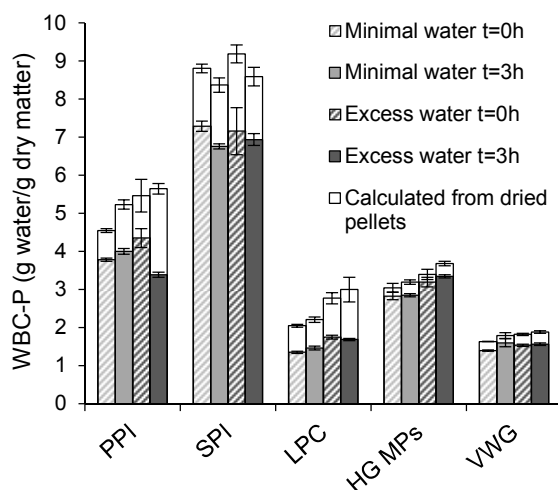


**Fig. 37.** The water-holding capacity (amount of water hold by samples when present in excess water) of fresh and dried (2 days at 50 °C) whey protein isolate (WPI) gels made with various concentrations of WPI. The standard deviation given is based on results of three measurements.

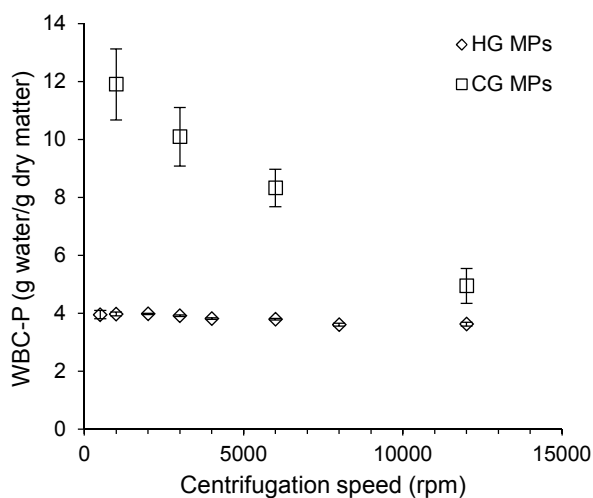
## 3.2 METHODOLOGY

This research focuses on the central important characteristic of the protein particles: their WBC. Although the WBC is a very important and frequently investigated property of proteins (and other food ingredients), it is poorly defined. In literature, several definitions can be found, various terms are utilized, and different methods are used to determine the WBC.<sup>[30][42][77][85][148]</sup> Therefore, the WBC as such does not exist, and needs further specification.

To quantify the WBC of protein particles, we employed the frequently used method in which a dispersion is made from the particles, and the WBC of the pellet (WBC-P) is subsequently determined via the pellet weight that is obtained after centrifugation. In this method, the WBC-P depends upon the temperature, hydration time, amount of water used (excess or minimal amount of water), quality of the water (e.g., pH and amount of ions present), centrifugation speed and time, and type of centrifugation tube (without or with filter that facilitates a separation of supernatant and pellet, to prevent reabsorption after removal of the centrifugation force). Additionally, various calculations for the WBC are reported in literature. Fig. 38 and 39 show an example of the effect on the WBC-P of some variations of the method. These differences in methods have an advantage as well, because comparing the effect of a change in one of the above parameters on the WBC-P gives insight into factors that determine the WBC-P. For example, Fig. 38 shows that all particles absorbed water quickly, because similar values were obtained after 0 h and 3 h of hydration. Fig. 39 shows that the centrifugation speed has barely any effect on the WBC-P of HG MPs, but a major effect on the WBC-P of the CG MP pellets.

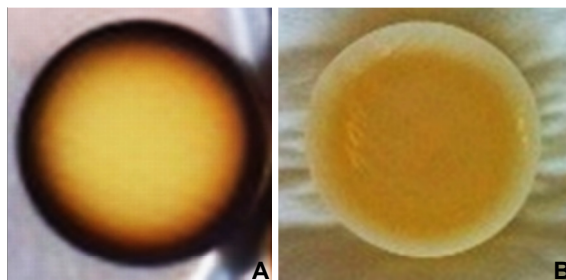


**Fig. 38.** The water-binding capacity of pellets (WBC-P) of pea protein isolate (PPI), soy protein isolate (SPI), lupin protein concentrate (LPC), heat-gelated whey protein microparticles (HG MPs) and vital wheat gluten (VWG), after a minimal amount of water was added and the proteins were hydrated for 0 h (i.e., centrifugation was applied directly after suspending particles in water) or 3 h; and after excess water was added and the proteins were hydrated for 0 h or 3 h. Here, the WBC-P was calculated from the weight of the material added before hydration, compared to the weight of the pellet after centrifugation. The WBC-P was also calculated from comparing the weight of the pellet after drying it in an oven with its weight immediately after centrifugation (open bars). The standard deviation given is based on results of four measurements.



**Fig. 39.** The WBC-P of heat-gelated microparticles (HG MPs) and cold-gelated microparticles (CG MPs) measured over a range of centrifugation speeds (rpm). The standard deviation given is based on results of three measurements for the HG MPs and four measurements for the CG MPs.

Our research indicates the importance of interstitial water to the WBC-P (Fig. 36; image pellet). In hindsight, it would therefore have been better not to measure the WBC of a pellet of particles, but instead merely to look at the swelling of the particles to determine the effect of variations in the micro- and nanostructures on the WBC. The accurate determination of the swelling of particles of this size is, however, difficult, because water is easily trapped between particles (for example, when determining the swelling via the isotherm of the particles, liquid bridges will form at a critical moisture content),<sup>[112]</sup> or because one would have to make many assumptions in the interpretation of the measurements (e.g., during the determination of the particle size distribution). An alternative approach is to investigate macro-gels instead of micro-gels, to determine which properties proteins and their structures should have to absorb a lot of water. However, making relevant macro-gels is not trivial either. For instance, one has to make sure that no air bubbles are introduced. They need to be subjected to an external force field for a long time, because the moisture permeation is quite slow. Further, the pore structures inside and around the particles are not necessarily the same as in a larger (macro)gel. Finally, a large amount of chemicals and longer treatment times are needed to induce, for example, a change in the crosslink density, while the homogeneity in larger gels is always subjected to discussion (Fig. 40).



**Fig. 40.** Whey protein isolate macro-gels after incubation in a (A) genipin, or (B) transglutaminase solution at 25 °C for 24 h. Both gels have a diameter of 20 mm. One can see that the components have penetrated only slightly into the matrix; demonstrating that investigating a macro-gel instead of microparticles can pose its own challenges.

## 4 SCIENTIFIC IMPLICATIONS AND FUTURE RESEARCH

### 4.1 SUPER-ABSORBENT PROTEIN PARTICLES DUE TO MICROSTRUCTURING?

Based on the existing knowledge of synthetic super-absorbent polymers and the understanding of swollen polymeric networks through theories like the Flory–Rehner equation, we envision two routes to enhance the swelling in water of MPs: decreasing the crosslink density and incorporating pores into the MPs.

#### 4.1.1 CROSSLINK DENSITY

The Flory–Rehner equation states that the crosslink density determines the extent of swelling of polymers from water-activity ( $a_w$ )-values of 0.8 and above.<sup>[111][156]</sup> A decrease in the crosslink density of HG MPs, effected by reducing the amount of disulphide bridges, resulted in an increase of the WBC-P of unheated pellets from 4 to 7 g water/g dry matter (**Chapters 2 and 3**). Increasing the crosslink density, by reducing the pH of the starting WPI solution closer to the isoelectric point of WPI, caused a reduction in the WBC-P of unheated pellets from 4 to 2 g water/g dry matter (**Chapter 3**). Unexpectedly, these changes in the crosslink density did not have a clear effect on the swelling of the MPs themselves; the change as observed with the pellets was not as pronounced (**Chapters 2 and 3**). We hypothesized that the crosslink density of the HG MPs was already too large to have a significant impact on their swelling. This implies that, if the effect of crosslink density is the property to observe, dried HG MPs made from a 40% w/w WPI solution are not the most ideal starting point; however using HG MPs with a lower WPI content may result in a more significant effect on swelling and additionally result in particles that can absorb the desired amount of water.

#### 4.1.2 PORES

The presence of pores can enhance the WBC of protein particles by binding water through capillary forces. However, the effect of pores has not been a main topic of investigation in our research on protein particles, due to the fact that we discovered the high degree of relevance at the final stage of the project. The presence of micropores in dry PPI and SPI particles, in combination with the particles' increase in size after hydration, and their relatively large WBC-P, suggest that the presence of pores is important for water-binding. For superporous synthetic polymer hydrogels it was reported that they were able to absorb more water than hydrogels with much fewer pores.<sup>[108]</sup> It is even thought that the WBC of a gel can be explained by the presence of pores, especially when considering a gel as a network in which interconnected capillaries are present.<sup>[11][20][23][67][68]</sup> The pore size affects the strength of water-binding. A pore size smaller than 100 nm can prevent water leakage

from the pores.<sup>[43][67][68][186]</sup> The pore size distribution is also reported to be important in foods. A finer distribution of pores enhances water-binding.<sup>[43][67]</sup> An even distribution of circular pores causes swelling to occur homogeneously.<sup>[107]</sup> Finally, interconnectivity between the pores can lead to faster water adsorption.<sup>[107]</sup> Incorporating pores in protein particles can be accomplished by, e.g., phase separation during synthesis, or by introducing air during processing.<sup>[71]</sup>

To conclude, future research has to show the viability of purposely nanostructuring (e.g., the crosslink density) and microstructuring (e.g., the amount, size, shape, distribution and interconnectivity of pores) as a tool to increase the WBC of the particles to  $\geq 9$  g water/g dry matter.

## 4.2 SUPER-ABSORBENT PROTEIN PARTICLES OR SUPER-ABSORBENT PROTEIN NETWORKS?

**Chapters 2, 3 and 4** show that it was possible to increase the WBC of the pellets originating from the MPs to  $\geq 9$  g water/g dry matter. The WBC of the MPs themselves could not be increased to that extent. This suggests that, to increase the water content in a product, it may be more practicable to use a pellet of MPs instead of the MPs themselves. The analyses on the pellets of MPs revealed there were two factors that influence the WBC of these pellets: the amount of internal water and interstitial water (Fig. 35 and Fig. 36; image pellet).

### 4.2.1 INTERNAL WATER

The WBC-P of the HG MPs and CG MPs consisted of two water-domains: internal and interstitial water (**Chapters 2, 3 and 4**; Fig. 36; image pellet). In case of HG MPs, TD NMR results revealed that an increase in the WBC-P was only to a very small degree due to an increase in internal water (**Chapter 3**). The importance of internal water to the overall WBC-P of CG MPs was small as well, according to the microscopic image of the pellets (**Chapter 4**). Pellets made from plant protein particles all consisted of swollen protein structures, either as separate particles or as a building block of a (semi-)continuous protein network (**Chapter 5**). The latter will not be discussed in great detail, because a (semi-)continuous protein network may be considered a larger version of a protein particle; albeit one that is too big to be utilized in our proposed application. Microscopic images of pellets of plant protein particles suggested that internal water played a larger role on the overall WBC-P than interstitial water. In conclusion, these results imply that internal water is an important factor on the overall WBC-P, though it is not always the largest fraction.

It was further noticed that internal water frequently seemed to be less important when the particles remained distinct from one another in the pellet than when they formed a (semi-)continuous network. It is possible that all those particles had a certain toughness

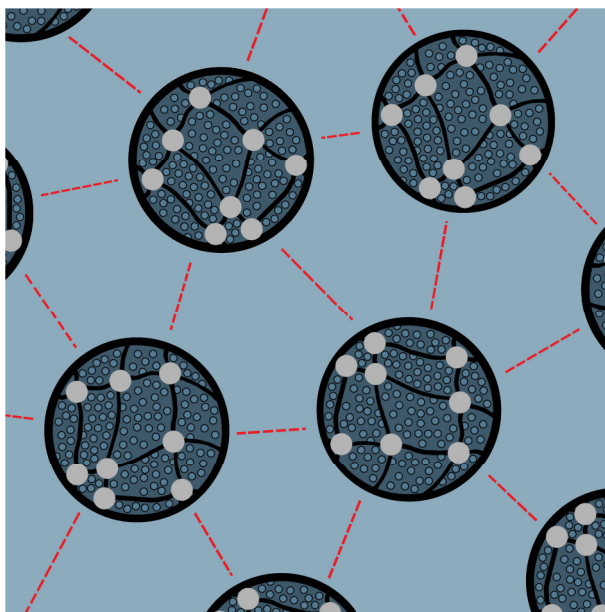
with which they could withstand the centrifugal force, but which also reduced their swelling. We hypothesize that this toughness is predominantly determined by the crosslink density and the presence of pores (Section 4.1). Extra experiments need to be performed to determine the effect of toughness and to find the optimal combination of swelling and toughness for the particles' proposed applications. An indication of the force that the particles can withstand can be obtained by, for example, capillary micromechanics<sup>[179]</sup> or atomic force microscopy. In conclusion, the above suggests that there is a connection between the toughness of particles (nanostructure) and the structure of the pellet (microstructure).

#### 4.2.2 INTERSTITIAL WATER

The WBC-P of HG MPs and CG MPs was predominantly determined by the amount of interstitial water. It was hypothesized that two different phenomena were responsible for the water-binding between the MPs. It was thought that highly swollen protein structures were present in the interstitial water in the HG MP pellets (**Chapter 3**). The water between the CG MPs seemed to be bound due to particle–particle interactions (**Chapter 4**). These interactions may have played a role in the water-binding between the HG MPs as well. There are several interactions possible between proteins, ranging from strong, long-range interactions (e.g. hydrophobic interactions) to weak, short-range interactions (e.g., Van der Waals interactions).<sup>[23]</sup>

A further understanding of the mechanism by which water is bound between particles, is an important step in formulating design guidelines for the preparation of particles or networks that have a large WBC. We therefore suggest investigating which particle–particle interactions play a role between the MPs in the pellet. This may, however, pose a challenge. Methods are known that can measure which interactions act *within* the particles, by following their dissolution in solutions with reagents that break specific bonds; e.g., disulphide bridges.<sup>[88]</sup> However, as far as we know, there are no methods that investigate which specific interactions *between* the particles play a role. A second research question is whether we can identify highly swollen particles between the HG MPs with, for example, a RAMAN microscope that is sensitive enough for low protein concentrations. The identification of those particles and their structure may provide insight about the characteristics of particles that have a large swelling capacity.

Overall, pellets are an interesting alternative to particles that are themselves highly swellable, providing that they can retain a network within the product to which they are applied. Therefore, we hypothesize that the protein structure that can bind the largest amount of water will be a network of particles (with a low crosslink density and a large amount of pores), that through particle interaction can also include a large amount of water between the particles (Fig. 41).



**Fig. 41.** Proposed structure that can bind the largest amount of water: particles with a low amount of crosslinks and a lot of pores, which, due to interaction with each other, can bind a large amount of water between them.

### 4.3 CAN TIME DOMAIN NUCLEAR MAGNETIC RESONANCE BE USED AS A TOOL TO MEASURE THE WATER-BINDING CAPACITY OF A PELLET OF PROTEIN PARTICLES AND ITS WATER DOMAINS SIMULTANEOUSLY?

#### 4.3.1 WATER-BINDING CAPACITY AND WATER DOMAINS MEASURED WITH TD NMR

Currently, the WBC obtained through centrifugation is often considered as a measure for the water-binding of protein particles.<sup>[15][45][75][175][183]</sup> However, the results in this thesis show that water is bound in a pellet of particles in two different ways: within and between the particles (**Chapters 2, 3, 4 and 5**), or in a protein network (**Chapter 5**). Consequently, the WBC-P frequently does not represent the WBC of its constituent particles. We therefore suggest that one should discriminate between the WBC-P and WBC of the particles. This will raise awareness of the difference in behaviour of single particles as compared to that of a pellet of particles. In addition, it will result in a more accurate value for the WBC in the application in which particles, or a pellet thereof, are used. This distinction is not only recommended for protein particles, but for all materials for which the WBC is investigated. With regard to fibres, for example, it has also been reported that a significant amount of water was found between the fibres<sup>[65]</sup> and consequently, a distinction between the WBC-P and that of the fibres themselves is needed here as well.

Differentiating between internal and interstitial water in a pellet or a protein network is not trivial. One cannot easily separate interstitial water from either the particles or the network. In this research, we used TD NMR for this purpose. TD NMR could be used to calculate the amount of water that is present in each water domain via a calibration curve when no fast exchange took place between the different water domains (Fig. 36;  $T_2$ -spectrum), as was the case for HG MPs (**Chapter 3**; Fig. 36;  $T_2$ - $D$  correlation). For these calculations we assumed that the  $T_2$ -value is only related to the protein concentration. However, it should be noted that we cannot discount the possibility that these calculations are incomplete, because the  $T_2$ -value may also be affected by other interactions (like capillary forces). In case of fast exchange of water, for example in a CG MP pellet (Fig. 36;  $T_2$ - $D$  correlation), TD NMR data was implemented in a fast exchange model to estimate the amount water present in each water domain (**Chapter 4**). The estimation requires additional information about the  $T_2$ -values of both the swollen particles and the environment wherein they are present (water without or with a certain concentration of proteins). TD NMR could not be used straightforwardly to obtain this information for the plant protein particles that were investigated (**Chapter 5**). Hence, extra experiments have to be performed to, for example, determine the effect of the centrifugal force, or give an indication of the  $T_2$ -values that have to be used in the fast exchange model.

#### 4.3.2 USING TD NMR AS A TOOL TO PROVIDE INFORMATION ABOUT THE MICROSTRUCTURE AND TYPE OF WATER-BINDING

Besides being useful to measure the WBC-P and the WBC of the particles, TD NMR may also yield more insight into the effect that the structure has on the protein(structure)-water interactions. This information can be obtained from the  $R_2$ -dry matter content calibration curves. For whey proteins, for example, three hydration regions were defined by others, and for each region the relevant water type was determined—(a possible combination of) water bound to the polymers, water bound in capillaries or free water.<sup>[110]</sup> Comparison of such graphs for various protein samples might reveal why one sample has a larger WBC than others. The combination of calibration curves for various protein samples can be useful as well. For soy-gluten blends, the distribution of water over the different phases in blends of these proteins was determined in this way.<sup>[41]</sup> In addition, diffusion experiments can be used to determine the resistance water encounters when it diffuses through the pellet. This provides insight into the structure in which water is present. Finally, more in-depth research, on which water domain is represented by every peak of the  $T_2$ -graphs, can also give more information about the microstructure of the pellet.



### 4.3.3 FURTHER TECHNIQUES TO GAIN INSIGHT INTO THE WATER DOMAINS IN A PELLET

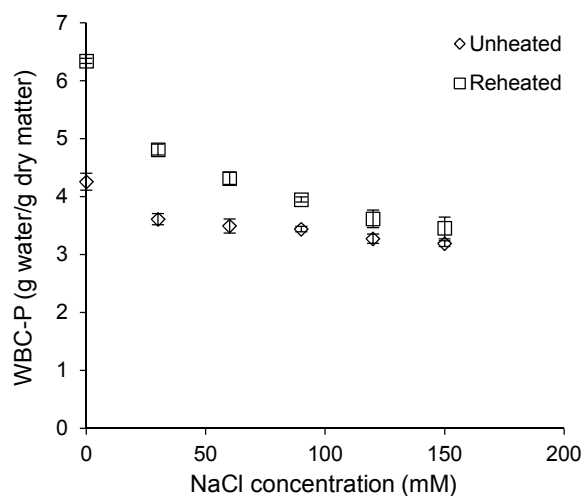
Other techniques than TD NMR may be used to differentiate between internal and interstitial water. These techniques can potentially be used for protein particles, to measure both the WBC-P and the WBC of the particles themselves. Furthermore, insight gained through these techniques may provide a greater understanding of the  $T_2$ -curves of these protein particle pellets. An interesting extension of the TD NMR technique, is to include freezing of the pellets and dispersions of various concentrations of protein particles, and subsequently using both TD NMR and differential scanning calorimetry to analyse those samples. This combination of techniques may give an indication of the concentration in each water domain. Another option to determine the composition of the various water domains is using a RAMAN microscope that is sensitive enough for low protein concentrations. A final route to gain more insight into the protein concentration within the protein particles is to collect them with optical tweezers and subsequently dry them to determine their WBC.

In conclusion, TD NMR on its own was found to be a useful additional technique to obtain more information about protein particle pellets, such as the number of water-domains present and the diffusivity of water. By combining data about the number of  $T_2$ -peaks, diffusion coefficient ( $D$ )-peaks and microscopy, information on the structure and permeability of the particles may be gained (**Chapters 3, 4, and 5**). Further experiments with different techniques, as described above, will provide an even greater understanding about how water is bound in the various domains that are present in the pellets, and how water-binding can be influenced.

#### 4.4 CAN WE INCREASE THE WATER CONTENT OF A PRODUCT WITHOUT AFFECTING ITS SENSORIAL PROPERTIES BY APPLYING PROTEIN PARTICLES?

Eventually, protein particles with an enhanced WBC may be applied to (dairy) products to decrease their caloric content without affecting their sensorial properties. Therefore, it is recommended to investigate the effect that adding MPs will have on either the mechanical, the rheological, or both types of characteristics of dairy products—or a model system for such a product—over time.

MPs can be added to a product in several ways. The dry HG MPs can be added to a product without hydration, which will cause them to absorb water from the product. This will lower the product's water content, and the product will, depending on the amount of HG MPs added, most likely be perceived as harder and more brittle. This can be compensated by adding more of the liquid phase that is used in the product. The HG MPs and CG MPs can also be added to the product as wet particles, or as a pellet of particles. The latter could be interesting because the WBC-P is often larger than the WBC of the particles. If the pellet material keeps its coherence when added to the product, an even larger amount of water may be added. It is likely that the HG MP pellets are tougher than CG MP pellets, given the difference in the effect of the centrifugal force on the MPs (Fig. 39). Depending on the  $a_w$  of the product, the MPs will shrink or swell (see Fig. 42 for an example of the effect of salt on the WBC-P of HG MPs) which may affect the product's sensorial characteristics.



**Fig. 42.** The effect of the presence of NaCl on the water-binding capacity of a pellet of heat-gelated microparticles, of which the particles were reheated and were not reheated (referred to in the graph above as unheated) before centrifugation at 90 °C for 30 min.

The addition of the MPs to a dairy product ought not result in a negative sensorial perception. An important parameter therefore is the size of the MPs.<sup>[135]</sup> Their current size will most probably be perceived as gritty, according to the rough division of the effects of size of MPs on the sensory perception,<sup>[135]</sup> and probably needs to be adapted before industrial use. When a pellet of MPs is added to the product, its size is larger than that of separate MPs. However, we think that if the MPs are small enough not to impart a gritty sensation to the product, then neither will the pellet, due to the large amount of interstitial water. In addition, we anticipate that the MPs or their pellets will not be perceived as gritty—contrary to expectations due to their size—when the MPs are highly swollen. In that case, they are soft enough to deform with the product matrix upon mastication.

Previous research on HG MPs showed the effect of the addition of HG MPs on the mechanical characteristics of a WPI gel.<sup>[115][116]</sup> This was done by replacing part of the WPI of the continuous phase with HG MPs. At similar effective protein concentrations (i.e., “the protein concentration of the composite gel as if it contained only native WPI leading to a similar gel stiffness”),<sup>[115]</sup> it was reported that the strength of a gel with HG MPs was equal to that of a WPI gel, with a concentration between that of the continuous phase and the total protein concentration. The HG MPs would absorb some water, and therefore one would indeed expect the continuous phase to be stronger with HG MPs than without. We estimated the amount of water that was absorbed by the HG MPs in this experiment with the WBC of the HG MPs themselves, as reported in **Chapter 3**. This amount of water was subtracted from the amount of water in the continuous phase, and the concentration in this phase was recalculated. This recalculation, using the data reported by Purwanti, et al. (2012),<sup>[115]</sup> shows that water-binding by HG MPs can explain the small increase in strength of the continuous phase (Table 11). This suggests that only the absorption of water by HG MPs affected the strength of the continuous phase, and that our data on swelling of the HG MPs explain the data of Purwanti, et al. (2012)<sup>[115]</sup> and Purwanti, et al. (2013).<sup>[116]</sup>

In summary, it may be interesting to determine the behaviour (e.g., water division) of MPs and their pellets in (model) products to investigate their applicability. We recommend using model products besides WPI gels, to determine the interaction of the whey MPs with proteins other than whey.

**Table 11.** The intended concentration of the continuous phase; the added amount of heat-gelated whey protein microparticles (HG MPs); the added amount of water; the amount of water within the HG MPs compared to the overall composition in the HG MPs, assuming that the dry matter content of the HG MPs was 35% (**Chapter 3**); the concentration of WPI in the continuous phase, after correction of water absorption by the HG MPs; and the effective concentration.

Continuous phase (% w/w WPI)*	HG MPs (% w/w)*	Overall water content (% w/w)	Water within HG MPs (% w/w)	Continuous phase corrected for water absorption (% w/w WPI)	Effective concentration (% w/w)*
12.8	2.5	84.7	4.6	13.8	13.5
13.2	5.0	81.8	9.3	15.4	15.2
13.5	7.5	79	13.9	17.2	17.3

\*Data from Purwanti, et al. (2012)<sup>[115]</sup>

## 4.5 RISK ASSESSMENT OF WHEY PROTEIN MICROPARTICLES

The application of MPs in food products requires an analysis of potential hazards and the effect that these new materials may have on human health and the environment. Firstly, the ingredients used to make the MPs should be proven safe and be present in a concentration that is regarded as safe for human consumption, according to the requirements of food safety authorities. HG MPs and CG MPs are produced using ingredients that are also available with a GRAS (generally regarded as safe) status for manufacturing on an industrial scale.<sup>[56]</sup> In addition, the concentrations of glucono- $\delta$ -lactone and locust bean gum that are used to produce CG MPs are below the concentration of acceptable daily intake, and are in that sense regarded as safe.<sup>[48][49]</sup> Furthermore, the particulate whey protein products Simplesse® and Dairy-Lo™ have a GRAS status,<sup>[57][180]</sup> suggesting that HG MPs and CG MPs are eligible for the same status. Secondly, hazards may be introduced during food production, which can be of biological (bacteria, viruses etc.); chemical (chemicals, environmental contaminants etc.); and physical (stones, splinters, etc.) origin.<sup>[31][99]</sup> Therefore, when the ingredients used for the MPs are biologically and chemically safe (i.e., do not contain contaminants such as herbicides, pesticides, and pathogenic bacteria etc.); equipment damage (that can cause foreign material to be present in a product) does not occur; and no cross-contamination (with, for instance, allergens) takes place; the MPs ought to be safe to human health. Therefore, the only way a hazard may be introduced is when the characteristics of the ingredients change during and due to processing.

A possible hazard may be introduced when, unintentionally, nanoparticles (NPs) or nanomaterials (NMs) that are insoluble and biopersistent are formed during processing of the MPs. NPs are “a discrete entity that has all three dimensions in the nanoscale”, while

“any form of a material that has one or more dimensions in the nanoscale” is defined as a nanomaterial (NM). The nanoscale size ranges from 1 to 100 nm.<sup>[50]</sup> Recent interest in NMs has increased due to their unique characteristics that are useful for society. For instance, the bioavailability of nutrients and health supplements increases when they are carried in NMs.<sup>[130][181]</sup> NMs are also thought to be useful in low-fat products, because less fat is needed when smaller droplets can be formed.<sup>[51]</sup> An emulsion with nano-sized water droplets in fat is thought to result in a product with a reduced fat content and a similar creaminess compared to its full-fat equivalent.<sup>[29]</sup> In addition, NMs have a relatively large surface-to-volume ratio, which may result in an increased WBC.<sup>[131]</sup> However, the size of NMs might pose a risk to human health. The small size of NMs is believed to give them the ability to cross cell membranes and to enter regions that are inaccessible to larger particles that were not digested earlier in the gastrointestinal tract.<sup>[29]</sup> This may be hazardous when NMs accumulate in cells.<sup>[29][177]</sup> However, the exact nature of those risks is still under investigation.<sup>[29]</sup>

The mentioned potential risks of NMs depend on size and several other characteristics of the NMs. The maximum size NMs can have that still enables crossing cell membranes was found to vary among various cell types and was also dependent on the surface properties of the NMs.<sup>[132]</sup> The solubility of NMs gives an indication of the biopersistence (non-digestibility) of the NMs; the complexity of the composition about its effect on the biocorona (the interaction and formation of complexes with biomolecules),<sup>[177]</sup> and, lastly, the surface charge on the potentiality of forming Trojan horses.<sup>[50]</sup> The largest concern is about insoluble NMs that are biopersistent (e.g., SiO<sub>2</sub> and TiO<sub>2</sub>), while soluble NMs are of least concern.<sup>[29]</sup> However, NMs are not dangerous per se. Digestible NMs from natural origin have been present in our food for as long as humans exist (e.g., casein micelles,<sup>[170]</sup> fat globules in human breast milk,<sup>[94]</sup> polysaccharides and globular proteins),<sup>[98]</sup> and are not suspected to be unsafe.

The information above is used to evaluate the potential hazards related to the HG MPs and CG MPs. First, we investigated the size of the HG MPs and CG MPs. The size distribution of both types of MPs was broad (**Chapters 2 and 4**).<sup>[159][160]</sup> Therefore, it is possible that some of the particles had dimensions in the nanoscale. Unfortunately, the static light scatter equipment, used to measure the size distributions, can only measure particle sizes 20 nm and larger, so it does not cover the whole nano-range. In addition, part of the range is close to the limitations of the equipment, making the size distribution in this range somewhat more uncertain. However, in both size distributions (measuring the volume and number of particles with a certain size) of the HG MP and CG MPs, no peak appeared close to 100 nm. Apart from possible sizes of MPs into the NM-range which might carry health problems as described above, it is well-known that the size distribution of the MPs, in the range that was measured, can cause health problems as well, especially when particles are in the dry state. Inhalation of dry particulate materials with a size larger than 10 µm may cause irritation; particles between 5 and 10 µm may cause asthmatic reactions;

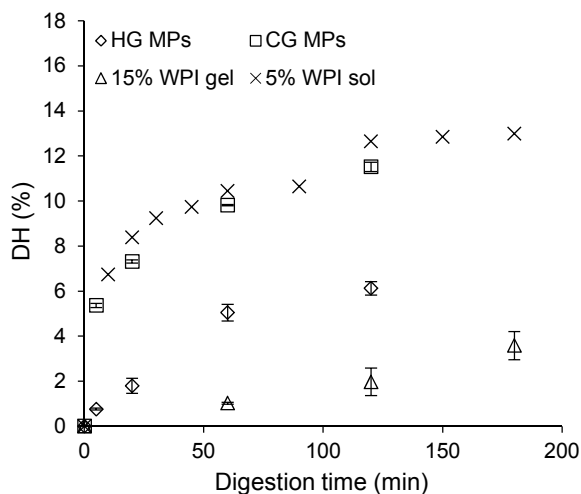
and particles smaller than 5  $\mu\text{m}$  can lead to allergic reactions.<sup>[140]</sup> Therefore, one should be careful during processing and handling of dry HG MPs.

In addition, unexpected characteristics could point to the presence of possible hazardous NMs. As far as the HG MPs and CG MPs have been characterised, no special attributes were found. For example, the water-binding capacity of these MPs was not extreme, compared to the water-binding capacity of other food proteins.

Furthermore, process conditions used to produce HG MPs and CG MPs from WPI have been applied to dairy proteins safely for years. In both cases, a dispersion of WPI was heated at temperatures at which (low) pasteurization (applied to milk industrially since 1880)<sup>[9]</sup> occurs, but for longer durations. In the process of making CG MPs, the pH was changed to pH 5, which is in the range of the pH of some dairy products (such as Cheddar),<sup>[173]</sup> but larger than the pH of, for instance, yogurt.<sup>[172]</sup> The processes that were applied to make HG MPs and CG MPs, spontaneously caused the whey proteins to make new structures on the molecular level due to self-assembly, and more controllably on a macroscopic level due to forced-assembly.<sup>[151]</sup> In case of the HG MPs, a combination of heating (self-assembly) and mixing (forced-assembly) was applied that caused the whey proteins to unfold, aggregate and form gel particles. CG MPs were made in a two-step gelling process in which structures were formed by self-assembly. First, a whey protein solution with a concentration below the gelling concentration was heated. This led to the formation of aggregated protein molecules. The second step was lowering of the pH to the isoelectric point of the whey proteins (pH 5.2–5.4),<sup>[58][147]</sup> which resulted in phase separation and spontaneous restructuring of the proteins at the molecular level. When shearing or mixing was applied during incubation, forced-assembly also played a role during MP formation. Restructuring of proteins always involves the risk that the proteins restructure during processing in a way they can become less safe.<sup>[14][123]</sup> Because regular process conditions were used for the production of both MPs, it is thought that the chance that this might have happened or might happen in the future is low for these MPs. Therefore, it is expected that restructuring of the whey proteins did not result in unsafe new structures.

To investigate the digestibility of the HG MPs and CG MPs, both kinds of MPs were subjected to a 2 h long digestion by pepsin in gastric juice at pH 2.0. The degree of hydrolysis (DH) increased in time for both MPs, and the increase was faster at the beginning of the digestion (Fig. 43). This trend is comparable to the trend found for the digestion of a 5% w/w non-denatured WPI solution, digested at a concentration of around 2 g proteins/L gastric juice, just like HG MPs and CG MPs. The WPI solution had DH-values comparable to the CG MPs, during the whole time the digestion was followed, while the DH-values of the HG MPs were lower. Compared to a 15% w/w WPI gel that was digested at a concentration of 2 g protein/L gastric juice, both HG MPs and CG MPs had larger DH values over the whole digestion–time range. These results show that the digestibility of both MPs is similar, if not faster compared with a WPI solution and gel.

This also means that the nutritional value of whey is preserved. Overall, it can be concluded that both MPs are safe with respect to the aspects that were taken into account here.



**Fig. 43.** The degree of hydrolysis (DH) (%) during digestion (min) of heat- (HG MPs) and cold-gelated whey protein microparticles (CG MPs). Error bars are based on the standard deviation of two experiments. Values of the DH of a 15% WPI gel and 5% WPI solution were given by Qi Luo and are related to the data of Luo, Q., Boom, R. M. & Janssen, A. E. M. (2015).<sup>[89]</sup>

## **5 KEY FINDINGS**

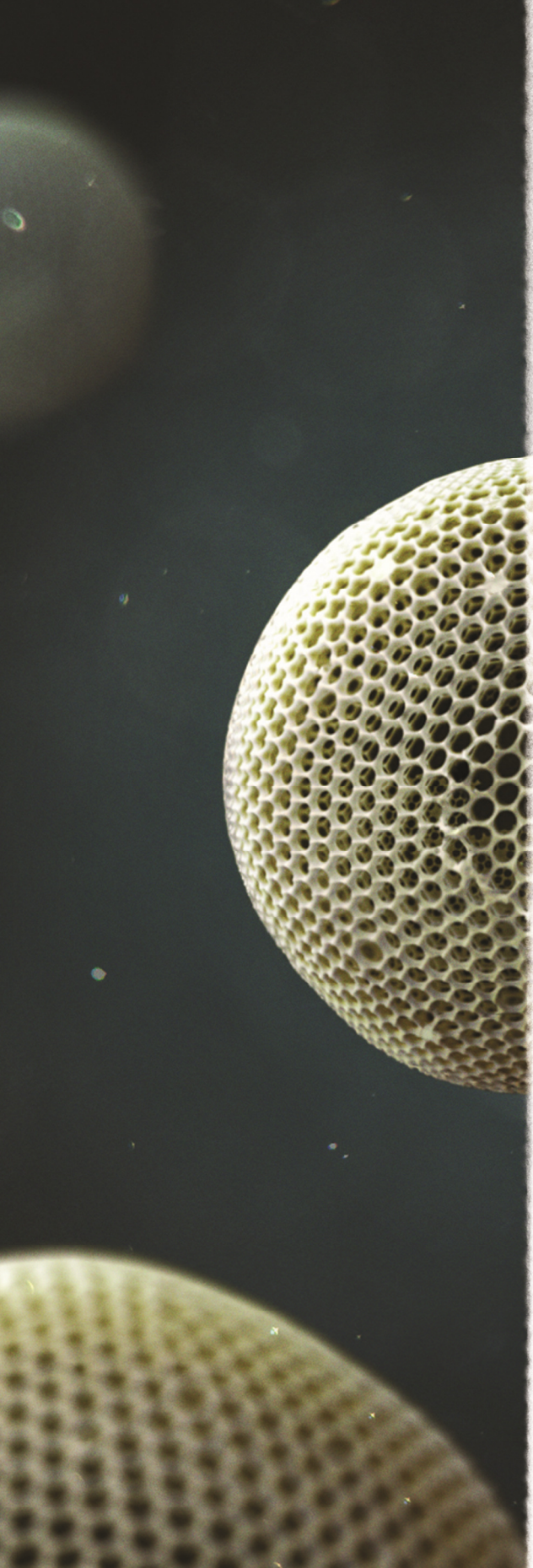
- The water-binding capacity of a pellet consisting of protein particles can be  $\geq 9$  g water/g dry matter.
- The water-binding capacity of a pellet of protein particles is always unequal to the water-binding capacity of the protein particles themselves.
- The structure of protein particles (nanostructure) and between particles (microstructure) is a determining factor for the water-binding capacity of pellets of protein particles.
- Pellets can be used as an alternative to highly swellable particles, providing they stay present as a network in the product.
- Time domain nuclear magnetic resonance, in combination with microscopy, is a useful tool to gain insight into the water-binding of a pellet and its water domains.

## **ACKNOWLEDGEMENTS**

We would like to thank Mauricio Opazo Navarette and Qi Luo for their help with the digestibility experiments and the fruitful discussions about these results. In addition, we would like to thank Wouter Perk for proofreading the general discussion.







# SUMMARY

## SUMMARY

With the increased prevalence of overweight and obesity, there is an increasing demand for food products that facilitate body weight control. In case of dairy products, this may be achieved by increasing their water content, thereby reducing the protein and fat content. However, just adding water may result in softening of the product or expulsion of water. In this thesis, we explored the creation of protein microparticles (MPs) that can bind  $\geq 90\%$  w/w water tightly, and, when added to the product, will increase the overall water content without negatively affecting its sensory perception. To design these particles, it is necessary to have a solid understanding of the water-binding mechanisms in these MPs. The aim of this thesis was therefore to understand the relation of nano- and microstructural characteristics of MPs and their resulting water-binding properties.

The first step in this research was to determine which factors would most strongly influence the water-binding of MPs. According to the Flory–Rehner theory, for our purpose, the crosslink-density of the MPs network is the most predominant factor. In **Chapter 2**, we therefore investigated the effect of the crosslink density on the water-binding capacity of heat-gelated whey protein microparticles (HG MPs). These HG MPs were made by heating a 40% w/w whey protein isolate (WPI) solution while mixing, which resulted in broken gel pieces. The pieces were dried and subsequently milled, producing HG MPs. The crosslink density of HG MPs was both increased and decreased. Remarkably, an *increase* in crosslink density did not result in a significant decrease of the water-binding capacity of a pellet (WBC-P) of HG MPs obtained after centrifuging an aqueous dispersion containing HG MPs. On the other hand, a *decrease* in crosslink density resulted in an increase of the WBC-P from 6 to 9 g water/g dry matter. Although the WBC of the *pellets* (i.e., the concentrated cake of particles) was significantly increased by decreasing the crosslink density, no clear increase in the swelling of the individual HG MPs was found, measured by both the size of the HG MPs and their sorption isotherm. It is hypothesized that the HG MPs already had a very high crosslink density, consisting of both non-covalent and covalent crosslinks, and that therefore no significant change in the overall crosslink density was achieved. This discrepancy, between the effect of altering the crosslink density on the swelling of the HG MPs and the WBC-P, showed that the method to find the WBC-P does not give a value for the WBC of just the HG MPs; it may be that a significant amount of water remained between the HG MPs in the pellet.

The discrepancy between the WBC-P and the WBC of the individual HG MPs was further investigated in **Chapter 3**. As in **Chapter 2**, pellets were made by centrifuging a dispersion of HG MPs with varying crosslink densities. The WBC-P was determined from the pellet weight. In addition, the same pellets were analysed with time domain nuclear magnetic resonance (TD NMR). Spectra obtained with TD NMR showed two peaks that were related to water present within and between the HG MPs.

By making this distinction, it was found that an increased WBC-P was caused by an increase of the amount of water in the HG MPs (swelling) to some extent and, more importantly, by an increase in the amount of water present between the HG MPs. Therefore, we concluded that the WBC-P is predominantly determined by water present between the HG MPs. In addition, this showed that the WBC-P is not equal to the WBC of the HG MPs themselves. Remarkably, though a larger WBC-P resulted in an increased amount of water between the HG MPs, we discovered that the protein concentration between the HG MPs was similar for all particles investigated. We hypothesized that the protein between the particles comprises small, highly swollen protein aggregates that were co-sedimented, and settled between the HG MPs. In addition, we showed that the WBC-P could be measured accurately with TD NMR.

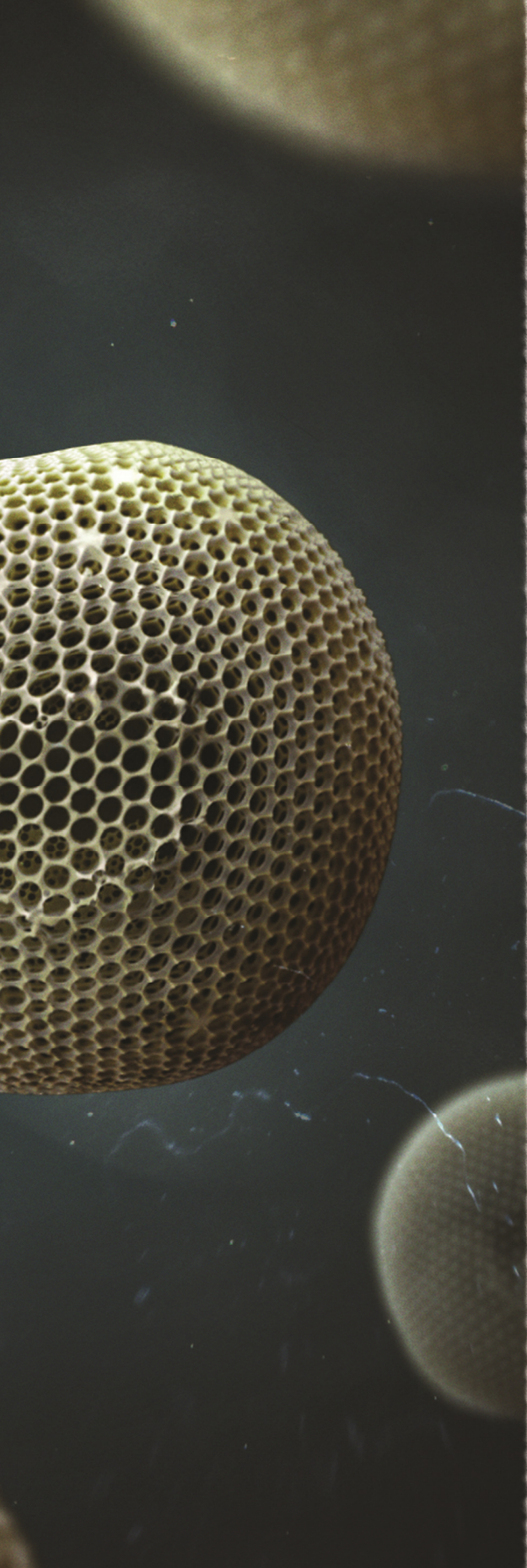
In **Chapter 4**, the WBC-P of cold-gelated whey protein microparticles (CG MPs) was examined. These MPs were made by a two-step process. First, a 9% w/w WPI solution was heated, which resulted in the formation of reactive aggregates. Second, an acidifier was added that induced gelation of the proteins at room temperature. To form CG MPs, a locust bean gum solution was added to the aggregates prior to gelation, resulting in phase separation. CG MPs were thought to have a larger swelling capacity due to a lower crosslink density, which was expected to lead to a higher WBC-P range to study. Additionally, previous research had shown that the interactions between these MPs could be altered by varying their size and shape. Therefore, we changed the size and shape of the CG MPs by applying a shearing or mixing force during gelation. When no shearing or mixing was applied (further referred to as unsheared and unmixed particles), spherical CG MPs were obtained, while applying a shearing or mixing force resulted in smaller and irregularly shaped CG MPs. All these MPs had a remarkably large WBC-P, ranging from 11 to 18 g water/g dry matter. Notably, the WBC-P was significantly larger for sheared and mixed CG MPs, compared with unsheared and unmixed CG MPs. This may be caused by the creation of smaller particles during shearing or mixing, leading to more particle–particle interactions and therefore higher water inclusion between the MPs. The significance of particle–particle interactions to the WBC-P was confirmed by blocking the thiol groups of the CG MPs. This blocking resulted in a lower WBC-P, which was explained by fewer particle–particle interactions and therefore supports the supposition that the particle–particle interactions are important for the value of the WBC-P.

The pellets of these CG MPs were further investigated with TD NMR. Although images of these pellets showed the presence of two water domains (water within and between the CG MPs), only one main peak was found in the TD NMR spectra. The presence of only one peak was caused by fast diffusional exchange of water between these two water domains. Such a fast exchange suggests that the CG MPs have a rather open structure compared to HG MPs. A fast diffusional exchange model was applied to estimate the amount of water that was present within and between the CG MPs. To perform this calculation, we assumed that no proteins were present between the CG MPs, based on the

fact that the supernatant which was obtained after centrifuging the pellets, showed a relaxation time equal to that of water without proteins. By applying this model, the significance of water between the CG MPs on the total WBC-P was confirmed once more.

The behaviour of MPs in a pellet suggested that the water-binding by MPs is predicated upon a few general principles. That is why, in **Chapter 5**, we investigated the water-binding properties of the protein-rich particles: pea protein isolate, soy protein isolate, lupin protein concentrate, and vital wheat gluten. Images of the pellets of these particles showed that in all cases, except for the pellets from pea particles, water was present between the protein structures. In addition, two kinds of pellet microstructures were roughly distinguished: structures suspended in water, and a (semi-)continuous protein network with pores. Most likely, a protein network does not represent the interaction of *particles* with water anymore, due to changed protein–water interactions. In conclusion, the WBC-P is unequal to the WBC of its constituent particles, because additional water was present between the particles, or because a new structure had formed. Therefore, the protein(structure)–water properties of the particles and their pellets were further investigated with, inter alia, TD NMR. This showed that differences in the WBC-P were caused by variations in the toughness of the particles (i.e., their ability to swell and to resist disintegration and expulsion of water during centrifugation, which was probably influenced by the crosslink density of the particles and the presence of pores) and the ability to include water between the particles or within the pores of the protein network.

**Chapter 6** summarizes and discusses the main outcomes of this research. We evaluated the parameters that influence the water-binding of particles and networks of particles, resulting in guidelines to make microstructures that can bind large quantities of water. In addition, we discuss the applicability of MPs in a product, and methods to measure the WBC of MPs and their pellets. Additionally, the scientific challenges to gaining further insight into the water-binding characteristics of protein systems are described. The chapter ends with a risk assessment of the MPs made in this thesis. That assessment revealed no clear risks that hinder application of MPs in food products. In closing, there are many potentially valuable topics left to uncover with regards to the WBC of particles and pellets, e.g., the evaluation of the effects on the WBC of particles, or a network of particles, when applied to a (model) product.



# APPENDIX

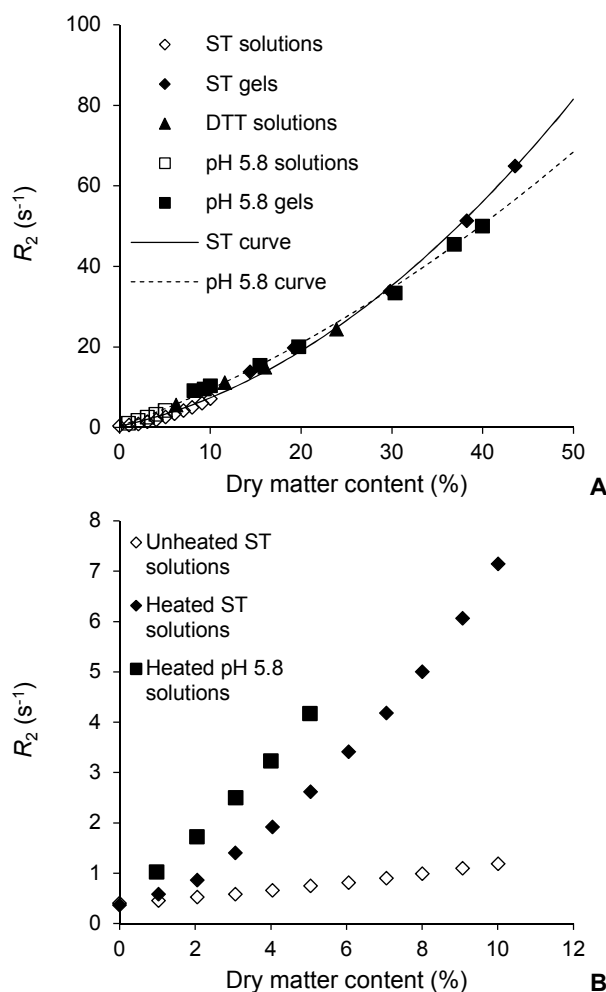
## APPENDIX A

### CALIBRATION CURVES FROM TIME DOMAIN NUCLEAR MAGNETIC RESONANCE

A standard calibration curve was made for all whey protein microparticles (MPs) to estimate the amount of water present inside and between the MPs, and the water-binding capacity (WBC) of the samples. The transverse relaxation rates ( $R_2$ ) obtained from the mono-exponential transverse decay curves of standard heated whey protein isolate (WPI) samples were plotted against the dry matter content (Fig. S1A). The heated WPI samples made at pH 5.8 (instead of 6.8) gave a different relationship between  $R_2$  and the dry matter content (Fig. S1A). The incubation of gels in 40 mM DTT did not change the relationship between the dry matter content and  $R_2$ , compared with the standard curve. Therefore, the standard calibration curve was used for all MPs, except for the MPs made at pH 5.8, for which the calibration curve was used which was made with samples at pH 5.8.

For both the standard heated solutions and gels, and the heated solutions and gels made at pH 5.8 (Fig. S1A), non-linear relationships were found between  $R_2$  and the dry matter concentration. This is in agreement with the non-linear relationship described for native and thermally denatured bovine serum albumin solutions, and gels with concentrations ranging from 0 to 25% w/w.<sup>[104][105]</sup> Linear relationships were reported for whey protein solutions and gels with protein concentrations of 6 to 18% w/w<sup>[87]</sup> and 10 to 36% w/w,<sup>[33]</sup> which seems to correspond to the trend found here when only those concentration ranges were considered. Unexpectedly, the curve of the standard heated solutions was non-linear (Fig. S1B). In this region, a linear relationship was expected, as found for the unheated standard solutions and heated solutions made at pH 5.8, because water is thought to be present, either bound to the protein or as free water, and the water exchange between the two fractions is fast.<sup>[105][110]</sup>

The transition from a heated solution to a gel for standard WPI samples did not change the relationship between  $R_2$  and the dry matter content (Fig. S1A). However, the relationship for the concentration and  $R_2$  of solutions and gels made at pH 5.8 (Fig. S1A) shows a slight change around the gelation concentration (8%).

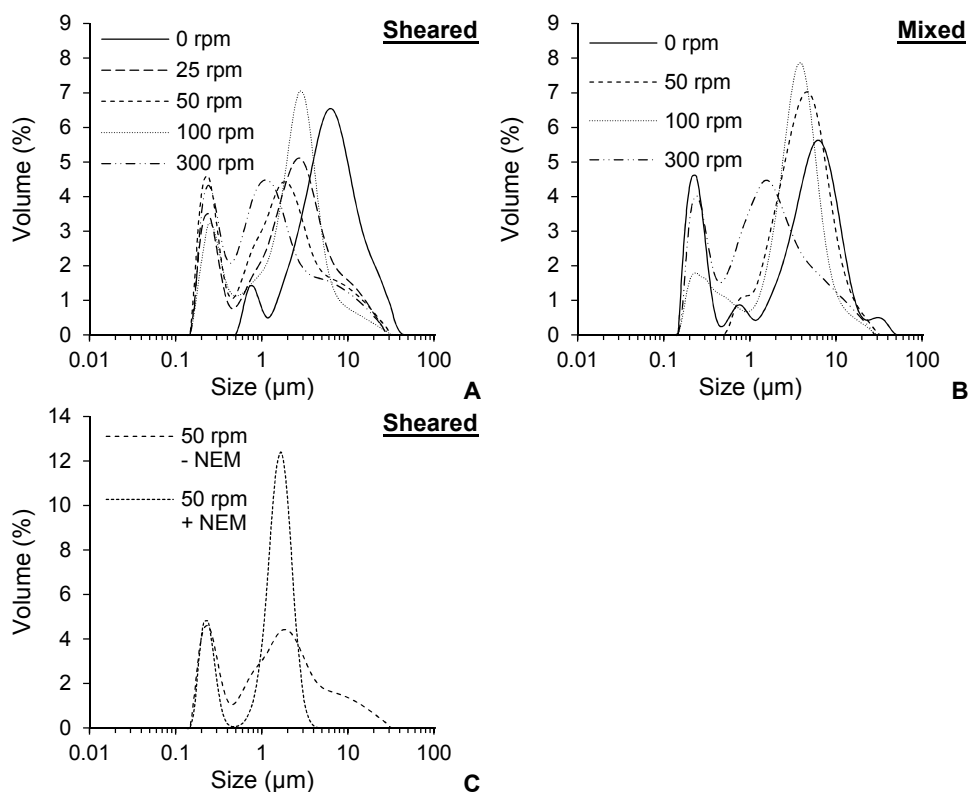


**Fig. S1.** Calibration curves of the dry matter content (%) against the transverse relaxation rate  $R_2$  (s<sup>-1</sup>) as determined by SPLMOD of (A) heated standard (ST) whey protein isolate (WPI) solutions (open diamond) and gels (closed diamond), solutions (open square) and gels (filled square) made at pH 5.8, and gels incubated in 40 mM dithiothreitol (DTT) (filled triangle); and (B) standard (ST) unheated (open diamond) and heated (filled diamond) WPI solutions, and heated solutions made at pH 5.8 (filled square). From the ST solutions and gels a standard calibration curve was drawn (Fig S1A; solid line) using the equation  $y = 0.023x^2 + 0.473x + 0.36$  ( $R_2 = 0.998$ ). Solutions and gels with a pH of 5.8 were used to obtain the pH 5.8 calibration curve (Fig S1A; dotted line) with the equation  $y = 0.011x^2 + 0.812x + 0.334$  ( $R_2 = 0.998$ ).



## APPENDIX B

## SIZE DISTRIBUTIONS OF COLD-GELATED WHEY PROTEIN MICROPARTICLES



**Fig. S2.** The size distributions measured with static light scattering of 6.5 % w/w pellets dispersed in water of cold-gelated whey protein microparticles (A) sheared and (B) mixed during gelation at 0 (solid black line), 25 (long dashed line), 50 (dashed line), 100 (dotted line) and 300 rpm (dashed-dotted line) and (C) cold-gelated whey protein microparticles made without (dashed line) and with N-ethylmaleimide (NEM) (short dashed line) at 50 rpm during gelation.

## APPENDIX C

### SIZE DISTRIBUTIONS OF PROTEIN-RICH PARTICLES

In our research on the water-binding properties of plant protein-rich particles we investigated their swelling via several methods. Below, we will explain the challenges that we encountered when we measured swelling by hydrating the particles and measuring their size with static light scattering.

#### METHOD

Swelling of the plant protein-rich particles in water was determined 20 min after hydration (this equals the centrifugation time; further referred to as hydrated for 0 h) and after 3 h of hydration. To accomplish this, a 10% w/w dispersion was made from the powders. During hydration, the dispersions were placed in an incubator at 25 °C. In addition, samples that were hydrated for 3 h were rotated at 16 rpm in a rotator and mixed with a vortex for a few seconds every 15 min. After hydration, the size of the protein-rich particles was determined using static light scattering (Mastersizer 2000, Malvern Instruments). During these measurements, water was used as a carrier fluid. The rotation speed of the vessel containing the carrier fluid was set at 1200 rpm. Refractive indices of 1.545 (particles), 1.33 (water) and an absorption index of 0.001 (particles) were assumed for the calculations on the particle size distribution. The measurements were performed for four dispersions per type of protein-rich particle; the size distribution was measured in quintuplicate. The size of the dry particles was measured as well. This was done with a Scirocco 2000 dry dispersion unit (Malvern Instruments, Malvern, UK) connected to the Mastersizer. The size of the dry particles was measured at least in triplicate.

From the measurements, the average particle diameter  $d_{4,3}$  (volume mean diameter) was calculated assuming that the particles were spherical. The average diameter  $d_{4,3}$  was used to approximate the average volume of the dry and hydrated particles. With this information, the volume of all hydrated particles together in the pellet was estimated with:

$$V_{\text{hpp}} = \frac{M_{\text{dpp}} V_{\text{hp}}}{\rho_p V_{\text{dp}}} \quad (\text{S1})$$

in which  $V_{\text{hpp}}$  is the total volume of all hydrated particles in the pellet,  $M_{\text{dpp}}$  the weight of all dry particles in the pellet,  $V_{\text{hp}}$  the volume of one hydrated particle,  $\rho_p$  the density of proteins that was assumed to be  $1330 \text{ kg m}^{-3}$ , and  $V_{\text{dp}}$  the volume of one dry particle. Then, the volume of the pellet was approximated with the equation:

$$V_{\text{wet\_pellet}} = \frac{M_{\text{wet\_pellet}} \text{WBC}_{\text{pellet}}}{\rho_w (\text{WBC}_{\text{pellet}} + 1)} + \frac{M_{\text{wet\_pellet}}}{\rho_p (\text{WBC}_{\text{pellet}} + 1)} \quad (\text{S2})$$

with  $V_{\text{wet\_pellet}}$  as the volume of the pellet,  $M_{\text{wet\_pellet}}$  as the weight of the pellet, and  $\rho_w$  as the density of water that was assumed to be  $1000 \text{ kg m}^{-3}$ . After that, the amount of dry matter between the particles was estimated, assuming that the dry matter concentration between the particles was equal to the dry matter concentration of the supernatant (**Chapter 5**; Table 9). For SPI hydrated at 0 h it was not possible to calculate the dry matter concentration. In that case, the dry matter concentration of SPI that was hydrated for 3 h was used in the calculations. The amount of dry matter between the particles was estimated with the following equation:

$$M_{\text{dm\_between}} = \frac{(V_{\text{wet\_pellet}} - V_{\text{hpp}}) \rho_p \rho_w w_{\text{dm\_between}}}{(w_{\text{dm\_between}} \rho_w + w_{\text{water\_between}} \rho_p)} \quad (\text{S3})$$

In this equation  $w_{\text{dm\_between}}$  is the weight-fraction of dry matter in between the particles and  $w_{\text{water\_between}}$  the weight-fraction of water in between the particles according to Table 9 (**Chapter 5**). Subsequently, the WBC of the particles themselves was roughly calculated according to:

$$\text{WBC}_{\text{particles}} = \frac{(V_{\text{hpp}} \rho_p [\text{WBC}_{\text{pellet}} + 1] - [M_{\text{wet\_pellet}} - M_{\text{dm\_between}} (\text{WBC}_{\text{pellet}} + 1)]) \rho_w}{(M_{\text{wet\_pellet}} - M_{\text{dm\_between}} [\text{WBC}_{\text{pellet}} + 1]) \rho_p} \quad (\text{S4})$$

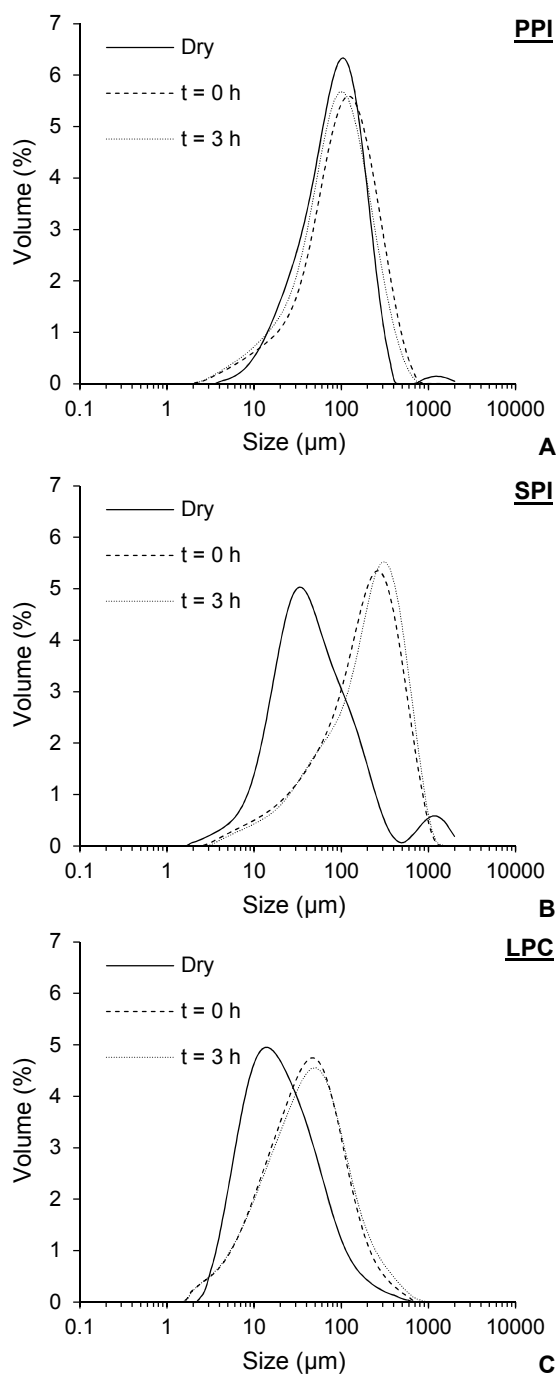
Finally, the ratio *water inside* : *water between* the particles was calculated with:

$$1 : \frac{M_{\text{dm\_between}} w_{\text{water\_between}} (\text{WBC}_{\text{pellet}} + 1)}{(M_{\text{pellet}} \text{WBC}_{\text{pellet}} w_{\text{dm\_between}} - M_{\text{dm\_between}} w_{\text{water\_between}} [\text{WBC}_{\text{pellet}} + 1])} \quad (\text{S5})$$

## RESULTS

The effects of hydration and hydration time on the size of the protein-rich particles were investigated by measuring the size distribution of the particles after 0 h and 3 h of hydration. The results showed that hydration time had no noticeable effect on the particle size (Fig. S3A, B and C). Furthermore, the size distribution of pea protein isolate (PPI) particles became broader when water was added, while the average size became smaller (Fig. S3A), which may indicate that they dissolved, or fell apart. Soy protein isolate (SPI) and lupin protein concentrate (LPC) particles increased in size when water was added (Fig. S3B and C). The effect of hydration and hydration time on the size of the vital wheat gluten (VWG) particles could not be measured, because VWG formed one clump directly after the addition of water.

The WBC of the particles themselves was calculated using the average size of the dry and hydrated protein-rich particles (Table S1). This did only result in a meaningful value for SPI hydrated for 0 h, because it is likely that the assumptions that were made for these calculations were not fully correct. For example, particles had an irregular shape, and due to centrifugation, the concentration of material between the particles was probably larger than in the supernatant. In addition, the size distributions may have also included small aggregates of particles, and therefore did not represent the size of separate particles. Furthermore, it might be that the particles expelled water due to centrifugation, resulting in a lower WBC of the particles (and the pellet thereof). This effect did not occur when the particles were only hydrated (which was the method performed for the size distributions). Consequently, the WBC of the particles, as calculated via their size distribution, will not be taken into account for further discussion.



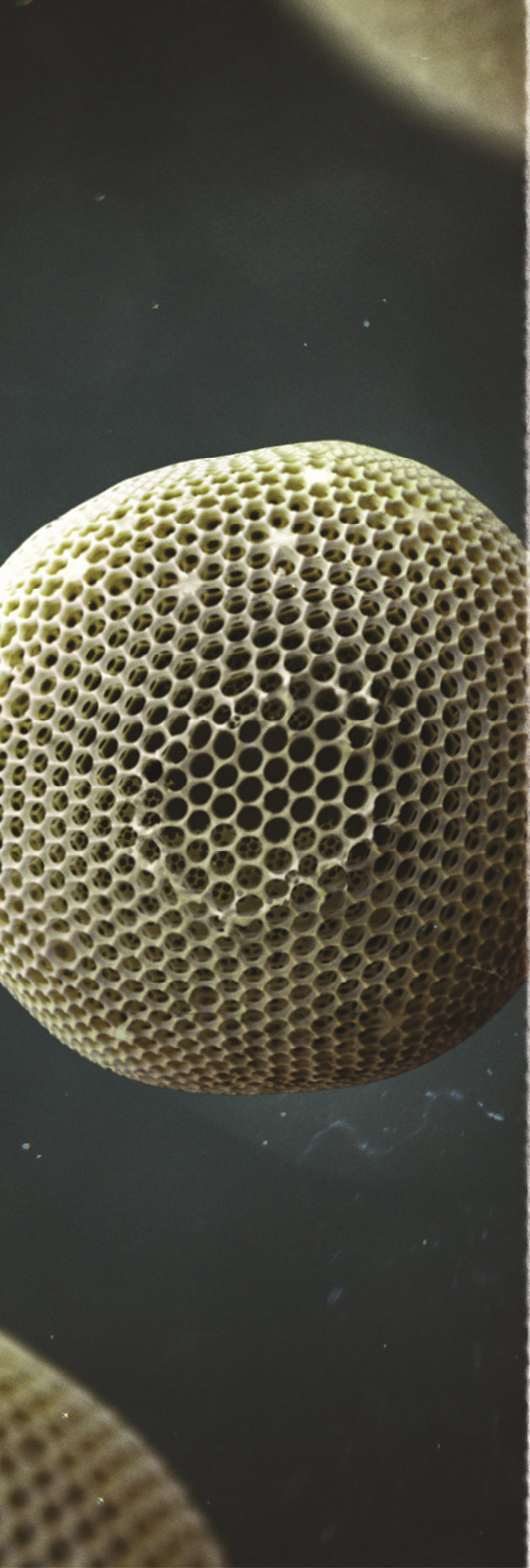
**Fig. S3.** Size distributions of (A) pea protein isolate (PPI), (B) soy protein isolate (SPI), (C) lupin protein concentrate (LPC) when the protein-rich particles were dry (solid line), hydrated for 0 h (dashed line), and hydrated for 3 h (dotted line).

**Table S1.** The water-binding capacity of the pellets (WPC-P) (g water/g dry matter) of pea protein isolate (PPI), soy protein isolate (SPI), lupin protein concentrate (LPC) and vital wheat gluten (VWG), measured via the pellet weight after hydrating the protein-rich particles for either 0 h or 3 h. In addition, the water-binding capacity of the structures (WBC-structures) (g water/g dry matter), and the ratio of water within : water between the structures inside these pellets; calculated via the average size that was obtained from the size distributions.

Method → Material ↓	WBC-P (g water/g dry matter)		WBC-structures (g water/g dry matter)		Ratio in pellet water within : between structures	
	By pellet weight		By size		By size	
	0 h	3 h	0 h	3 h	0 h	3 h
PPI	5.5 (0.4)	5.6 (0.1)	0.9	0.8	1 : 6.0	1 : 8.6
SPI	9.2 (0.2)	8.6 (0.2)	8.9	10.2	1 : 0.0	1 : -0.2
LPC	2.8 (0.1)	3.0 (0.3)	4.7	6.8	1 : -0.4	1 : -0.6
Gluten	1.8 (0.0)	1.9 (0.0)	n.d.	n.d.	n.d.	n.d.

The standard deviation is given within parentheses and is based on four measurements.





## REFERENCES



- [1] Ahmed, J., Al-Jassar, S., & Thomas, L. (2015). A comparison in rheological, thermal, and structural properties between Indian Basmati and Egyptian Giza rice flour dispersions as influenced by particle size. *Food Hydrocolloids*, 48, 72–83.
- [2] Akkermans, C., Venema, P., van der Goot, A. J., Gruppen, H., Bakx, E. J., Boom, R. M., & van der Linden, E. (2008). Peptides are building blocks of heat-induced fibrillar protein aggregates of  $\beta$ -lactoglobulin formed at pH 2. *Biomacromolecules*, 9(5), 1474–1479.
- [3] Alting, A. C., de Jongh, H. H. J., Visschers, R. W., & Simons, J.-W. F. A. (2002). Physical and chemical interactions in cold gelation of food proteins. *Journal of Agricultural and Food Chemistry*, 50(16), 4682–4689.
- [4] Alting, A. C., Hamer, R. J., de Kruif, C. G., Paques, M., & Visschers, R. W. (2003). Number of thiol groups rather than the size of the aggregates determines the hardness of cold set whey protein gels. *Food Hydrocolloids*, 17(4), 469–479.
- [5] Alting, A. C., Hamer, R. J., de Kruif, C. G., & Visschers, R. W. (2000). Formation of disulfide bonds in acid-induced gels of preheated whey protein isolate. *Journal of Agricultural and Food Chemistry*, 48(10), 5001–5007.
- [6] Alting, A. C., Weijers, M., de Hoog, E. H. A., van de Pijpekamp, A. M., Cohen Stuart, M. A., Hamer, R. J., de Kruif, C. G., & Visschers, R. W. (2004). Acid-induced cold gelation of globular proteins: effects of protein aggregate characteristics and disulfide bonding on rheological properties. *Journal of Agricultural and Food Chemistry*, 52(3), 623–631.
- [7] Anker, M., Stading, M., & Hermansson, A.-M. (1999). Effects of pH and the gel state on the mechanical properties, moisture contents, and glass transition temperatures of whey protein films. *Journal of Agricultural and Food Chemistry*, 47(5), 1878–1886.
- [8] Anuradha, S. N., & Prakash, V. (2009). Altering functional attributes of proteins through cross linking by transglutaminase—A case study with whey and seed proteins. *Food Research International*, 42(9), 1259–1265.
- [9] Atkins, P. J. (2000). The pasteurisation of England: the science, culture and health implications of milk processing, 1900–1950. In D. F. Smith & J. Phillips (Eds.), *Food, science, policy and regulation in the twentieth Century: International and comparative perspectives* (37–52). Routledge.
- [10] Banks, J. M. (2004). The technology of low-fat cheese manufacture. *International Journal of Dairy Technology*, 57(4), 199–207.
- [11] Barbut, S. (1995). Effect of sodium level on the microstructure and texture of whey protein isolate gels. *Food Research International*, 28(5), 437–443.

- [12] Barbut, S., & Foegeding, E. A. (1993).  $\text{Ca}^{2+}$ -induced gelation of pre-heated whey protein isolate. *Journal of Food Science*, 58(4), 867–871.
- [13] Basu, S., Shivhare, U. S., & Mujumdar, A. S. (2006). Models for sorption isotherms for foods: A review. *Drying Technology*, 24(8), 917–930.
- [14] Bekard, I. B., Asimakis, P., Bertolini, J., & Dunstan, D. E. (2011). The effects of shear flow on protein structure and function. *Biopolymers*, 95(11), 733–745.
- [15] Berghout, J. A. M., Boom, R. M., & van der Goot, A. J. (2014). The potential of aqueous fractionation of lupin seeds for high-protein foods. *Food Chemistry*, 159, 64–70.
- [16] Berghout, J. A. M., Boom, R. M., & van der Goot, A. J. (2015). Understanding the differences in gelling properties between lupin protein isolate and soy protein isolate. *Food Hydrocolloids*, 43, 465–472.
- [17] Bertram, H. C., Andersen, H. J., & Karlsson, A. H. (2001). Comparative study of low-field NMR relaxation measurements and two traditional methods in the determination of water holding capacity of pork. *Meat Science*, 57(2), 125–132.
- [18] Bertram, H. C., Dønstrup, S., Karlsson, A. H., & Andersen, H. J. (2002). Continuous distribution analysis of  $T_2$  relaxation in meat—An approach in the determination of water-holding capacity. *Meat Science*, 60(3), 279–285.
- [19] Bosmans, G. M., Lagrain, B., Deleu, L. J., Fierens, E., Hills, B. P., & Delcour, J. A. (2012). Assignments of proton populations in dough and bread using NMR relaxometry of starch, gluten, and flour model systems. *Journal of Agricultural and Food Chemistry*, 60(21), 5461–5470.
- [20] Boye, J. I., Alli, I., Ramaswamy, H., & Raghavan, V. G. S. (1997). Interactive effects of factors affecting gelation of whey proteins. *Journal of Food Science*, 62(1), 57–65.
- [21] Brøndum, J., Munck, L., Henckel, P., Karlsson, A., Tornberg, E., & Engelsen, S. B. (2000). Prediction of water-holding capacity and composition of porcine meat by comparative spectroscopy. *Meat Science*, 55(2), 177–185.
- [22] Bryant, A., Ustunol, Z., & Steffe, J. (1995). Texture of Cheddar cheese as influenced by fat reduction. *Journal of Food Science*, 60(6), 1216–1219.
- [23] Bryant, C. M., & McClements, D. J. (1998). Molecular basis of protein functionality with special consideration of cold-set gels derived from heat-denatured whey. *Trends in Food Science & Technology*, 9(4), 143–151.

- [24] Buchert, J., Ercili Cura, D., Ma, H., Gasparetti, C., Monogioudi, E., Faccio, G., Mattinen, M., Boer, H., Partanen, R., Selinheimo, E., Lantto R., & Kruus, K. (2010). Crosslinking food proteins for improved functionality. *Annual Review of Food Science and Technology*, 1, 113–138.
- [25] Butler, M. F., & Heppenstall-Butler, M. (2003). Phase separation in gelatin/dextran and gelatin/maltodextrin mixtures. *Food Hydrocolloids*, 17(6), 815–830.
- [26] Butler, M. F., Ng, Y.-F., & Pudney, P. D. A. (2003). Mechanism and kinetics of the crosslinking reaction between biopolymers containing primary amine groups and genipin. *Journal of Polymer Science Part A: Polymer Chemistry*, 41(24), 3941–3953.
- [27] Caillard, R., Remondetto, G. E., Mateescu, M. A., & Subirade, M. (2008). Characterization of amino cross-linked soy protein hydrogels. *Journal of Food Science*, 73(5), C283–C291.
- [28] Centraal Bureau voor de Statistiek. (2015). *Lengte en gewicht van personen, ondergewicht en overgewicht; vanaf 1981*. [statline.cbs.nl/Statweb/publication/?DM=SLNL&PA=81565ned&D1=5&D2=a&D3=0-1,5&D4=0&D5=0,10,20,30,33-34&VW=T](http://statline.cbs.nl/Statweb/publication/?DM=SLNL&PA=81565ned&D1=5&D2=a&D3=0-1,5&D4=0&D5=0,10,20,30,33-34&VW=T). Accessed 24 December 2015.
- [29] Chaudhry, Q., & Castle, L. (2011). Food applications of nanotechnologies: An overview of opportunities and challenges for developing countries. *Trends in Food Science & Technology*, 22(11), 595–603.
- [30] Chou, D. H., & Morr, C. V. (1979). Protein–water interactions and functional properties. *Journal of the American Oil Chemists' Society*, 56(1), 53A–62A.
- [31] Codex Alimentarius Comission. (2001). *Joint FAO/WHO Food Standards Programme; Procedural Manual* (12th ed.). Rome, Italy.
- [32] Cohen, Y., Avram, L., & Frish, L. (2005). Diffusion NMR spectroscopy in supramolecular and combinatorial chemistry: An old parameter—New insights. *Angewandte Chemie International Edition*, 44(4), 520–554.
- [33] Colsenet, R., Mariette, F., & Cambert, M. (2005). NMR relaxation and water self-diffusion studies in whey protein solutions and gels. *Journal of Agricultural and Food Chemistry*, 53(17), 6784–6790.
- [34] Cumming, D. B., & Tung, M. A. (1975). The ultrastructure of commercial wheat gluten. *Canadian Institute of Food Science and Technology Journal*, 8(2), 67–73.
- [35] Damodaran, S. (2008). Chemical and enzymatic modification of proteins. In S. Damodaran, K. L. Parkin, & O. R. Fennema (Eds.), *Fennema's food chemistry* (4th ed.; 318–323). CRC Press/Taylor & Francis.

- [36] Davisco. (2014). *BiPRO whey protein isolate—Amino acid profile*. [www.daviscofoods.com](http://www.daviscofoods.com). Accessed 23 January 2014.
- [37] Davisco. (2015). *BiPRO whey protein isolate—BiPRO specifications*. [www.daviscofoods.com](http://www.daviscofoods.com). Accessed 29 December 2015.
- [38] Day, L., Augustin, M. A., Batey, I. L., & Wrigley, C. W. (2006). Wheat-gluten uses and industry needs. *Trends in Food Science & Technology*, 17(2), 82–90.
- [39] De Jong, S., Klok, H. J., & van de Velde, F. (2009). The mechanism behind microstructure formation in mixed whey protein–polysaccharide cold-set gels. *Food Hydrocolloids*, 23(3), 755–764.
- [40] De Jong, S., & van de Velde, F. (2007). Charge density of polysaccharide controls microstructure and large deformation properties of mixed gels. *Food Hydrocolloids*, 21(7), 1172–1187.
- [41] Dekkers, B., De Kort, D. W., Grabowska, K. J., Tian, B., Van As, H., & van der Goot, A. J. (2016). A combined rheology and time domain NMR approach for determining water distribution in protein blends. *Food Hydrocolloids*, 60, 525–532.
- [42] De Kruif, C. G., Anema, S. G., Zhu, C., Havea, P., & Coker, C. (2015). Water holding capacity and swelling of casein hydrogels. *Food Hydrocolloids*, 44, 372–379.
- [43] DeMan, J. M. (1999). Water. In *Principles of Food Chemistry* (3rd ed.; 1–32). Springer.
- [44] Doi, E. (1993). Gels and gelling of globular proteins. *Trends in Food Science & Technology*, 4(1), 1–5.
- [45] Draganovic, V., van der Goot, A. J., Boom, R., & Jonkers, J. (2011). Assessment of the effects of fish meal, wheat gluten, soy protein concentrate and feed moisture on extruder system parameters and the technical quality of fish feed. *Animal Feed Science and Technology*, 165(3–4), 238–250.
- [46] Ellman, G. L. (1959). Tissue sulphydryl groups. *Archives of Biochemistry and Biophysics*, 82(1), 70–77.
- [47] Færgemand, M., Otte, J., & Qvist, K. B. (1998). Cross-linking of whey proteins by enzymatic oxidation. *Journal of Agricultural and Food Chemistry*, 46(4), 1326–1333.

- [48] FAO, & WHO. (1967). Toxicological evaluation of some antimicrobials, antioxidants, emulsifiers, stabilizers, flour treatment agents, acids and bases. *10th Report of the joint FAO/WHO expert committee on food additives. WHO food additive series 67.29. FAO nutrition meetings report series 40A, B, C. 620. Glucono- $\delta$ -lactone*. Geneva.
- [49] FAO, & WHO. (1975). Toxicological evaluation of some food colours, thickening agents, and certain other substances. *9th Report of the joint FAO/WHO expert committee on food additives. WHO food additive series 8. FAO nutrition meetings report series 55A. 405. Carob bean gum*. Geneva.
- [50] FAO, & WHO. (2010). FAO/WHO Expert meeting on the application of nanotechnologies in the food and agriculture sectors: potential food safety implications. *Meeting report*. Rome.
- [51] Farhang, B. (2007). Nanotechnology and lipids. *Lipid Technology*, 19(6), 132–135.
- [52] Fennema, O. R. (1996). Amino acids, peptides and proteins. In *Food chemistry* (3rd ed.; 366–370). Marcel Dekker, Inc.
- [53] Flory, P. J., & Rehner, J. Jr. (1943a). Statistical mechanics of cross-linked polymer networks I. Rubberlike elasticity. *The Journal of Chemical Physics*, 11(11), 512–520.
- [54] Flory, P. J., & Rehner, J. Jr. (1943b). Statistical mechanics of cross-linked polymer networks II. Swelling. *The Journal of Chemical Physics*, 11(11), 521–526.
- [55] Foegeding, E. A., Davis, J. P., Doucet, D., & McGuffey, M. K. (2002). Advances in modifying and understanding whey protein functionality. *Trends in Food Science & Technology*, 13(5), 151–159.
- [56] Food and Drug Administration. (2014). *Food Additive Status*. [www.fda.gov/Food/IngredientsPackagingLabeling/FoodAdditivesIngredients/ucu091048.htm](http://www.fda.gov/Food/IngredientsPackagingLabeling/FoodAdditivesIngredients/ucu091048.htm). Accessed 3 May 2016.
- [57] Food and Drug Administration. (2015). Food and drugs; Food and Drug Administration; Food for human consumption; Part 184 Direct food substances affirmed as generally recognized as safe; Subpart B Listing of specific substances affirmed as GRAS; Section 184.1498 Microparticulated protein product. In *Code of Federal Regulations*. Silver Spring.
- [58] Gentès, M.-C., St-Gelais, D., & Turgeon, S. L. (2010). Stabilization of whey protein isolate-pectin complexes by heat. *Journal of Agricultural and Food Chemistry*, 58(11), 7051–7058.

- [59] Gerrard, J. A. (2002). Protein–protein crosslinking in food: methods, consequences, applications. *Trends in Food Science & Technology*, 13(12), 391–399.
- [60] Goetz, J., & Koehler, P. (2005). Study of the thermal denaturation of selected proteins of whey and egg by low resolution NMR. *LWT—Food Science and Technology*, 38(5), 501–512.
- [61] Gosal, W. S., & Ross-Murphy, S. B. (2000). Globular protein gelation. *Current Opinion in Colloid & Interface Science*, 5(3–4), 188–194.
- [62] Gosline, J. M. (1978). The temperature-dependent swelling of elastin. *Biopolymers*, 17(3), 697–707.
- [63] Gunasekaran, S., Ko, S., & Xiao, L. (2007). Use of whey proteins for encapsulation and controlled delivery applications. *Journal of Food Engineering*, 83(1), 31–40.
- [64] Gwartney, E. A., Foegeding, E. A., & Larick, D. K. (2002). The texture of commercial full-fat and reduced-fat cheese. *Journal of Food Science*, 67(2), 812–816.
- [65] Hardacre, A. K., Yap, S.-Y., Lentle, R. G., Janssen, P. W. M., & Monro, J. A. (2014). The partitioning of water in aggregates of undigested and digested dietary particles. *Food Chemistry*, 142, 446–454.
- [66] Havea, P., Carr, A. J., & Creamer, L. K. (2004). The roles of disulphide and non-covalent bonding in the functional properties of heat-induced whey protein gels. *Journal of Dairy Research*, 71(03), 330–339.
- [67] Hermansson, A.-M. (1994). Microstructure of protein gels related to functionality. In R. Y. Yada, R. L. Jackman, J. L. Smith (Eds.), *Protein Structure—Function Relationships in Foods* (22–42). Springer Science + Business Media, L.L.C.
- [68] Hermansson, A.-M. (2008). Structure water by gelation. In J. M. Aguilera & P. J. Lillford (Eds.), *Food Materials Science: Principles and Practice* (255–280). Springer.
- [69] Hinrichs, R., Götz, J., Noll, M., Wolfschoon, A., Eibel, H., & Weisser, H. (2004). Characterisation of the water-holding capacity of fresh cheese samples by means of low resolution nuclear magnetic resonance. *Food Research International*, 37(7), 667–676.
- [70] Hinrichs, R., Götz, J., & Weisser, H. (2003). Water-holding capacity and structure of hydrocolloid-gels, WPC-gels and yogurts characterised by means of NMR. *Food Chemistry*, 82(1), 155–160.

- [71] Hoffman, A. S. (2012). Hydrogels for biomedical applications. *Advanced Drug Delivery Reviews*, 64, Supplement, 18–23.
- [72] Hongsprabhas, P., & Barbut, S. (1997). Protein and salt effects on  $\text{Ca}^{2+}$ -induced cold gelation of whey protein isolate. *Journal of Food Science*, 62(2), 382–385.
- [73] Huppertz, T., & de Kruif, C. G. (2008). Structure and stability of nanogel particles prepared by internal cross-linking of casein micelles. *International Dairy Journal*, 18(5), 556–565.
- [74] Hürlimann, M. D., & Venkataramanan, L. (2002). Quantitative measurement of two-dimensional distribution functions of diffusion and relaxation in grossly inhomogeneous fields. *Journal of Magnetic Resonance*, 157(1), 31–42.
- [75] Ige, M. M., Ogunsua, A. O., & Oke, O. L. (1984). Functional properties of the proteins of some Nigerian oilseeds: Conophor seeds and three varieties of melon seeds. *Journal of Agricultural and Food Chemistry*, 32(4), 822–825.
- [76] Jain, A., Prakash, M., & Radha, C. (2015). Extraction and evaluation of functional properties of groundnut protein concentrate. *Journal of Food Science and Technology*, 52(10), 6655–6662.
- [77] Jauregui, C. A., Regenstein, J. M., & Baker, R. C. (1981). A simple centrifugal method for measuring expressible moisture, a water-binding property of muscle foods. *Journal of Food Science*, 46(4), 1271, 1273.
- [78] Katsuta, K., Rector, D., & Kinsella, J. E. (1990). Viscoelastic properties of whey protein gels: mechanical model and effects of protein concentration on creep. *Journal of Food Science*, 55(2), 516–521.
- [79] Kaufmann, I., Seiberlich, N., Haase, A., & Jakob, P. (2008). Diffusion generated  $T_1$  and  $T_2$  contrast. *Journal of Magnetic Resonance*, 192(1), 139–150.
- [80] Kilara, A., & Sengupta T. (2014). Multi-textures foods. In Y. Lal Dar, J. M. Light (Eds.), *Food Texture Design and Optimization* (15–221). John Wiley & Sons, Ltd. Published.
- [81] Kilara, A. & Vaghela, M.N. (2004). Whey proteins. In R. Yada (Ed.), *Proteins in Food Processing* (72–99). CRC Press/Woodhead publishing limited.
- [82] Kinsella, J. E. (1982). Relationships between structure and functional properties of food proteins. In P. F. Fox, & J. J. Condon (Eds.), *Food Proteins* (51–104). Springer.
- [83] Kinsella, J. E., Fox, P. F., & Rockland, L. B. (1986). Water sorption by proteins: Milk and whey proteins. *CRC Critical Reviews in Food Science and Nutrition*, 24(2), 91–139.

- [84] Kneifel, W., Paquin, P., Abert, T., & Richard, J.-P. (1991). Water-holding capacity of proteins with special regard to milk proteins and methodological aspects—A review. *Journal of Dairy Science*, 74(7), 2027–2041.
- [85] Kocher, P. N., & Foegeding, E. A. (1993). Microcentrifuge-based method for measuring water-holding of protein gels. *Journal of Food Science*, 58(5), 1040–1046.
- [86] Labuza, T. P., & Altunakar, B. (2007). Water activity prediction and moisture sorption isotherms. In G. V. Barbosa-Cánovas, A. J. Fontana, Jr., S. J. Schmidt, T. P. Labuza (Eds.), *Water Activity in Foods* (109–154). IFT Press/Blackwell Publishing.
- [87] Lambelet, P., Berrocal, R., Desarzens, C., Froehlicher, I., & Ducret, F. (1988). Pulsed low-resolution NMR investigations of protein sols and gels. *Journal of Food Science*, 53(3), 943–946.
- [88] Liu, K., & Hsieh, F.-H. (2008). Protein–protein interactions during high-moisture extrusion for fibrous meat analogues and comparison of protein solubility methods using different solvent systems. *Journal of Agricultural and Food Chemistry*, 56(8), 2681–2687.
- [89] Luo, Q., Boom, R. M., & Janssen, A. E. M. (2015). Digestion of protein and protein gels in simulated gastric environment. *LWT—Food Science and Technology*, 63(1), 161–168.
- [90] Mahmoudi, N., Mehalebi, S., Nicolai, T., Durand, D., & Riaublanc, A. (2007). Light-scattering study of the structure of aggregates and gels formed by heat-denatured whey protein isolate and  $\beta$ -lactoglobulin at neutral pH. *Journal of Agricultural and Food Chemistry*, 55(8), 3104–3111.
- [91] Mariette, F. (2006). NMR relaxation of dairy products. In G. A. Webb (Ed.), *Modern magnetic resonance* (1697–1701). Springer.
- [92] Mariette, F. (2009). Investigations of food colloids by NMR and MRI. *Current Opinion in Colloid & Interface Science*, 14(3), 203–211.
- [93] Mayor, L., & Sereno, A. M. (2004). Modelling shrinkage during convective drying of food materials: a review. *Journal of Food Engineering*, 61(3), 373–386.
- [94] Michalski, M. C., Briard, V., Michel, F., Tasson, F., & Poulain, P. (2005). Size distribution of fat globules in human colostrum, breast milk, and infant formula. *Journal of Dairy Science*, 88(6), 1927–1940.
- [95] Mistry, V. V. (2001). Low fat cheese technology. *International Dairy Journal*, 11(4–7), 413–422.



- [96] Mitchell, J., Gladden, L. F., Chandrasekera, T. C., & Fordham, E. J. (2014). Low-field permanent magnets for industrial process and quality control. *Progress in Nuclear Magnetic Resonance Spectroscopy*, 76, 1–60.
- [97] Mokdad, A. H., Ford, E. S., Bowman, B. A., Dietz, W. H., Vinicor, F., Bales, V. S., & Marks, J. S. (2003). Prevalence of obesity, diabetes, and obesity-related health risk factors, 2001. *The Journal of the American Medical Association*, 289(1), 76–79.
- [98] Morris, V. J. (2010). Natural food nanostructures. In Q. Chaudhry, L. Castle & R. Watkins (Eds.), *Nanotechnologies in Food* (50–68). RSC Publishing.
- [99] Mortimore, S., & Wallace, C. (1998). An introduction to hazards, their significance and control. In *HACCP: A Practical Approach* (2nd ed.; 69–100). Springer Science + Business Media, B.V.
- [100] Motoki, M., & Seguro, K. (1998). Transglutaminase and its use for food processing. *Trends in Food Science & Technology*, 9(5), 204–210.
- [101] Nielsen, P. M., Petersen, D., & Dambmann, C. (2001). Improved method for determining food protein degree of hydrolysis. *Journal of Food Science*, 66(5), 642–646.
- [102] NPD. (2014). *Youngest U.S. Generations and Hispanics Will Drive Country's Eating Behaviors Over the Next Five Years, Reports NPD*. [www.npd.com/wps/portal/npd/us/news/press-releases/youngest-us-generations-and-hispanics-will-drive-countrys-eating-behaviors-over-the-next-five-years-reports-npd](http://www.npd.com/wps/portal/npd/us/news/press-releases/youngest-us-generations-and-hispanics-will-drive-countrys-eating-behaviors-over-the-next-five-years-reports-npd). Accessed 9 April 2016.
- [103] Oakenfull, D., Pearce, J., & Burley, R. W. (1997). Protein gelation. In S. Damodaran & A. Paraf (Eds.), *Food Proteins and Their Applications* (111–142). Marcel Dekker, Inc.
- [104] Oakes, J. (1976a). Protein hydration. Nuclear magnetic resonance relaxation studies of the state of water in native bovine serum albumin solutions. *Journal of the Chemical Society, Faraday Transactions 1: Physical Chemistry in Condensed Phases*, 72, 216–227.
- [105] Oakes, J. (1976b). Thermally denatured proteins. Nuclear magnetic resonance, binding isotherm and chemical modification studies of thermally denatured bovine serum albumin. *Journal of the Chemical Society, Faraday Transactions 1: Physical Chemistry in Condensed Phases*, 72, 228–237.
- [106] Omidian, H., & Park, K. (2008). Swelling agents and devices in oral drug delivery. *Journal of Drug Delivery Science and Technology*, 18(2), 83–93.

- [107] Omidian, H., & Park, K. (2010). Introduction to hydrogels. In R. M. Ottenbrite, K. Park & T. Okano (Eds.), *Biomedical Applications of Hydrogels Handbook* (1–16). Springer.
- [108] Omidian, H., Rocca, J. G., & Park, K. (2005). Advances in superporous hydrogels. *Journal of Controlled Release*, 102(1), 3–12.
- [109] Oztop, M. H., Rosenberg, M., Rosenberg, Y., McCarthy, K. L., & McCarthy, M. J. (2010). Magnetic resonance imaging (MRI) and relaxation spectrum analysis as methods to investigate swelling in whey protein gels. *Journal of Food Science*, 75(8), E508–E515.
- [110] Padua, G. W., Richardson, S. J., & Steinberg, M. P. (1991). Water associated with whey protein investigated by pulsed NMR. *Journal of Food Science*, 56(6), 1557–1561.
- [111] Paudel, E., Boom, R. M., & van der Sman, R. G. M. (2015). Change in water-holding capacity in mushroom with temperature analyzed by Flory–Rehner theory. *Food and Bioprocess Technology*, 8(5), 960–970.
- [112] Peleg, M., & Mannheim, C. H. (1977). The mechanism of caking of powdered onion. *Journal of Food Processing and Preservation*, 1(1), 3–11.
- [113] Provencher, S. W. (1982). A constrained regularization method for inverting data represented by linear algebraic or integral equations. *Computer Physics Communications*, 27(3), 213–227.
- [114] Provencher, S. W., & Vogel, R. H. (1983). Regularization techniques for inverse problems in molecular biology. In P. Deuffhard, & E. Hairer (Eds.), *Numerical treatment of inverse problems in differential and integral equations* (Vol 2, 304–319). Birkhäuser.
- [115] Purwanti, N., Moerkens, A., van der Goot, A. J., & Boom, R. (2012). Reducing the stiffness of concentrated whey protein isolate (WPI) gels by using WPI microparticles. *Food Hydrocolloids*, 26(1), 240–248.
- [116] Purwanti, N., Peters, J. P. C. M., & van der Goot, A. J. (2013). Protein micro-structuring as a tool to texturize protein foods. *Food & Function*, 4(2), 277–282.
- [117] Purwanti, N., Smiddy, M., van der Goot, A. J., de Vries, R., Alting, A., & Boom, R. (2011). Modulation of rheological properties by heat-induced aggregation of whey protein solution. *Food Hydrocolloids*, 25(6), 1482–1489.
- [118] Purwanti, N., van der Goot, A. J., Boom, R., & Vereijken, J. (2010). New directions towards structure formation and stability of protein-rich foods from globular proteins. *Trends in Food Science & Technology*, 21(2), 85–94.

- [119] Purwanti, N., van der Veen, E., van der Goot, A. J., & Boom, R. (2013). Stiffening in gels containing whey protein isolate. *International Dairy Journal*, 28(2), 62–69.
- [120] Pusch, W. (1988). Transport of water across synthetic membranes. In F. Franks (Ed.), *Water Science Reviews 3: Volume 3: Water Dynamics* (278–349). Cambridge University Press.
- [121] Qi, P. X., Nuñez, A., & Wickham, E. D. (2012). Reactions between  $\beta$ -lactoglobulin and genipin: Kinetics and characterization of the products. *Journal of Agricultural and Food Chemistry*, 60(17), 4327–4335.
- [122] Qiao, Y., Galvosas, P., Adalsteinsson, T., Schönhoff, M., & Callaghan, P. T. (2005). Diffusion exchange NMR spectroscopic study of dextran exchange through polyelectrolyte multilayer capsules. *The Journal of Chemical Physics*, 122(21), 214912.1–9.
- [123] Raynes, J. K., Carver, J. A., Gras, S. L., & Gerrard, J. A. (2014). Protein nanostructures in food—Should we be worried? *Trends in Food Science & Technology*, 37(1), 42–50.
- [124] Ritzoulis, C., & Karayannakidis, P. D. (2015). Proteins as texture modifiers. In J. Chen & A. Rosenthal (Eds.), *Modifying Food Texture: Volume 1: Novel Ingredients and Processing Techniques* (51–70). Woodhead Publishing.
- [125] Roccia, P., Ribotta, P. D., Pérez, G. T., & León, A. E. (2009). Influence of soy protein on rheological properties and water retention capacity of wheat gluten. *LWT—Food Science and Technology*, 42(1), 358–362.
- [126] Russ, J. C. (2005). Volume fraction. In *Image Analysis of Food Microstructure* (11–20). CRC Press.
- [127] Ryabov, Y. E., & Feldman, Y. (2002). The relationship between the scaling parameter and relaxation time for non-exponential relaxation in disordered systems. In F. Family, M. Daoud, H. J. Herrmann & H. E. Stanley (Eds.), *Scaling and Disordered Systems* (173–184). World scientific.
- [128] Sağlam, D., Venema, P., de Vries, R., van Aelst, A., & van der Linden, E. (2012). Relation between gelation conditions and the physical properties of whey protein particles. *Langmuir*, 28(16), 6551–6560.
- [129] Sağlam, D., Venema, P., de Vries, R., & van der Linden, E. (2014). Exceptional heat stability of high protein content dispersions containing whey protein particles. *Food Hydrocolloids*, 34, 68–77.
- [130] Salvia-Trujillo, L., Qian, C., Martín-Belloso, O., & McClements, D. J. (2013). Influence of particle size on lipid digestion and  $\beta$ -carotene bioaccessibility in emulsions and nanoemulsions. *Food Chemistry*, 141(2), 1472–1480.

- [131] Sanguansri, P., & Augustin, M. A. (2006). Nanoscale materials development—A food industry perspective. *Trends in Food Science & Technology*, 17(10), 547–556.
- [132] Shang, L., Nienhaus, K., & Nienhaus, G. U. (2014). Engineered nanoparticles interacting with cells: size matters. *Journal of Nanobiotechnology*, 12.
- [133] Shewan, H. M., & Stokes, J. R. (2013). Review of techniques to manufacture micro-hydrogel particles for the food industry and their applications. *Journal of Food Engineering*, 119(4), 781–792.
- [134] Shimada, K., & Cheftel, J. C. (1988). Texture characteristics, protein solubility, and sulfhydryl group/disulfide bond contents of heat-induced gels of whey protein isolate. *Journal of Agricultural and Food Chemistry*, 36(5), 1018–1025.
- [135] Singer, N. S. (1996). Microparticulated proteins and fat mimetics. In S. Roller & S. A. Jones (Eds.), *Handbook of Fat Replacers* (175–190). CRC Press.
- [136] Song, F., Zhang, L.-M., Yang, C., & Yan, L. (2009). Genipin-crosslinked casein hydrogels for controlled drug delivery. *International Journal of Pharmaceutics*, 373(1-2), 41–47.
- [137] Song, Y. Q., Venkataramanan, L., Hürlimann, M. D., Flaum, M., Frulla, P., & Straley, C. (2002).  $T_1$ – $T_2$  correlation spectra obtained using a fast two-dimensional Laplace inversion. *Journal of Magnetic Resonance*, 154(2), 261–268.
- [138] Sowers, J. R. (2003). Obesity as a cardiovascular risk factor. *The American Journal of Medicine*, 115(8, Supplement 1), 37–41.
- [139] Spyros, A., & Dais, P. (2013). Theoretical Aspects. In *NMR spectroscopy in food analysis* (5–66). Cambridge: Royal Society of Chemistry. RSC Publishing.
- [140] Stobnicka, A., & Górny, R. L. (2015). Exposure to flour dust in the occupational environment. *International Journal of Occupational Safety and Ergonomics*, 21(3), 241–249.
- [141] Straadt, I. K., Rasmussen, M., Andersen, H. J., & Bertram, H. C. (2007). Aging-induced changes in microstructure and water distribution in fresh and cooked pork in relation to water-holding capacity and cooking loss—A combined confocal laser scanning microscopy (CLSM) and low-field nuclear magnetic resonance relaxation study. *Meat Science*, 75(4), 687–695.
- [142] Sullivan, S. T., Khan, S. A., & Eissa, A. S. (2009). Whey proteins: Functionality and foaming under acidic conditions. In C. Onwulata, & P. Huth (Eds.), *Whey Processing, Functionality and Health Benefits* (99–132). Wiley.

- [143] Sun, Q., & Xiong, C. S. L. (2014). Functional and pasting properties of pea starch and peanut protein isolate blends. *Carbohydrate Polymer*, 101, 1134–1139.
- [144] Thalmann, C. R., & Lötzbeyer, T. (2002). Enzymatic cross-linking of proteins with tyrosinase. *European Food Research and Technology*, 214(4), 276–281.
- [145] Totosaus, A., Montejano, J. G., Salazar, J. A., & Guerrero, I. (2002). A review of physical and chemical protein-gel induction. *International Journal of Food Science & Technology*, 37(6), 589–601.
- [146] Truong, V.-D., Clare, D. A., Catignani, G. L., & Swaisgood, H. E. (2004). Cross-linking and rheological changes of whey proteins treated with microbial transglutaminase. *Journal of Agricultural and Food Chemistry*, 52(5), 1170–1176.
- [147] Turgeon, S. L., & Beaulieu, M. (2001). Improvement and modification of whey protein gel texture using polysaccharides. *Food Hydrocolloids*, 15(4–6), 583–591.
- [148] Urbonaite, V., de Jongh, H. H. J., van der Linden, E., & Pouvreau, L. (2014). Origin of water loss from soy protein gels. *Journal of Agricultural and Food Chemistry*, 62(30), 7550–7558.
- [149] Urbonaite, V., de Jongh, H. H. J., van der Linden, E., & Pouvreau, L. (2015). Protein aggregates may differ in water entrapment but are comparable in water confinement. *Journal of Agricultural and Food Chemistry*, 63(40), 8912–8920.
- [150] Van den Berg, L., van Vliet, T., van der Linden, E., van Boekel, M. A. J. S., & van de Velde, F. (2007). Serum release: The hidden quality in fracturing composites. *Food Hydrocolloids*, 21(3), 420–432.
- [151] Van der Goot, A. J., Peighambaroust, S. H., Akkermans, C., & van Oosten-Manski, J. M. (2008). Creating novel structures in food materials: The role of well-defined shear flow. *Food Biophysics*, 3(2), 120–125.
- [152] Van der Sman, R. G. M. (2007a). Moisture transport during cooking of meat: An analysis based on Flory–Rehner theory. *Meat Science*, 76(4), 730–738.
- [153] Van der Sman, R. G. M. (2007b). Soft condensed matter perspective on moisture transport in cooking meat. *AIChE Journal*, 53(11), 2986–2995.
- [154] Van der Sman, R. G. M. (2012). Thermodynamics of meat proteins. *Food Hydrocolloids*, 27(2), 529–535.
- [155] Van der Sman, R. G. M. (2013). Moisture sorption in mixtures of biopolymer, disaccharides and water. *Food Hydrocolloids*, 32(1), 186–194.

- [156] Van der Sman, R. G. M., Paudel, E., Voda, A., & Khalloufi, S. (2013). Hydration properties of vegetable foods explained by Flory–Rehner theory. *Food Research International*, 54(1), 804–811.
- [157] Van Dusschoten, D., Moonen, C. T. W., de Jager, P. A., & Van As, H. (1996). Unraveling diffusion constants in biological tissue by combining Carr–Purcell–Meiboom–Gill imaging and pulsed field gradient NMR. *Magnetic resonance in medicine*, 36(6), 907–913.
- [158] Van Duynhoven, J., Voda, A., Witek, M., & Van As, H. (2010). Time-domain NMR applied to food products. In A. W. Graham (Ed.), *Annual reports on NMR spectroscopy* (Vol. 69; 145–197). Academic Press.
- [159] Van Riemsdijk, L. E., Snoeren, J. P. M., van der Goot, A. J., Boom, R. M., & Hamer, R. J. (2011). New insights on the formation of colloidal whey protein particles. *Food Hydrocolloids*, 25(3), 333–339.
- [160] Van Riemsdijk, L. E., Sprakel, J. H. B., van der Goot, A. J., & Hamer, R. J. (2010). Elastic networks of protein particles. *Food Biophysics*, 5(1), 41–48.
- [161] Veerman, C. (2003). Method for improving the functional properties of a globular protein, protein thus prepared, use thereof and products containing the protein. Patent US20060204454 A1, EP1565067 A2, WO2004049819 A2, WO2004049819 A3.
- [162] Venkataramanan, L., Song, Y.-Q., & Hürlimann, M. D. (2002). Solving Fredholm integrals of the first kind with tensor product structure in 2 and 2.5 dimensions. *IEEE Transactions on Signal Processing*, 50(5), 1017–1026.
- [163] Voedingscentrum. (2011). *Meer consumenten willen gezonder eten*. [www.voedingscentrum.nl/nl/nieuws/meer-consumenten-willen-gezonder-eten.aspx](http://www.voedingscentrum.nl/nl/nieuws/meer-consumenten-willen-gezonder-eten.aspx). Accessed 9 April 2016.
- [164] Walkenström, P., Nielsen, M., Windhab, E., & Hermansson, A.-M. (1999). Effects of flow behaviour on the aggregation of whey protein suspensions, pure or mixed with xanthan. *Journal of Food Engineering*, 42(1), 15–26.
- [165] Walsh, K. (2015). Nondestructive assessment of fruit quality. In R. B. H. Wills, & J. B. Golding (Eds.), *Advances in Postharvest Fruit and Vegetable Technology* (39–64). CRC Press/Taylor & Francis Group.
- [166] Walstra, P. (2003a). Concentrated dispersions. In *Physical Chemistry of Foods* (99). Marcel Dekker, Inc.
- [167] Walstra, P. (2003b). Proteins. In *Physical Chemistry of Foods* (203–249). Marcel Dekker, Inc.

- [168] Walstra, P. (2003c). Sedimentation. In *Physical Chemistry of Foods* (504–514). Marcel Dekker, Inc.
- [169] Walstra, P., Wouters, J. T. M., & Geurts, T. J. (2006a). Proteins. In *Dairy Science and Technology* (2nd ed.; 63–84). CRC Press/Taylor & Francis.
- [170] Walstra, P., Wouters, J. T. M., & Geurts, T. J. (2006b). Casein micelles. In *Dairy Science and Technology* (2nd ed.; 140–156). CRC Press/Taylor & Francis.
- [171] Walstra, P., Wouters, J. T. M., & Geurts, T. J. (2006c). Protein preparations. In *Dairy Science and Technology* (2nd ed.; 537–550). CRC Press/Taylor & Francis.
- [172] Walstra, P., Wouters, J. T. M., & Geurts, T. J. (2006d). Yogurt. In *Dairy Science and Technology* (2nd ed.; 558–569). CRC Press/Taylor & Francis.
- [173] Walstra, P., Wouters, J. T. M., & Geurts, T. J. (2006e). Cheddar-type cheese. In *Dairy Science and Technology* (2nd ed.; 712–717). CRC Press/Taylor & Francis.
- [174] Wang, A., Cui, Y., Li, J., & van Hest, J. C. M. (2012). Fabrication of gelatin microgels by a “cast” strategy for controlled drug release. *Advanced Functional Materials*, 22(13), 2673–2681.
- [175] Wang, J. C., & Kinsella, J. E. (1976). Functional properties of novel proteins: Alfaalfa leaf protein. *Journal of Food Science*, 41(2), 286–292.
- [176] Wang, W., Zhong, Q., & Hu, Z. (2013). Nanoscale understanding of thermal aggregation of whey protein pretreated by transglutaminase. *Journal of Agricultural and Food Chemistry*, 61(2), 435–446.
- [177] Westmeier, D., Chen, C., Stauber, R. H., & Docter, D. (2015). The bio-corona and its impact on nanomaterial toxicity. *European Journal of Nanomedicine*, 7(3), 153–168.
- [178] Wolf, B., Scirocco, R., Frith, W. J. & Norton, I. T. (2000). Shear-induced anisotropic microstructure in phase-separated biopolymer mixtures. *Food Hydrocolloids*, 14(3), 217–255.
- [179] Wyss, H. M., Franke, T., Mele, E., & Weitz, D. A. (2010). Capillary micromechanics: Measuring the elasticity of microscopic soft objects. *Soft Matter*, 6(18), 4550–4555.
- [180] Yazici, F., & Akgun, A. (2004). Effect of some protein based fat replacers on physical, chemical, textural, and sensory properties of strained yogurt. *Journal of Food Engineering*, 62(3), 245–254.

- [181] Yi, J., Li, Y., Zhong, F., & Yokoyama, W. (2014). The physicochemical stability and in vitro bioaccessibility of beta-carotene in oil-in-water sodium caseinate emulsions. *Food Hydrocolloids*, 35, 19–27.
- [182] Yokoyama, K., Nio, N., & Kikuchi, Y. (2004). Properties and applications of microbial transglutaminase. *Applied Microbiology and Biotechnology*, 64(4), 447–454.
- [183] Yu, J., Ahmedna, M., & Goktepe, I. (2007). Peanut protein concentrate: Production and functional properties as affected by processing. *Food Chemistry*, 103(1), 121–129.
- [184] Yuan, Y., Chesnutt, B. M., Utturkar, G., Haggard, W. O., Yang, Y., Ong, J. L. & Bumgardner, J. D. (2007). The effect of cross-linking of chitosan microspheres with genipin on protein release. *Carbohydrate Polymers*, 68(3), 561–567.
- [185] Zayas, J. F. (1997a). Water holding capacity of proteins. *Functionality of proteins in food* (76–133). Springer–Verlag Berlin Heidelberg GmbH.
- [186] Zayas, J. F. (1997b). Gelling properties of proteins. *Functionality of Proteins in Food* (310–366). Springer–Verlag Berlin Heidelberg GmbH.
- [187] Zirbel, F., & Kinsella, J. E. (1988). Effects of thiol reagents and ethanol on strength of whey protein gels. *Food Hydrocolloids*, 2(6), 467–475.
- [188] Zohuriaan-Mehr, M. J., & Kabiri, K. (2008). Superabsorbent polymer materials: A review. *Iranian Polymer Journal*, 17(6), 451–477.





## ACKNOWLEDGEMENTS

Hereby I present to you the result of four years of hard work and the offering of quite some blood, sweat and tears. Even though it was not always easy, I am happy to have had the chance to pursue a PhD and I appreciate the guidance, advice, support and company I enjoyed. A lot of people have helped me during the last years in one way or another, and I would like to thank all of them. Additionally, there are some people I would like to thank in particular.

Dear Atze Jan. Without you this thesis would not have been here. I do not have the words to describe how thankful I am for all that you have done for me. For all the time and energy that you have invested in me and my project; for the way you kept supporting me. You are an extraordinary supervisor who still stood behind me where others might have walked away. I feel very fortunate that you were my supervisor.

Dear Hannemieke, thank you for all the pleasant and productive meetings we had together, and all the valuable ideas you came up with. I appreciate your positive attitude towards me and my results a lot. Thank you for believing in me.

Dear Frank, thank you for introducing me to the “world of NMR”. I really enjoyed working with you, and in particular all the discussions we have had. Those discussions gave me a lot of energy and you inspired me to go further with my work and to try to understand it better.

Dear Remko and Henk, I would like to thank you for your time and valuable contributions to my project. Your input has improved the quality of my work.

Furthermore I would like to thank all my colleagues at FPE for the pleasant times. I would like to give special thanks to Jos, Maurice and Jarno for saving me from flooding water baths and all the other technical assistance you provided, especially when equipment was not working the way it should. Furthermore, I would thank Jarno for the good conversations, and his interest in me. Also thanks to Barbara, Marjan and Martin for organizing everything outside the lab smoothly.

In addition, I would like to thank all the students that worked on one of my projects. Martin, Sevinç, Anita, Mareike, Vivian, Xinyi, Charlotte and Maryam, I have learned a lot from you.

Thanks to all my office mates. Laura, Jue, Rupali, Sebastian, Angelica, Jacqueline, Birgit and Fiona, thank you for all the laughs, talks, discussions, relaxing moments (like during the repainting of our office!) etc.

Luckily, life did not consist of only work the last four years. Jue, Sami, Ekaraj, Filippas, Jacqueline, Angelica, Victor, Feifei thanks for all the nice meals, cosy evenings and leisure time activities. Special thanks to Jue and Victor for being my paranympths.

Daarnaast wil ik ook mijn (schoon)familie bedanken voor hun steun en interesse in mij en mijn werk. Oma, bedankt voor je belangstellende praatjes, mailtjes, appjes en belletjes. Ik kom binnenkort weer eens op de koffie. Pap en mam, bedankt dat jullie er altijd voor mij zijn. Ruben bedankt dat je me altijd hebt willen helpen met de grafische aspecten die bij mijn project kwamen kijken. Deze thesis is een plaatje geworden mede dankzij jou! Elmar en Elvie, bedankt dat jullie voor mij klaar staan. Daarnaast, Elmar bedankt voor de muzikale ontspanning, en Elvie voor alle kledingadviezen :).

Tenslotte mijn lieve Wouter. Bedankt dat je er voor mij bent. Ik ben blij dat je de stap hebt gezet om mij wat beter te leren kennen. Jij zorgt voor de verrijking in mijn leven waar ik heel lang naar verlangd heb. Ik ben ontzettend dankbaar en blij met je gezelligheid, steun, luisterende oor, warmte en liefde. Ik zie uit naar onze toekomst samen!

## ABOUT THE AUTHOR

Jorien Petronella Cornelia Mathilde Peters was born in Sittard, the Netherlands, on the 11<sup>th</sup> of October 1988. She attended secondary school at Theresialyceum Tilburg and graduated in 2006 with a major in Nature and Health.

In the same year she started studying Food Technology at Wageningen University. She completed her BSc with a thesis on *“Influence of the protein content on the crispness of bread”* at the Food Chemistry department in 2009. Jorien conducted her MSc thesis research at the department of Food Process Engineering 2011, which was regarding *“The characteristics and solidification behaviour of commercial lupin concentrates.”* In the same year she also performed an internship at Skretting, Stavanger (Norway) about *“Hydrolysis of soy protein concentrate and wheat gluten.”*

In 2011 Jorien graduated from Wageningen University with a MSc degree and started as a PhD student on the project *“Microstructuring of dairy proteins”* at the Food Process Engineering department. The results of this work are represented in this thesis.





## LIST OF PUBLICATIONS

### PEER REVIEWED PAPERS

**Peters, J. P. C. M.**, Vergeldt, F. J., Boom, R. M., van der Goot, A. J. Water-binding capacity of protein-rich particles. *Submitted for publication*.

**Peters, J. P. C. M.**, Vergeldt, F. J., Van As, H., Luyten, H., Boom, R. M., van der Goot, A. J. Unravelling of the water-binding capacity of cold-gelated whey protein microparticles. *Submitted for publication*.

**Peters, J. P. C. M.**, Vergeldt, F. J., Van As, H., Luyten, H., Boom, R. M., & van der Goot, A. J. (2016). Time domain nuclear magnetic resonance as a method to determine and characterize the water-binding capacity of whey protein microparticles. *Food Hydrocolloids*, 54 Part A, 170–178.

**Peters, J. P. C. M.**, Luyten, H., Alting, A. C., Boom, R. M., & van der Goot, A. J. (2015). Effect of crosslink density on the water-binding capacity of whey protein microparticles. *Food Hydrocolloids*, 44(0), 277–284.

Purwanti, N., **Peters, J. P. C. M.**, & van der Goot, A. J. (2013). Protein micro-structuring as a tool to texturize protein foods. *Food & Function*, 4(2), 277–282.

### PATENT APPLICATIONS

J. M. J. G. Luyten, A. Koning, T. J. Faber, **J. P. C. M. Peters**, and J. P. Paques. Hard and semi-hard cheese comprising water-retaining particles, a method for preparing such hard or semi-hard cheese, and use of such particles in the preparation of cheese. *Patent WO2015060715*, 2015.



## OVERVIEW OF COMPLETED TRAINING ACTIVITIES

### DISCIPLINE SPECIFIC

#### COURSES

Industrial Food Proteins, Wageningen (NL)	2013
Advanced Food Analysis, Wageningen (NL)	2013
Summer school Boulder “Polymers in Soft and Biological matter,” Boulder (US)	2012
Food Structure and Rheology, Wageningen (NL)	2012

#### CONFERENCES

NanoCity 2016, Amsterdam (NL) <sup>a</sup>	2016
NanoCity 2015, Amersfoort (NL) <sup>a</sup>	2015
9 <sup>th</sup> NIZO Dairy conference (2015), Papendal (NL) <sup>b</sup>	2015
NPS14, Utrecht (NL) <sup>a</sup>	2014
7 <sup>th</sup> International Whey Conference, Rotterdam (NL) <sup>a</sup>	2014
IDF Symposium on Microstructure of Dairy Products, Melbourne (AU) <sup>b *</sup>	2014
MicroNanoConference '13, Ede (NL) <sup>b</sup>	2013
International Symposium on the Properties of Water XII, Fiskebäckskil (SE) <sup>b</sup>	2013
9th European Congress of Chemical Engineering, The Hague (NL) <sup>a</sup>	2013
MicroNanoConference '12, Ede (NL)	2012
FoodBalt 2012, Kaunas (LT) <sup>a</sup>	2012
The 6th International Symposium on Food Rheology and Structure, Zürich (CH) <sup>b</sup>	2012

#### GENERAL COURSES

Last Stretch of the PhD, Wageningen (NL)	2016
Orientation on Teaching for PhD students, Wageningen (NL)	2015
Analytic Storytelling, Utrecht (NL)	2014
Risk Analysis and Technology Assessment, Amersfoort (NL)	2013
Techniques for Writing and Presenting a Scientific Paper, Wageningen (NL)	2013
Scientific Writing, Wageningen (NL)	2013



Effective Behaviour in your Professional Surroundings, Wageningen (NL)	2012/2013
IP Awareness and Valorisation, Oegstgeest (NL)	2012
Organising and Supervising Thesis Projects, Wageningen (NL)	2012
VLAG PhD week, Baarlo (NL)	2012
Stress Identification and Management, Wageningen (NL)	2012

### **OPTIONAL ACTIVITIES**

NanoNextNL Project Meetings <sup>a, b</sup>	2011-2016
Food Process Engineering Group Meetings <sup>b</sup>	2011-2016
RATA day <sup>b</sup>	2013
Scientific PhD excursion to Finland and the Baltic States <sup>b</sup>	2012

<sup>a</sup>Poster <sup>b</sup>Oral

\*Best Early Career Scientist Presentation



The work presented in this thesis has received funding from FrieslandCampina and NanoNextNL, a micro and nanotechnology consortium of the Government of the Netherlands and 130 partners.

Cover and layout were designed by Måriboe, Ruben Peters

This thesis was printed by GVO drukkers & vormgevers B.V.

